Polarization phenomena in photo- and electrodisintegration of the lightest nuclei at medium energies

V. V. Kotlyar, Yu. P. Mel'nik, and A. V. Shebeko
National Science Center, Khar'kov Physico–Technical University, Khar'kov, Ukraine

Fiz. Elem. Chastits At. Yadra **26**, 192–274 (January–February 1995)

This review discusses the dependence of the target asymmetries and the nucleon polarizations in electrodisintegration of polarized and unpolarized deuterons and the beam asymmetry in disintegration of the ^{3}He nucleus induced by linearly polarized photons on the choice of model of the nuclear electromagnetic current (in particular, the meson-exchange currents). Special attention is given to the effects of the final-state interaction of the np pair in the $d(e,e'\vec{n})p$ reaction. The effect of the spin–orbit electromagnetic interaction of the nucleons and of other relativistic corrections to the electromagnetic current density of the nucleus on the formation of the angular and energy dependences of the polarization observables in these processes is demonstrated. The possibilities of extracting the neutron electric form factor from the inelastic scattering of longitudinally polarized electrons on the deuteron and the ^{3}He nucleus in inclusive and exclusive reactions are considered. The kinematical regions in which the polarization observables take values which can be measured at c.w. electron accelerators of the CEBAF type are determined. Various proposals for isolating (in particular, in the cumulative region) the structure functions characterizing the response of the hadronic system to its interaction with electromagnetic probes are discussed. For this purpose the disintegration of the lightest nuclei induced by longitudinally polarized electrons under the conditions of the MIT–Bates experiments is analyzed theoretically. The results of the calculations are compared with the data obtained by the Amsterdam, Bonn, MIT–Bates, Novosibirsk, Frascati, Saclay, and Khar'kov groups. In the Conclusion are some ideas which might prove useful for developing a covariant and gauge-independent description of electromagnetic interactions with nuclei.

1. INTRODUCTION

The study of the polarization characteristics in electromagnetic (EM) interactions involving nuclei is at the leading edge of contemporary research (Refs. 1–21). The interest in this topic has been stimulated by the construction of continuously working electron accelerators such as MAMI in Mainz, ELSA in Bonn, AmPS in Amsterdam, SHR at MIT–Bates Laboratory, and CEBAF in Newport News. A fairly complete presentation of the role and goals of polarization experiments in the research programs of these centers is given in the reviews of Refs. 22–28. The problems and achievements of the measurements and theoretical descriptions of polarization observables in the photodisintegration of few-nucleon systems at medium photon energies have been discussed in Refs. 29–31. Various aspects of spin physics in EM interactions of nuclei (in particular, in electrodisintegration of polarized targets by polarized electrons) have been reviewed in Refs. 32–35 and in the lecture of Ref. 36.

The corresponding observables (for example, the beam and target asymmetries) can contain information on the reaction mechanisms and nuclear structure which is richer than that from unpolarized particles. These spin observables, which depend on the interference of various reaction amplitudes (the structure functions) can be very sensitive to the contributions of non-nucleon degrees of freedom and final-state-interaction (FSI) effects. The results of studies of the role of FSI effects in the $(e,e'N)$ reaction on nuclei are discussed in Refs. 37 and 38.

Special attention is given to the study of the polarization of knocked-out nucleons in the electrodisintegration of the simplest nuclear system, the deuteron (Refs. 4–7, 11–13, 15, 16, 18, 20, and 21). This observable in the $d(e,e'\vec{N})N$ reaction with unpolarized electrons and deuterons is expressed in terms of the structure functions, which are not encountered in the cross section. Only one of them survives if the momenta of the virtual photon and the knocked-out nucleon are collinear (the case of the so-called parallel kinematics). This feature makes it possible to extract the interference of certain reaction amplitudes without resorting to the complicated procedures of structure-function isolation (for example, in out-of-plane experiments; Ref. 33). We also note that this polarization is completely determined by FSI effects, viz., it vanishes if this interaction is neglected (at least, in descriptions without P and T violation). Accordingly, it can be expected that study of this observable as a function of the nucleon emission angle for different relative energies in the np pair can provide additional information about the np interaction.

In contrast to the preceding case, in the $d(\vec{e},e\vec{N})N$ reaction with polarized electrons there is, in addition to the nucleon polarization induced by the FSI, polarization transfer owing to the $\vec{e}d$ interaction in the entrance channel of the reaction.[5,11] This difference is reflected in the appearance of new structure functions. Owing to the weak coupling of the nucleons in the deuteron, it can be expected that for quasifree $\vec{e}d$ scattering the polarization transfer will be proportional (like the nucleon polarization in $\vec{e}N$ scattering) to the product $G_E^N G_M^N$, where G_E^N (G_M^N) is the nucleon electric (magnetic) form factor. Therefore, the idea arises of obtaining additional

 1063-7796/95/010079-35$10.00

information about the neutron electric form factor G_E by analyzing this observable in the $d(\vec{e},e'\vec{n})p$ reaction (Refs. 4–6, 11). Of course, information about the EM properties of the bound nucleon can be distorted by FSI and meson-exchange-current (MEC) effects (Refs. 7, 12, 13, 15, and 18). The combined effect of these distortion factors is discussed in detail in the present review.

We should stress the fact that the true role played by FSI and MEC effects is difficult to understand unless the MECs and the NN interaction that is used are compatible. In fact, as was shown in Ref. 39 (see also Ref. 12), the FSI and MEC contributions separately can be important, but only if they are taken together is it possible to obtain (owing to the destructive interference between them) a satisfactory description of the data.[40,41] This result reflects the general statement (Ref. 42; see also Refs. 7, 43, and 44) that satisfaction of the continuity equation for the EM current-density operator of a system of charged particles is not sufficient to ensure the gauge independence of the EM transition amplitudes in the system. Below, we shall touch upon questions related to the gauge independence of the description of EM processes on nuclei.

The asymmetries in the $d(e,e'p)n$ reaction with tensorially polarized deuterons can be a source of additional information about the deuteron structure (in particular, at short distances). In fact, the corresponding structure functions calculated in the impulse approximation (IA) are determined by the interference of the S and D waves of the deuteron wave function. This fact has become an important motivation for the measurement of the cross section for the $\vec{D}(e,pn)e'$ reaction near the photon point.[8]

The experiment of Ref. 8 was carried out at Novosibirsk using the VÉPP-2 accelerator with electron energy $E=180$ MeV and an internal target (a polarized deuterium jet). Later these studies were extended using the VÉPP-3 accelerator with $E=2$ GeV (Ref. 45) in order to extract the high-momentum components of the deuteron wave function. We note that there are plans to measure the asymmetries in the reaction $\vec{D}(\vec{e},e'p)n$ with vectorially polarized deuterons and longitudinally polarized electrons at CEBAF.[46]

Of course, the predictions based on the IA need to be corrected to include more complicated reaction mechanisms (for example, the FSI in the np system). In addition, as the energy–momentum transfer increases it becomes necessary to take into account the contributions of non-nucleon degrees of freedom, viz., isobaric configurations in the deuteron, MECs, and other relativistic effects (Refs. 13, 17, and 19).

The search for relativistic effects in the disintegration of the lightest nuclei induced by photons and electrons (in particular, their manifestations in the spin observables) is of great interest for a deeper understanding of the mechanisms of EM processes and nuclear dynamics. In the matrix elements of the EM current between the initial and final hadron states it is possible to distinguish relativistic corrections (RCs) to the current operators and the wave functions, where in the latter case there are understood to be two types of contribution, namely, those originating in the internal dynamics of the wave function in the rest frame and those from the boosts transforming this frame to a moving frame. It has been shown (see Refs. 30, 47–53, 20, and 21 and references therein) that even at moderate energy–momentum transfers the RCs can significantly affect the various observables in deuteron and ^{3}He photodisintegration and in electron inclusive and exclusive scattering on the deuteron. The corresponding calculations (Refs. 47, 52, and 53) of the longitudinal–transverse (LT) structure functions are confirmed by the data on the azimuthal asymmetry (see below) of the cross sections for the $D(e,e'p)n$ reaction at NIKHEF (Ref. 54) and Saclay.[55]

Among the theoretical methods for including the requirements of special relativity, three approaches are noteworthy. In the description of photo- and electrodisintegration of the deuteron one of them is based on the Bethe–Salpeter (BS) formalism (Refs. 53 and 56–60) and uses for practical calculations various quasipotential versions of the BS equation (in particular, three-dimensional Blankenbecler–Sugar reduction[53,56]) and simplified BS kernels.

Another approach, the S-matrix approach, is based on the invariant functions in terms of which the elements of the t matrix can be expressed. In principle, these functions are determined by the corresponding dispersion relations,[61] but usually only a certain class of diagrams is considered. An example of the use of this method is Ref. 62, where the $(p/m)^2$ expansion is used to calculate the near-threshold amplitudes for deuteron electrodisintegration.

Finally, a very attractive approach is that of transformation from the field-theoretic description in terms of *in* and *out* vectors from the complete Fock space of hadron states and operators acting on them to the description traditional in nuclear physics. This transformation, which involves the use of the unitary Okubo transformation (Ref. 63; see also Ref. 64), leads to a three-dimensional formalism with state vectors and effective operators which have the correct transformation properties under transformations from the Poincaré group. In contrast to the BS amplitudes, these vectors retain their probabilistic interpretation, since, in the final analysis, one deals only with on-shell particles. We shall demonstrate a possible development of these ideas[65,66] (in particular, certain prescriptions for constructing off-shell γNN vertices).

This review is organized as follows. In Sec. 2 we systematize the definitions of the observables of interest relative to a particular coordinate system. We stress the consequences of the general and auxiliary symmetry properties. In Sec. 3 the Okubo method is described, first of all to help the reader (particularly one not working in this field) follow the path from the description with certain Lagrangians for interacting nucleon and meson fields to the formulation of the theory with multiparticle operators (Hamiltonians, currents, and boosts), second, to propose recipes for taking into account off-shell effects in photon absorption by a bound nucleon, and, third, to indicate effective methods of satisfying the requirements of gauge and relativistic invariance. Various aspects of the spin physics of EM interactions of few-nucleon systems are discussed in Sec. 4 for a wide range of kinematical conditions, both in the vicinity of the quasifree peak and far from it, including the results of our calculations[67] for the $(e,e'N)$ reaction with cumulative nucleons. The Conclusion

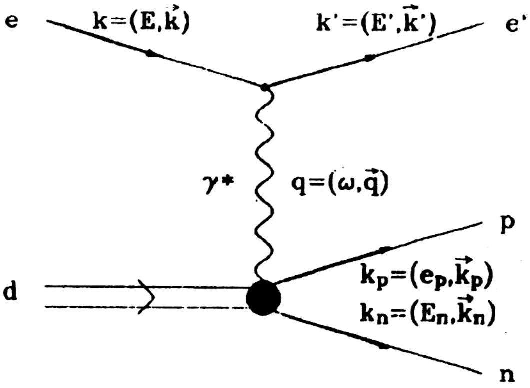

FIG. 1. One-photon exchange diagram.

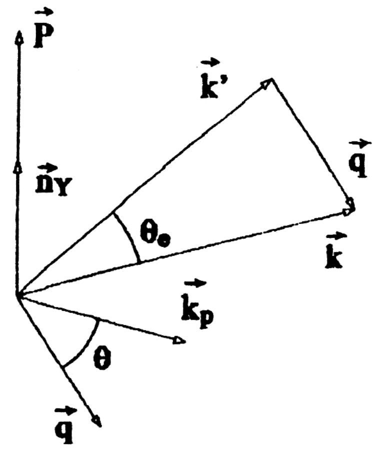

FIG. 2. Proton polarization vector in the reaction $d(e,e'\vec{p})n$ for coplanar geometry.

(Sec. 5) is followed by appendices containing useful kinematical relations.

There is no discussion of spin phenomena in deuteron photodisintegration in this review, because it has already been covered in a separate study[30] with an atlas of polarization observables[68] below the pion production threshold.

2. BASIC DEFINITIONS AND RELATIONS

Although in the following discussion we shall use as examples electron exclusive and inclusive scattering on the deuteron and the ^{3}He nucleus and also two-particle breakup of ^{3}He by linearly polarized photons, many of the results will remain valid for other reactions (for example, for $A(e,e'X)B$ in which the scattered electron is detected in coincidence with the fragment X, which can be a set of nucleons, mesons, etc.

2.1. Proton angular distributions and polarization in the reaction $d(e,e'p)n$

In the one-photon exchange approximation (Fig. 1) the cross section for the reaction $d(e,e'p)n$ with unpolarized particles in the lab frame can be written as

$$\sigma_0 \equiv \frac{d^3\sigma}{dE'd\Omega_e d\Omega_p} = \frac{4\alpha^2 E'^2 l^{\mu\nu} W_{\mu\nu} R}{(q_\lambda^2)^2}, \tag{2.1}$$

$$W_{\mu\nu} = \tfrac{1}{3}\,\mathrm{Tr}[F_\mu(\vec{p}_0,\vec{q})F_\nu^+(\vec{p}_0,\vec{q})], \tag{2.2}$$

where $l_{\mu\nu} = (k'_\mu k_\nu + k'_\nu k_\mu - g_{\mu\nu} k'k)/2E'E$ is the lepton tensor, $k=(E,\vec{k})$ and $k'=(E',\vec{k}')$ are the 4-momenta of the incident and scattered electrons, $\vec{q}=\vec{k}-\vec{k}'$ is the 3-momentum transfer, and α is the fine-structure constant.

The kinematical factor R is

$$R = k_p E_p\left[1 - E_p\left(\frac{q}{k_p}\cos\vec{q}\vec{k}_p - 1\right)/E_n\right]^{-1}.$$

The energies and momenta involved here are shown in Fig. 1.

The quantity $F_\mu(\vec{p}_0,\vec{q})$ is the matrix element

$$F_\mu(\vec{p}_0,\vec{q}) = \langle\Psi^{(-)}_{\vec{p}_0 S M_s}|J_\mu(\vec{q})|\Psi_{1M_d}\rangle \tag{2.3}$$

of the operator $J_\mu=(J_0\vec{\mathbf{J}})$ of the deuteron EM current between the initial state $|\Psi_{1M_d}\rangle$ and the final state $|\Psi^{(-)}_{\mathbf{p}_0 S M_s}\rangle = (1/\sqrt{2})\,\Sigma_T|\Psi^{(-)}_{\mathbf{p}_0 S M_s T_O}\rangle$ of the np pair with spin S (and projection M_S), isospin T, and momentum of the relative motion $\vec{p}_0$.

Let us consider the case of coplanar geometry[1)] and introduce the orthonormal basis

$$\vec{n}_z=\vec{q}/q, \quad \vec{n}_y=\frac{\vec{k}\times\vec{k}'}{|\vec{k}\times\vec{k}'|}, \quad \vec{n}_X=\vec{n}_Y\times\vec{n}_Z,$$

assuming that $\vec{n}_X$ and $\vec{n}_Z$ form the scattering plane (Fig. 2). According to Ref. 69, we have

$$\frac{4\alpha^2 E'^2 l^{\mu\nu}W_{\mu\nu}}{(q_\lambda^2)^2} = \sigma_M\left\{\xi^2 W_C + \left(\frac{1}{2}\,\xi+\eta\right)W_T + (\xi+\eta)W_S + \xi\sqrt{\xi+\eta}\,W_I\right\},$$

$$\xi = q_\mu^2/\vec{q}^2, \quad \eta = \tan^2\frac{\theta_e}{2}, \tag{2.4}$$

where σ_M is the Mott cross section, θ_e is the electron scattering angle, $q_\mu^2=\vec{q}^2-\omega^2\geqslant 0$, and $\omega=E-E'$ is the energy transfer. The W_i, with $i=C,T,S,I$, represent bilinear combinations of the amplitudes (2.3): the Coulomb function $W_C=W_{00}$ is determined by the longitudinal component of the current, $W_T=2W_{YY}$ and $W_S=W_{XX}-W_{YY}$ depend only on its transverse components, while $W_I=-W_{X0}-W_{0X}$ is the interference term and therefore is often called R_{LT} (see, for example, Ref. 3).

It is important to stress the fact that in deriving (2.4) we have used the condition of gauge independence,

$$q_\mu F^\mu(\vec{p}_0,\vec{q}) = 0, \tag{2.5}$$

in order to eliminate the matrix elements of the longitudinal component of the current.

In the coplanar kinematics the proton polarization vector

$$\vec{P} = \mathrm{Tr}\{\vec{\sigma}(1)FF^+\}/\mathrm{Tr}FF^+ \tag{2.6}$$

in the reaction $d(e,e'\vec{p})n$ with unpolarized electrons and deuteron is perpendicular to the reaction plane (Fig. 2):

$$\vec{P}=P\vec{n}_Y. \tag{2.7}$$

Again using the condition (2.5), it can be shown that

$$\sigma_0 P=4\alpha^2 E'^2 l^{\mu\nu}\Sigma_Y^{\mu\nu}R/(q_\mu^2)^2=\sigma_M\{\xi^2\Sigma_C+(\xi+\eta)\Sigma_T$$
$$+(\xi+\eta)\Sigma_S+\xi\sqrt{\xi+\eta}\Sigma_I,\} \tag{2.8}$$

where the polarization structure functions Σ_i $(i=C,T,S,I)$ are related to the components of the hadron spin tensor as

$$\Sigma_{\mu\nu}=\tfrac{1}{3}\,\mathrm{Tr}\{\vec{\sigma}(1)F_\mu(\vec{p}_0,\vec{q})F_v^+(\vec{p}_0,\vec{q})\} \tag{2.9}$$

by the same relations as those between W_i and $W_{\mu\nu}$. Obviously, the new structure functions contain the contributions of spin-flip transitions and therefore differ from the structure functions W_i.

Furthermore, in the theory without P and T violation, when

$$U_P(U_T)J_\mu(\vec{q})(U_T^{-1})U_P^{-1}=-g_{\mu\mu}J_\mu(-\vec{q}), \tag{2.10}$$

it can be shown that the proton polarization vanishes when the FSI is switched off. In other words, for a current with the properties (2.10), where U_P (U_T) is a transformation in the space of hadron states corresponding to spatial (temporal) inversion of the coordinates, the vector $\vec{P}$ vanishes when the distorted wave $|\Psi^{(-)}_{p_0SM_s}\rangle$ is replaced by a plane wave $|\vec{p}_0SM_S\rangle$.

Therefore, a nonzero value of P, which could be measured, would first of all give information about the properties of the np interaction (more precisely, about half-off-energy-shell effects). In fact, our research has shown that FSI effects in S, P, D and higher partial-wave states significantly affect the value of P (the details can be found in Refs. 7, 12, and 15; see also Sec. 4 below).

2.2. The reaction $d(\vec{e},e'\vec{p})n$ with polarized electrons. Polarization transfer

The polarization vector of the protons in the reaction $d(\vec{e},e'\vec{p})n$,

$$\vec{P}_e=\mathrm{Tr}\{\vec{\sigma}(1)F\rho_e F^+\}/\mathrm{Tr}\,F\rho_e F^+ \tag{2.11}$$

depends on the density matrix ρ_e of the incident electrons. In the coplanar kinematics in the breakup of unpolarized deuterons by longitudinally polarized electrons this vector acquires a component related to the beam helicity λ:

$$\vec{P}_\lambda=\vec{P}+\lambda\vec{P}', \tag{2.12}$$

where $\vec{P}$ is the proton polarization vector in the reaction $d(e,e'\vec{p})n$.

As already noted, the vector $\vec{P}$ is perpendicular to the reaction plane, while the polarization transfer $\vec{P}'$ lies in this plane. According to Ref. 18, we have

$$\sigma_0 P'_{X,Z}=\sigma_M\sqrt{\eta}\left\{\xi\Sigma_I'^{X,Z}+\sqrt{\eta+\xi}\Sigma_T'^{X,Z}\right\}R, \tag{2.13}$$

$$\sigma_0 P_Y=\sigma_M R\{\xi^2\Sigma_C+(\tfrac{1}{2}\,\xi+\eta)\Sigma_T+(\xi+\eta)\Sigma_S$$
$$+\xi\sqrt{\xi+\eta}\Sigma_I\,)\}, \tag{2.14}$$

$$P'_Y=0,\quad P_{X,Z}=0, \tag{2.15}$$

where, by definition,

$$\Sigma_I'=i[\Sigma_{0Y}-\Sigma_{Y0}], \tag{2.16}$$

$$\Sigma_T'=i[\Sigma_{YX}-\Sigma_{XY}], \tag{2.17}$$

or

$$\Sigma_I'=-\tfrac{2}{3}\,\mathrm{Im}\,\mathrm{Tr}\{\vec{\sigma}F_0(\vec{p}_0,\vec{q})F_Y^+(\vec{p}_0,\vec{q})\}, \tag{2.18}$$

$$\Sigma_T'=-\tfrac{2}{3}\,\mathrm{Im}\,\mathrm{Tr}\{\vec{\sigma}F_X(\vec{p}_0,\vec{q})F_Y^+(\vec{p}_0,\vec{q})\}. \tag{2.19}$$

Therefore, this observable depends on combinations of reaction amplitudes which are not encountered in the so-called induced polarization $\vec{P}$. In contrast to the latter, the polarization transfer $\vec{P}'$ does not, in general, vanish if the FSI is switched off. This fact can be used to obtain additional information about the EM properties of the bound nucleon (for example, the neutron) in situations where FSI effects are negligible [cf. the motivations for the experiment of Ref. 4[2)] for extracting the neutron electric form factor from the reaction $D(\vec{e},e'\vec{n})p$].

2.3. Electrodisintegration of polarized deuterons (exclusive and inclusive scattering). The target and beam asymmetries

Let us now consider the reaction $\vec{d}(e,e'p)n$ with a polarized target. The corresponding hadron tensor

$$W_{\mu\nu}=F_{SM_s\mu M_d'}\rho_{M_d'M_d}F^*_{SM_s\nu M_d}, \tag{2.20}$$

where we have explicitly indicated the spin dependence of the amplitudes

$$F_{SM_s\nu M_d}=\langle\Psi^{(-)}_{p_0SM_s}|J_\mu(\vec{q})|\Psi_{1M_d}\rangle,$$

contains the density matrix of the target, which can be expressed in terms of the so-called orientation parameters P_{JM} characterizing the degree of vector $(J=1)$ and tensor $(J=2)$ polarizations of the deuterons (Ref. 13; see also Ref. 19):

$$\rho_{M_d'M_d}=\sum_{JM}C^{JM}_{M_d'M_d}P^*_{JM},$$

$$C^{JM}_{M_d'M_d}=(-1)^{M_d'+1}(1M_d1-M_d'|JM)/\sqrt{3},\quad P_{00}=1,$$

$$P^*_{JM}=(-1)^M P_{J-M}. \tag{2.21}$$

Usually, polarized deuterons are obtained by populating atomic levels with various projections M_d along the direction of an external magnetic field $\vec{H}$ (along the Z axis). Here the matrix ρ is diagonal in the basis formed by the vectors $|\Psi_{1M_d}\rangle$,

$$\rho_{M_d'M_d}=n_{M_d}\delta_{M_d'M_d}, \tag{2.22}$$

where n_{M_d} is the population of a level with given projection on the quantization axis, with

$$n_{+1}+n_{-1}+n_0=1.$$

Then only two parameters in (2.21) are independent:

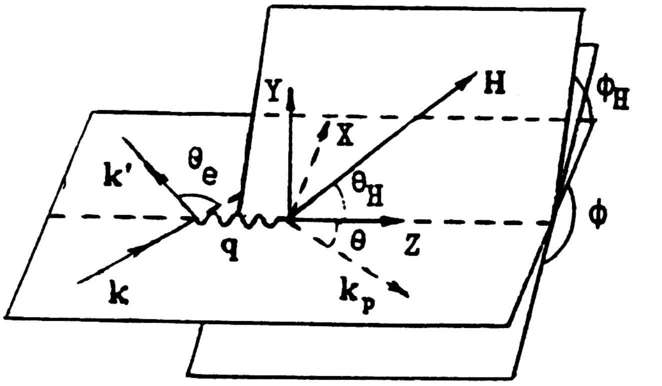

FIG. 3. Relative positions of vectors in the reaction $\vec{d}(e,e'p)n$ for out-of-plane geometry with direction of the polarizing magnetic field $\vec{H}$.

$$P_1=P_{10}=\sqrt{\frac{3}{2}}(n_1-n_{-1}),\quad P_2\equiv P_{20}=\frac{1}{\sqrt{2}}(1-3n_0).$$

If $\vec{H}$ has arbitrary orientation with angles θ_H and ϕ_H, then

$$P_{JM}=P_J e^{iM\phi_H}d^J_{M0}(\theta_H), \tag{2.23}$$

where $d^J_{M0}(\theta)$ is the Wigner function.

The general case of noncoplanar kinematics is shown in Fig. 3, where the electron scattering density coincides with the XZ plane. The angle between this plane and the reaction plane formed by the vectors $\vec{q}$ and $\vec{k}_p$ is denoted by ϕ.

Substituting (2.21) and (2.23) into (2.20) after isolating the dependence of $F_{SM_S\mu M_d}$ on the azimuthal angle ϕ, we obtain

$$W_{\mu\nu}=\sum_{JM} e^{iM(\phi-\phi_H)}P_J w^{JM}_{\mu\nu}d^J_{M0}(\theta_H), \tag{2.24}$$

$$w^{JM}_{\mu\nu}=C^{JM}_{M'_dM_d}f^*_{SM_S\mu M'_d}f_{SM_S\nu M_d}, \tag{2.25}$$

where $f_{SM_S\mu M_d}$ denotes the reaction amplitudes for coplanar geometry with $\phi=0$ (the vector $\vec{k}_p$ lies to the left of $\vec{q}$ if the xz plane is viewed from above; Fig. 4.)

Using the symmetry property of these amplitudes, it can be shown that the differential cross section of the reaction $\vec{d}(e,e'p)n$ is

$$\sigma(\vec{H})=d^3\sigma/dE'd\Omega_e d\Omega_p=K\sum_J \sigma^{(J)},$$

$$K=R\sigma_M, \tag{2.26}$$

where the terms $\sigma^{(J)}$ determine the contributions to this cross section arising from the disintegration of unpolarized ($J=0$) vector ($J=1$), and tensor ($J=2$) deuterons:[19]

$$\sigma^{(0)}=S^{00}, \tag{2.27}$$

$$\sigma^{(1)}=P_1\sum_{M\geq 0}\{S^{1M}\sin[M(\phi-\phi_H)]+\bar{S}^{1M}\cos[M(\phi-\phi_H)]\}d^1_{M0}(\theta_H), \tag{2.28}$$

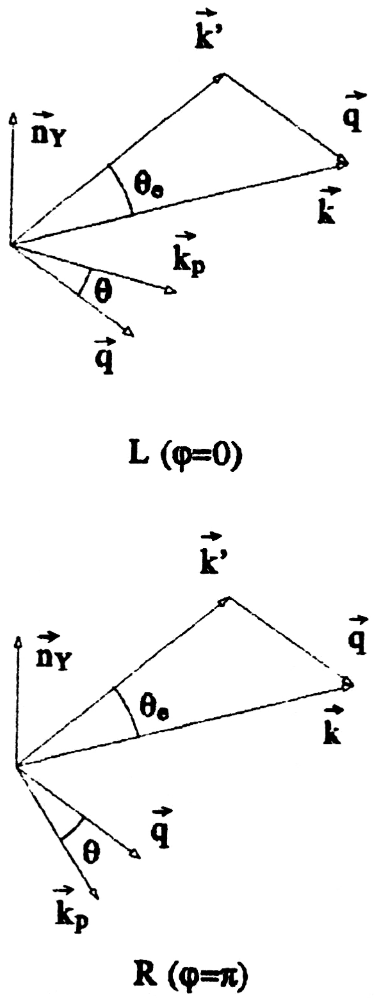

FIG. 4. Left-hand (L) and right-hand (R) cases for $d(e,e'p)n$.

$$\sigma^{(2)}=P_2\sum_{M\geq 0}\{S^{2M}\cos[M(\phi-\phi_H)]+\bar{S}^{2M}\sin[M(\phi-\phi_H)]\}d^2_{M0}(\theta_H). \tag{2.29}$$

The quantities S^{JM} and $\bar{S}^{JM}$ are expressed in terms of the structure functions W^{JM}_i ($i=L,LT,T,TT$) and $\bar{W}^{JM}_i$ ($i=LT,TT$) as

$$S^{JM}=\xi^2W^{JM}_L+\left(\frac{1}{2}\xi+\eta\right)W^{JM}_T+\frac{1}{2}\xi W^{JM}_{TT}\cos 2\phi+\xi\sqrt{\xi+\eta}W^{JM}_{LT}\cos\phi, \tag{2.30}$$

$$\bar{S}^{JM}=\tfrac{1}{2}\xi\bar{W}^{JM}_{TT}\sin 2\phi+\xi\sqrt{\xi+\eta}\bar{W}^{JM}_{LT}\sin\phi, \tag{2.31}$$

where we have introduced the following notation:

$$W^{JM}_T=W^{JM}_{XX}+W^{JM}_{YY},\quad W^{JM}_{TT}=W^{JM}_{XX}-W^{JM}_{YY},$$
$$\bar{W}^{JM}_{TT}=\bar{W}^{JM}_{XY},\quad W^{JM}_L=W^{JM}_{00},\quad W^{JM}_{LT}=-2W^{JM}_{X0},$$
$$\bar{W}^{JM}_{LT}=-\bar{W}^{JM}_{Y0}.$$

In other words, the structure functions W_{LT} ($\bar{W}_{LT}$) are determined by the interference of the longitudinal and transverse components of the current.

In turn, we have

$$W^{JM}_{\mu\nu}=b_{JM}\mathrm{Re}(i^J w^{JM}_{\mu\nu}), \qquad (2.32)$$

$$\bar{W}^{JM}_{\mu\nu}=b_{JM}\mathrm{Im}(i^J w^{JM}_{\mu\nu}), \qquad (2.33)$$

where

$$b_{JM}=(1-2\delta_{J2})[2-\delta_{M0}(1+\delta_{J1})],$$

$$\bar{b}_{JM}=-2[2-\delta_{M0}(1+\delta_{J2})].$$

For the reaction $\vec{d}(\vec{e},e'p)n$ with polarized beam and target, as for (2.12) we can write

$$\sigma_\lambda(\vec{H})\equiv d^3\sigma/dE'd\Omega_e d\Omega_p=K\sum_J (\sigma^{(J)}+\lambda\sigma'^{(J)}). \qquad (2.34)$$

Here we have the quantities:

$$S'^{JM}=\xi\sqrt{\eta}W'^{JM}_{LT}\sin\phi, \qquad (2.35)$$

$$\bar{S}'^{JM}=\xi\sqrt{\eta}\bar{W}'^{JM}_{LT}\cos\phi+\sqrt{\eta(\xi+\eta)}\bar{W}'^{JM}_{TT}, \qquad (2.36)$$

in terms of which the contributions $\sigma'^{(J)}$ $(J=0,1,2)$ are expressed, using (2.27)–(2.29), after replacing S^{JM} by S'^{JM} and $\bar{S}^{JM}$ by $\bar{S}'^{JM}$. The new structure functions W'_{LT} and $\bar{W}'_i$ $(i=LT,TT)$ are defined as follows:

$$W'^{JM}_{LT}=-2W'^{JM}_{X0}, \quad \bar{W}'^{JM}_{LT}=-\bar{W}'^{JM}_{Y0},$$

$$\bar{W}'^{JM}_{TT}=\bar{W}'^{JM}_{YX}.$$

The components $W'^{JM}_{\mu\nu}$ are obtained from $W^{JM}_{\mu\nu}$ by computing in (2.32) the imaginary part instead of the real part and in (2.33) the real part instead of the imaginary part.

Here we note that the structure functions contributing to $\sigma'^{(0)}$, $\sigma^{(1)}$, and $\sigma'^{(2)}$ vanish when the FSI is switched off. The structure functions Σ_i determining the proton polarization in the reaction $d(e,e'\vec{p})n$ with unpolarized deuterons possess the same property. This is a reflection of a general relation between this observable and the asymmetry for a vectorially polarized deuterium target.

In contrast, the contributions $\sigma'^{(1)}$ and $\sigma^{(2)}$ are, in general, not zero even when FSI effects are excluded, so that the polarization properties of the target and beam are transmitted to the observables which depend on the corresponding structure functions W'^{1M}_i, $\bar{W}'^{1M}_i$, W^{2M}_i, and $\bar{W}^{2M}_i$.

Let us define the beam asymmetry A'_e, the target asymmetry $A_{v,t}$, and the mixed asymmetry $A'_{v,t}$, respectively, for vector and tensor deuterons:

$$A'_e=\sigma'^{(0)}/\sigma^{(0)}, \quad A_{v,t}=\sigma^{(1,2)}/P_{1,2}\sigma^{(0)},$$

$$A'_{v,t}=\sigma'^{(1/2)}/P_{1,2}\sigma^{(0)}.$$

In this notation

$$\sigma_\lambda(\vec{H})=\sigma_0[1+P_1A_v+P_2A_t+\lambda(A'_e+P_1A'_v+P_2A'_t)]. \qquad (2.37)$$

Using the transformation properties

$$\sigma^{(J)}(-\vec{H})=(-1)^J\sigma^{(J)}(\vec{H}),$$

$$\sigma'^{(J)}(-\vec{H})=(-1)^J\sigma'^{(J)}(\vec{H}) \qquad (2.38)$$

$(J=1,2)$

under inversion of the polarizing magnetic field, we obtain

$$A_v=[\sigma(\vec{H})-\sigma(-\vec{H})]/2P_1\sigma_0, \qquad (2.39)$$

$$A_t=[\sigma(\vec{H})+\sigma(-\vec{H})-2\sigma_0]/2P_2\sigma_0, \qquad (2.40)$$

$$A'_{v(t)}\{[\sigma_\lambda(\vec{H})-\sigma_{-\lambda}(\vec{H})]-(+)[\sigma_\lambda(-\vec{H})-\sigma_{-\lambda}(-\vec{H})]\}/4\lambda P_{1(2)}\sigma_0. \qquad (2.41)$$

In this way the possibility arises of isolating the individual contributions (see Sec. 4.2 for more detail about this and other methods of isolating structure functions).

The nucleon polarization in the reaction $\vec{d}(\vec{e},e'\vec{N})N$ has recently been calculated in Ref. 47, where its dependence on the main ingredients of the theory (the FSI, MECs, and other relativistic effects) has been demonstrated.

Let us conclude this section by considering the scattering of polarized electrons on polarized deuterons with detection of only the scattered electrons. The corresponding double differential cross section can be obtained by integrating the exclusive cross section (2.37) over the solid angle $d\Omega_p$ (of course, taking into account the two branches of the dependence of the momentum of the knocked-out nucleon on the polar angle θ):

$$\begin{aligned}
d^2\sigma_\lambda/dE'd\Omega' &= \sigma_{\mathrm{inc}}[1+P_1a_v+P_2a_t+\lambda(P_1a'_v+P_2a'_t)],\\
P_1a_v &= \xi\sqrt{\xi+\eta}\,\mathrm{Im}\,P_{11}R^{11}_{LT}\sigma_M/\sigma_{\mathrm{inc}},\\
P_1a'_v &= [\sqrt{\eta(\xi+\eta)}P_{10}R'^{10}_T+\xi\sqrt{\eta}\,\mathrm{Re}\,P_{11}R'^{11}_{LT}]\sigma_M/\sigma_{\mathrm{inc}},\\
P_2a_t &= \Bigg[\left(\xi^2R^{20}_L+\left(\frac{1}{2}\xi+\eta\right)R^{20}_T\right]P_{20}+\xi\sqrt{\xi+\eta}\,\mathrm{Re}\,P_{21}R^{21}_{LT}+\frac{1}{2}\xi\,\mathrm{Re}\,P_{22}R^{22}_T\Bigg]\sigma_M/\sigma_{\mathrm{inc}},\\
P_2a'_t &= \xi\sqrt{\eta}\,\mathrm{Im}\,P_{21}R'^{21}_{LT}\sigma_M/\sigma_{\mathrm{inc}},
\end{aligned} \qquad (2.42)$$

with the inclusive cross section for unpolarized particles

$$\sigma_{\mathrm{inc}}=\sigma_M\left[\xi^2R_L+\left(\frac{1}{2}\xi+\eta\right)R_T\right], \qquad (2.43)$$

where we have introduced the response functions R_L, R_T, R^{JM}_i, and R^{IJM}_i. The various methods of isolating these functions are discussed in Ref. 16.

2.4. Inelastic scattering of longitudinally polarized electrons on polarized ^{3}He nuclei

In the case of interest to us, that of the two-particle breakup of the ^{3}He nucleus by longitudinally polarized electrons, the cross section in the lab frame can be written as

$$\sigma\equiv d^3\sigma/dE'd\Omega'd\Omega_p=\sigma_0[1+\vec{S}\vec{A}^0+\lambda(A^e+\vec{S}\vec{A}')], \qquad (2.44)$$

where $\vec{S}$ is a vector characterizing the ^{3}He spin orientation, $\vec{A}^0$ is the target asymmetry when the beam is unpolarized, $\vec{A}'$ (A^e) is the beam asymmetry in the reaction $^3\text{He}(\vec{e},e'p)d$ [$^3\text{He}(\vec{e},e'p)d$] with a polarized (unpolarized) target.

The cross section σ_0 for the $^3\text{He}(e,e'p)d$ reaction entering into this is expressed in terms of the corresponding structure functions W_i $(i=C,T,S,I)$ by using (2.4). In contrast to (2.1), the factor R is now equal to

$$R=k_pE_p\left[1-E_p\left(\frac{Q}{k_p}\cos\widehat{QK}_p-1\right)/E_d\right]^{-1},$$

where $E_d=[(\vec{Q}-\vec{k}_p)^2+m_d^2]^{1/2}$ is the deuteron recoil energy. Here and below in the expressions pertaining to ^{3}He breakup the momentum transferred to the hadron system is denoted by $\vec{Q}=\vec{k}-\vec{k}'$ in order to avoid confusion with the notation for the Jacobi momenta $\vec{p}$ and $\vec{q}$ in the theory of few-nucleon systems.

In this case the reaction amplitude

$$F_\mu(\vec{P}_0,\vec{Q})=\langle\Psi_{\vec{P}_0}^{(-)}|J_\mu(\vec{Q})|\Psi\rangle \tag{2.45}$$

is the matrix element of the current operator $J_\mu(\vec{Q})$ of the ^{3}He nucleus between the initial state $|\Psi\rangle$ and the final state $|\Psi_{\vec{P}_0}^{(-)}\rangle$ of the ^{3}He and pd systems, respectively, with relative momentum $\vec{P}_0$.

For coplanar geometry, when the vectors $\vec{k}_p$ and $\vec{k}_d=\vec{Q}-\vec{k}_p$ lie in the XZ plane (see Fig. 2), only the components A_Y^0, A_X', and A_Z' are nonzero. Again using the gauge-independence condition for (2.45), it can be shown [cf. (2.13)] that

$$\sigma_0A'_{X,Z}=\sigma_M\sqrt{\eta}\left\{\xi\Sigma_I'^{X,Z}\cos\phi+\sqrt{\eta+\xi}\Sigma_T'^{X,Z}\right\}R \tag{2.46}$$

with $\phi=0,\pi$. The structure functions $\Sigma_{I,T}'^{X,Z}$ are related to the tensor

$$\Sigma_{\mu\nu}=\tfrac{1}{2}\,\text{Tr}\{\vec{\sigma}F_\mu(\vec{P}_0,\vec{Q})F_\nu^+(\vec{P}_0,\vec{Q})\} \tag{2.47}$$

in the same way as the structure functions in Eq. (2.13) for the polarization transfer in the reaction $d(\vec{e},e'\vec{p})n$ with the tensor (2.2). We shall therefore retain the earlier notation for the other structure functions.

Extending the parallels between the spin observables for the reactions $d(\vec{e},e'\vec{p})n$ and $^3\text{He}(\vec{e},e'p)d$, we should note that if the FSI in the pd system is neglected, then independently of the relative location of the scattering and reaction planes $\vec{A}^0=A^e=0$.

Of course, this similarity, since it is a consequence of certain symmetry properties of the amplitudes in question, holds for the inclusive channel with complete breakup of the ^{3}He nucleus. In this respect the reactions $d(\vec{e},e'\vec{n})p$ and $^3\text{He}(\vec{e},e'n)pp$, in which the scattered electron is detected in coincidence with the knocked-out neutron, are partners. The first measurement of the asymmetries $A'_{X,Z}$ in the reaction $^3\text{He}(\vec{e},e'n)pp$ was made recently at the microtron in Mainz.[70] The results of this and other experiments performed to extract the neutron electric form factor are discussed in Sec. 4.

In connection with this, following Refs. 71–73, we introduce the asymmetry

$$A=\frac{\sigma(+)-\sigma(-)}{\sigma(+)+\sigma(-)}=\frac{\Delta(\theta_H,\phi_H)}{\Sigma} \tag{2.48}$$

for the cross section of the inclusive $^3\text{He}(\vec{e},e')X$ reaction,

$$\sigma(\lambda)\equiv\frac{d^2\sigma}{dE'd\Omega'}=\Sigma+\lambda\Delta(\theta_H,\phi_H), \tag{2.49}$$

which contains contributions dependent on and independent of the beam helicity:

$$\Delta=-\sigma_M[v_{T'}R_{T'}(Q^2,\omega)\cos\theta_H$$
$$+v_{TL'}R_{TL'}(Q^2,\omega)\sin\theta_H\cos\phi_H], \tag{2.50}$$

$$\Sigma=\sigma_M[v_LR_L(Q^2,\omega)+v_TR_T(Q^2,\omega)],$$

$$v_L=\xi^2,\quad v_T=\tfrac{1}{2}\xi+\eta,\quad v_{T'}=\sqrt{\eta(\xi+\eta)}, \tag{2.51}$$

$$v_{TL'}=-\xi\sqrt{\eta}/\sqrt{2}.$$

The definitions of the response functions $R_i(Q^2,\omega)$ with $Q^2=-q_\mu^2<0$ can be found in Ref. 3.

2.5. Two-particle breakup of the ^{3}He nucleus by linearly polarized photons

The amplitude of the reaction

$$\vec{\gamma}+{}^3\text{He}\rightarrow p+d \tag{2.52}$$

for absorption of a photon with polarization vector $\vec{\varepsilon}_\lambda$ and momentum $\vec{k}_\gamma$ in the Coulomb gauge has the form

$$T_\lambda=-e(2\pi/E\gamma)^{1/2}\vec{\varepsilon}_\lambda\langle\Psi_{pd}^{(-)}|\vec{J}(\vec{k}_\gamma)|\Psi\rangle, \tag{2.53}$$

where all the necessary discrete indices are understood.

The corresponding differential cross section

$$\frac{d\sigma_\lambda}{d\Omega_p}=\frac{d\sigma}{d\Omega_p}[1+P\Sigma(\theta_p)\cos2\phi_\lambda], \tag{2.54}$$

where P is the degree of polarization of the photon beam, $d\sigma/d\Omega_p$ is the cross section for unpolarized photons, $\Sigma(\theta_p)$ is the asymmetry coefficient, and $\theta_p(\phi_\lambda)$ is the proton emission angle [the angle between the vector $\vec{\varepsilon}_\lambda$ ($\vec{\varepsilon}_\lambda\vec{k}_\gamma=0$) and the reaction plane, formed by the vector $\vec{k}_\gamma$ and the emitted-proton momentum $\vec{k}_p$].

The coefficient Σ is defined as

$$\Sigma(\theta_p)=(d\sigma_\parallel-d\sigma_\perp)/(d\sigma_\parallel+d\sigma_\perp), \tag{2.55}$$

where $d\sigma_\parallel\equiv d\sigma_\parallel/d\Omega_p(d\sigma_\perp\equiv d\sigma_\perp/d\Omega_p)$ is the proton angular distribution for $\phi_\lambda=0$ $(\pi/2)$ for a completely polarized photon beam.

Our calculations (Refs. 9, 10, 31, 51, and 74–76) of the cross sections $d\sigma_\parallel$ and $d\sigma_\perp$ were to a considerable degree stimulated by the first measurements[77,78] using a quasimonochromatic photon beam at the Khar'kov Physico–Technical Institute. The purpose of these studies was to investigate the mechanisms of two-particle breakup of the ^{3}He nucleus by photons with energies in the range from the giant resonance ($E_\gamma\sim10$ MeV) to the Δ-isobar production region ($E_\gamma\approx300$ MeV). The relative roles of direct proton knockout and of the recoil mechanism, and the competition between one-body photoabsorption and the mechanisms arising from two-body meson-exchange currents were studied in connection with this (see Sec. 4).

We have given special attention to nuclear-structure effects (in particular, because the results of earlier[79,80] calculations of the cross sections for the reaction $^3\mathrm{He}(\gamma,p)d$ with unpolarized photons performed using Faddeev wave functions of the ^{3}He nucleus for the Reid soft-core potential[81] differed noticeably from each other). A two-body interaction of this type (cf., for example, the Paris potential; Ref. 82) is often used (see Ref. 83 and references therein) in the nonrelativistic eigenvalue problem for the nuclear Hamiltonian:

$$H=K+V,$$
$$K=\sum_{\alpha=1}^{3}\vec{p}_\alpha^{\,2}/2m,\quad V=\sum_{\alpha<\beta=1}^{3}V(\alpha,\beta), \tag{2.56}$$

where $\vec{p}_\alpha$ is the momentum operator of the nucleon numbered α, $V(\alpha,\beta)$ is the NN-interaction operator, and m is the nucleon mass. In this approach the wave functions $\Psi_{pd}^{(-)}$ and Ψ are eigenfunctions of H. Owing to the enormous computational difficulties in Refs. 79 and 80 and in our studies, the FSI in the pd system was not included, i.e., the function was chosen to be a symmetrized product of two plane waves.

Of course, in comparing the theory with experiment this FSI cannot *a priori* be neglected, although the question of its inclusion may not be so acute in the calculation of the coefficient Σ, which is determined by the cross-section ratio (2.55). An important step forward in solving this complicated problem for the continuous spectrum is the results of rigorous numerical calculations in momentum space obtained in Ref. 84 using relativistic NN forces (in particular, in the description of electron-induced two-particle breakup of the ^{3}He nucleus.[85] As was emphasized in Ref. 85, since the series[3)] of multiple scattering theory for the final state $\langle\Psi_{pd}^{(-)}|$ diverges, a cutoff of this series is not really justified. In connection with this, the results of Ref. 86 do not inspire trust (see the discussion in Ref. 87). In this context it is advisable to consider replacing, in the diagrammatic approach,[88] the transition matrix for the pd channel, which accumulates all the rescatterings in the $3N$ system, leading to proton and deuteron emission in the final state, by the on-shell elastic pd-scattering amplitude with some off-shell extensions. Uncontrollable factors with parameters for fitting to the experimental data are thereby introduced into the theory.

In addition to the FSI problem, another important problem is the study of three-body photoabsorption mechanisms in the reaction $^3\mathrm{He}(\gamma,p)d$. Strictly speaking, the corresponding contributions to the electromagnetic current of the nucleus must be consistent in the sense of the continuity equation for this current with $3N$ forces, which should be added to the Hamiltonian (2.56) (cf. Ref. 89). As is well known, the determination of these forces suffers from uncertainties even greater than the introduction of $2N$ forces (see Refs. 90 and 91, for example).

The formalism described above suggests a possible way of obtaining the various n-body contributions to the nuclear forces and electromagnetic current of the nucleus.

3. THE FORMALISM

The common belief that electromagnetic probes are the simplest instruments for studying nuclear structure can lead to errors. In fact, theories of electromagnetic interactions with nuclei possess many of the difficulties of strong-interaction theory.[92] A fixed ingredient of current studies in this area is the inclusion of meson-exchange currents or interaction currents. This is a reflection of Yukawa's idea that nuclear forces arise from meson exchange. Electromagnetic probes must affect exchanges of charged mesons at inter-nucleon separations of less than about the Comption wavelength of the pion (the lightest meson). The principle of gauge invariance, one consequence of which is the electromagnetic-current conservation law for a system of charged particles (a nucleus), is an important regulator in determining the relations between meson exchange in the NN interaction and MECs.

There is an extensive literature on the status of MECs in nuclear physics (see the reviews of Refs. 93 and 94 plus the reports of Refs. 7, 95, and 96). These currents are usually introduced either within the S-matrix approach (see the reviews of Chemtob and Riska in Ref. 93) or by the Okubo method.[65] There are other methods of constructing two-particle and more complicated currents consistent with the NN interaction (cf. Refs. 97 and 98, and our study in Ref. 99, where the Sachs approach[100] in the phenomenological theory of interaction currents in nuclei is developed). We should also mention our studies of Refs. 101 and 102, in which the ideas of Okubo are extended to the case of single pion photo- and electroproduction on nuclei.

3.1. The unitary-transformation method. Effective operators

As an illustration of this method, let us consider the absorption of a photon (real or virtual) by a hadron system consisting of interacting mesons and nucleons. The corresponding amplitude for the transition of the system from state i to state f can be written as

$$T_{\mathrm{if}}=\langle f|H_{\gamma MN}|i\rangle, \tag{3.1}$$
$$H_{\gamma MN}=\langle 0\gamma|\mathcal{H}_{\gamma MN}|1\gamma\rangle,$$

where $\mathcal{H}_{\gamma MN}$ is the operator for the interaction of the electromagnetic field with the nucleon and meson fields. The vectors $|i\rangle$ and $|f\rangle$, being eigenvectors of the Hamiltonian $\mathcal{H}_S$,

$$\mathcal{H}_S=\mathcal{H}_N+\mathcal{H}_M+\mathcal{H}_{MN}, \tag{3.2}$$

where $\mathcal{H}_N$, $\mathcal{H}_M$ and $\mathcal{H}_{MN}$ are the Hamiltonians of the nucleon and meson fields and their interaction, belong to the Fock space R_{MN} of states of the system.

Following Ref. 63, we write R_{MN} as a direct sum of the subspace R_0 without mesons and an addition, i.e., for any $|\Psi\rangle\in R_{MN}$ we take

$$|\Psi\rangle=P_0|\Psi\rangle+Q_0|\Psi\rangle,$$

where P_0 is the projector onto R_0, $Q_0=1-P_0$.

The vector $|\Psi\rangle$ is associated with a vector $|\chi\rangle\in R_0$ such that

$$|\Psi\rangle=\Omega_0\{P_0\Omega_0^+\Omega_0P_0\}^{-1/2}|\chi\rangle, \tag{3.3}$$

$$\Omega_0=1+A_0,$$

where the desired operator A_0 has the structure $A_0=Q_0A_0'P_0$ and satisfies the Okubo relation:

$$Q_0\{\mathscr{H}_S-[A_0,\mathscr{H}_S]-A_0\mathscr{H}_SA_0\}P_0=0. \tag{3.4}$$

This nonlinear equation gives the condition for diagonalization of $\mathscr{H}_S$ by a unitary transformation:

$$U_0=\begin{Bmatrix}(1+A_0^+A_0)^{-1/2}-A_0^+(1+A_0A_0^+)^{-1/2}\\ A_0(1+A_0^+A_0)^{-1/2}(1+A_0A_0^+)^{-1/2}\end{Bmatrix}. \tag{3.5}$$

Obviously, we have conservation of the scalar product

$$\langle\chi'/\chi\rangle=\langle\Psi'/\Psi\rangle \tag{3.6}$$

for the two pairs (Ψ,χ) and (Ψ',χ') i.e., the contraction of the space of states effected by (3.3) does not spoil the probabilistic interpretation characteristic of the field-theoretic description in the larger space R_{MN} This feature of the Okubo approach is one of its advantages over the projection method (see the review by Chemtob in Ref. 93).

Using such an algebraic procedure, each operator O in R_{MN} is associated with an effective operator O^{eff} in R_0:

$$O^{\text{eff}}=\Gamma_0^+O\Gamma_0, \tag{3.7}$$

$$\Gamma_0=\Omega_0\{P_0\Omega_0^+\Omega_0P_0\}^{-1/2}. \tag{3.8}$$

This operator is Hermitian ($O^{\text{eff}+}=O^{\text{eff}}$) as long as O is.

Furthermore, if $|\psi\rangle$ is a solution of the eigenvalue problem in R_{MN} i.e., for example, $\mathscr{H}_S|\Psi\rangle=E|\Psi\rangle$, then for the corresponding vector $|\chi\rangle$ we have

$$H^{\text{eff}}|\chi\rangle=E|\chi\rangle \tag{3.9}$$

with the effective Hamiltonian

$$H^{\text{eff}}=\Gamma_0^+\mathscr{H}_S\Gamma_0, \tag{3.10}$$

acting in R_0. Of course, R_0 contains nucleon and antinucleon components. The latter can be eliminated effectively, again using the Okubo procedure.

The Okubo approach makes it possible to determine the relation to the quantum-mechanical description traditional in nuclear physics. But most importantly, it makes it possible to avoid the empiricism of the phenomenological theory, although up to now several examples of its use for developing the three-dimensional (covariant) formalism in the theory of interacting nucleons are known (Refs. 65, 66, and 101–104). The central role here is played by the construction of effective operators (generators of the Poincaré group and currents). These operators are multiparticle operators. For example,

$$H^{\text{eff}}=H^{[1]}+H^{[2]}+\ldots, \tag{3.11}$$

where $H^{[n]}$ denotes the n-body contribution [cf. Eq. (2.56)]:

$$H^{[1]}=\sum_{\alpha=1}^{A}H_N(\alpha),\quad H^{[2]}=\sum_{\alpha<\beta}V(\alpha,\beta), \tag{3.12}$$

where $H_N(\alpha)$ is the free-nucleon Hamiltonian and $V(\alpha,\beta)$ is the NN-interaction potential. The latter can be calculated (at least, for the simplest meson-exchange mechanisms) on the basis of existing models of the meson–nucleon interaction. In this way, $3N$ forces and more complicated interactions arise naturally.

The same is true of the effective current

$$J_\mu^{\text{eff}}(\vec{x})=\Gamma_0^+J_\mu(\vec{x})\Gamma_0, \tag{3.13}$$

where $J_\mu(\vec{x})$ is the bare (Noether) current entering into the canonical expression

$$\mathscr{H}_{\gamma MN}=\int\langle0\gamma|A_\mu(\vec{x},0)|1\gamma\rangle J^\mu(\vec{x})d\vec{x}. \tag{3.14}$$

The current $J^\mu(\vec{x})\equiv J^{\mu}(\vec{x},0)$ is conserved,

$$i[J^0(\vec{x}),\mathscr{H}_S]=\text{div }\mathbf{J}(\vec{x}), \tag{3.15}$$

and consists of a nonminimal part which is conserved separately and a part which is obtained from the hadronic Lagrangian by using the recipe of minimal substitution. For example, in the PS-coupling scheme for the nucleon (Ψ) and pion ($\vec{\phi}$) fields this latter part is equal to

$$J^\mu(\vec{x})=J_N^\mu(\vec{x})+J_\pi^\mu(\vec{x}), \tag{3.16}$$

$$J_N^\mu(\vec{x})=e\bar{\Psi}(\vec{x})\gamma^\mu\pi_p\Psi(\vec{x}),$$

$$J_\pi^\mu(\vec{x})=e[\vec{\phi}(\vec{x})\times\partial^\mu\vec{\phi}(\vec{x})]_3,$$

where π_p is the projector onto the proton state.

The operators $J^{[n]}(\vec{x})$ entering into the expansion

$$J^{\text{eff}}(\vec{x})=J^{[1]}(\vec{x})+J^{[2]}(\vec{x})+\ldots, \tag{3.17}$$

can be classified according to the number of mesons participating in the exchange, the type of intermediate state for the virtual processes in the hadronic system, and other physical features. Therefore, an entire hierarchy of MECs arises (see Ref. 93).

Conservation of the current $J^{\text{eff}}(\vec{x})$ is a consequence of (3.15):

$$i[J_0^{\text{eff}}(\vec{x}),H^{\text{eff}}]=\text{div }\mathbf{J}^{\text{eff}}(\vec{x}). \tag{3.18}$$

For the photoabsorption amplitude with mesonless channels we find

$$T_{if}=\int\langle0\gamma|A^\mu(\vec{x},0)|1\gamma\rangle\langle\chi_f|J_\mu^{\text{eff}}(\vec{x})|\chi_i\rangle d\vec{x}, \tag{3.19}$$

where, by definition, $|i\rangle=\Gamma_0|\chi_i\rangle$ and $|f\rangle=\Gamma_0|\chi_f\rangle$, or, for photon states satisfying the Fermi condition,

$$T_{if}=[2(2\pi)^3E_\gamma]^{-1/2}\langle\chi_f|\varepsilon(\vec{k}_\gamma)J^{\text{eff}}(\vec{k}_\gamma)|\chi_i\rangle, \tag{3.20}$$

where $\varepsilon(\vec{k}_\gamma)$ is the polarization vector of a photon with momentum $\vec{k}_\gamma$ and energy E_γ [cf. Eq. (2.53)].

We see that the independence of the radiative transition amplitude of interest to us from the choice of gauge of the electromagnetic field, i.e., the fact that (3.20) vanishes upon the substitution $\varepsilon\to k_\gamma$, is ensured, first, when Eq. (3.18) is satisfied and, second, when the states χ_i and χ_f are eigenstates of the effective Hamiltonian H^{eff}. A more general discussion of the problems related to ensuring gauge invariance and gauge independence in the theory of electromagnetic interactions with nuclei is given in Sec. 3.3.

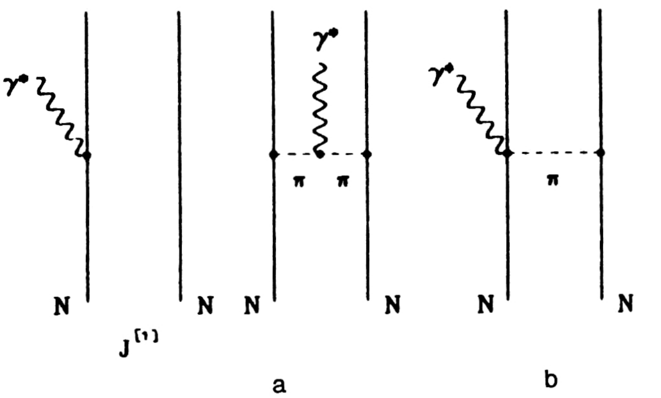

FIG. 5. Various contributions to the EM current of the nucleus.

Unfortunately, so far it has not been possible to solve Eq. (3.4) exactly, and the first requirement can be satisfied only approximately. This problem should be considered at the perturbative level, i.e., by expanding the operator A_0 in powers of the strong-interaction constant (Ref. 65).[4)] However, even after operators H^{eff} and J^{eff} consistent in the sense (3.18) are constructed, computational difficulties remain in the solution of the eigenvalue equation (3.9). The exception is the two-nucleon problem, for which an effective method of numerically solving the Lippmann–Schwinger equation with a nonlocal interaction has been developed (see, for example, Ref. 106 and references therein).

3.2. Model of the electromagnetic current of the nucleus. Off-shell effects. The simplest meson-exchange currents

We have studied the effects of MECs generated by π and ρ exchanges over several years (Refs. 7, 9, 10, 12, 15, 18, 19, 31, 38, 67, and 74–76). The current operator that we have used,

$$J_\mu(\vec{q}) \equiv \int \exp(i\vec{q}\vec{x}) J_\mu^{\text{eff}}(\vec{x}) d\vec{x} \tag{3.21}$$

consists of the one-body current $J_\mu^{[1]}(\vec{q})$ and the two-body MEC $J_\mu^{[2]}(\vec{q})$:

$$J_\mu = J_\mu^{[1]} + J_\mu^{[2]}. \tag{3.22}$$

Usually the nucleon current $J^{[1]}(\vec{x}) = \Sigma_{\alpha=1}^{A} J_\alpha(\vec{x})$ (Fig. 5), which includes Coulomb, convection, spin, and spin–orbit contributions, is obtained by applying the Foldy-Wouthuysen transformation to the Dirac equation for the nucleon in an external electromagnetic field. The resulting expressions[107,108] contain the Dirac, $F_1(q_\mu^2)$, and Pauli, $F_2(q_\mu^2)$, form factors of the nucleon. Here the fact that the nucleon absorbing the photon goes off-shell is neglected. Even though the calculations discussed below were carried out in this approximation, when the Okubo procedure is used the problem of including off-shell effects is simple to solve.

Actually, following Sec. 3.1, we find the following for the matrix element of the current-density operator $J_\mu(x)$ for $x = (\vec{x}, 0) = 0$ between *in* and *out* states of the nucleon in R_{MN}:

$$\langle p'; out | J_\mu(0) | p; in \rangle = \langle \vec{p}' | J_\mu^{[1]}(0) | \vec{p} \rangle, \tag{3.23}$$

where $|\vec{p}\rangle \equiv |\chi_{\vec{p}}\rangle$ and $|\vec{p}\rangle \equiv |\chi_{\vec{p}}\rangle \in R_0 \subset R_{MN}$ (the spin and isospin indices have been dropped). More detail about the differences between the *in* and *out* vectors and their Okubo partners can be found in Appendix A.

By definition (see, for example, Ref. 109, p. 242), for the left-hand side of (3.23) we have

$$\langle p'; out | J_\mu(0) | p; in \rangle = \bar{u}'(p') \Gamma_\mu(p', p) u(p) \tag{3.24}$$

with the γNN vertex function on the mass shell, $p'^2 = p^2 = m^2$:

$$\Gamma_\mu(p', p) = F_1[(p'-p)^2]\gamma_\mu + iF_2[(p'-p)^2] \times \sigma_{\mu\nu}(p'-p)^\nu / 2m. \tag{3.25}$$

The Dirac spinors in (3.24) can be expressed in terms of the two-component Pauli spinors φ:

$$u(p) = \left[\frac{E_{\vec{p}}+m}{2E_{\vec{p}}}\right]^{1/2} \begin{pmatrix} 1 \\ \dfrac{\vec{\sigma}\vec{p}}{E_{\vec{p}}+m} \end{pmatrix} \varphi, \tag{3.26}$$

$$E_{\vec{p}} = \sqrt{\vec{p}^2 + m^2}.$$

Combined with Eqs. (3.24)–(3.25), Eq. (3.22) gives a recipe for constructing the desired one-particle contribution in all orders in the strong-interaction constants (cf. the off-shell extrapolation of the CCI in Ref. 69). This construction is free of ambiguities, and it is logical to use it in calculations involving nuclear wave functions. It is rather constructive, since for on-shell nucleons $(p'-p)^2 = \vec{q}^2 - (E_{\vec{p}+\vec{q}} - E_{\vec{p}})^2 \geqslant 0$, i.e., we are dealing with the form factors $F_{1,2}$ in the physical (space-like) region.

In Ref. 110 we compared the results of the nonrelativistic reduction of (3.24) with those obtained in Refs. 107 and 108. The differences can be significant far from the quasifree region, when the difference $E_{\vec{p}+\vec{q}} - E_{\vec{p}}$ can noticeably differ from the value $\omega_{\max} = q_\mu^2/2m$. Since this reduction is based on the assumptions that $p/m \ll 1$ and $p'/m \ll 1$, as more and more high-momentum components of the wave function are probed and the momentum transfers increase, making the inequalities weaker, the equations of Appendix B for the coefficients in the expansion (3.24) in the complete set of matrices $\{1, \vec{\sigma}\}$ in the nucleon spin space can be useful.

We note that the conservation law

$$(p'-p)_\mu \bar{u}'(p') \Gamma^\mu(p', p) u(p) = 0 \tag{3.27}$$

is equivalent to four independent conditions for these coefficients. Upon nonrelativistic reduction, (3.27) generates a chain of equations for the components of $\langle p' | J(0) | p \rangle = (p, \mathbf{J})$:

$$\vec{q}\mathbf{J}^{(l)} = \sum_{m+n=l} (E_{\vec{p}+\vec{q}} - E_{\vec{p}})^{(m)} \rho^{(n)} \quad (l = 1, 3, \ldots), \tag{3.28}$$

where the superscripts denote the order of the contribution to the expansion in inverse powers of the nucleon mass. For example,

$$E' - E = (E'-E)^{(1)} - (E'-E)^{(3)} + \ldots,$$

$$(E'-E)^{(1)}=\vec{P}\vec{q}/2m,$$

$$(E-E')^{(3)}=-\vec{P}\vec{q}(\vec{P}^2+\vec{q}^2)/16m^3,$$

where $\vec{P}=\vec{p}'+\vec{p}=2\vec{p}+\vec{q}$. Obviously, each equation in (3.28) is satisfied separately for the parts of the current F_1 and F_2. In addition, the convection and spin–orbit parts of the current, together with the part corresponding to the Darwin–Foldy interaction, are conserved independently.

The nuclear matrix elements of the operator $J^{[1]}$ do not satisfy the condition of gauge independence, i.e., in general,

$$\omega\langle f|J_0^{[1]}(0)|i\rangle\neq\vec{q}\langle f|\mathbf{J}^{[1]}(0)|i\rangle. \tag{3.29}$$

Exceptions are discussed in Ref. 111.

Let us now consider meson-exchange currents generated by one-pion exchange:

$$J^{[2]}(\vec{q})=J_{\pi NN}(\vec{q})+J_{\pi CC}(\vec{q}),$$

where $J_{\pi CC}$ is the pion current (Fig. 5a) and $J_{\pi NN}$ is the seagull current (Fig. 5c).

After the nonrelativistic reduction we find that

$$J_0^{[2]}(\vec{q})=0, \tag{3.30}$$

$$\mathbf{J}_{\pi NN}=\sum_{\alpha<\beta}\mathbf{J}_{SG}(\alpha,\beta), \tag{3.31}$$

where in momentum space

$$\langle\vec{p}_\alpha',\vec{p}_\beta'|J_{SG}(\alpha,\beta)|\vec{p}_\alpha,\vec{p}_\beta\rangle=\delta(\vec{p}_\alpha'+\vec{p}_\beta'-\vec{p}_\alpha-\vec{p}_\beta-\vec{q})\mathbf{J}_{SG}(\vec{k}_\alpha,\vec{k}_\beta),$$

$$\mathbf{J}_{SG}(\vec{k}_\alpha,\vec{k}_\beta)=\frac{i}{2}\left(\frac{f}{\pi m_\pi}\right)^2[\vec{\tau}(\alpha)\times\vec{\tau}(\beta)]_3F_1^V(q_\mu^2)\times\left\{\frac{\vec{\sigma}(\alpha)\vec{k}_1}{\omega_\alpha^2}\vec{\sigma}(\beta)F_{\pi NN}^2(\vec{k}_\alpha^2)-\vec{\sigma}(\alpha)\frac{\vec{\sigma}(\beta)\vec{k}_2}{\omega_\beta^2}F_{\pi NN}^2(\vec{k}_\beta^2)\right\},$$

$$\omega_{\alpha,\beta}^2=\vec{k}_{\alpha,\beta}^2+m_\pi^2,\quad \vec{k}_{\alpha,\beta}=\vec{p}_{\alpha,\beta}'-\vec{p}_{\alpha,\beta}, \tag{3.32}$$

where f is the pseudovector πN coupling constant, m_π is the pion mass, $\vec{\tau}(i)$ is the Pauli isospin vector, and $F_1^V(q_\mu^2)$ is the isovector form factor of the nucleon. We also see that (3.32) contains the "strong" πNN form factor, the introduction of which makes it possible to include nucleon finite-size effects. For this form factor we used the monopole form of parametrization:

$$F_{\pi NN}(\vec{k}^2)=(\Lambda^2-m_\pi^2)/(\Lambda^2+\vec{k}^2), \tag{3.33}$$

where $\vec{k}$ is the pion momentum.

The operator $J_{\pi CC}$ satisfies the continuity equation (see Ref. 112 and references therein)

$$\vec{q}(\mathbf{J}_{\pi CC}(\mathbf{k})+\mathbf{J}_{\pi NN}(\vec{q}))=[J_0^{[1]}(\vec{q}),V_{\mathrm{OPEI}}], \tag{3.34}$$

where the interaction V_{OPEI} is obtained from the one-pion exchange potential by introducing the form factor (3.33) into the πNN vertex. As was emphasized in Ref. 112, for a certain optimal choice $\Lambda=4m_\pi$ the radial dependence of V_{OPEI} is reminiscent of the behavior of the Reid soft-core potential (especially its tensor part) at distances $r\gtrsim(4m_\pi)^{-1}$. The properties of V_{OPEI} are studied more carefully in Ref. 51. Therefore, the EM current of the nucleus used in our calculations satisfies the continuity equation with an NN interaction close to the realistic Reid soft-core potential.

3.3. The Weyl criterion. Conditions for gauge invariance of the theory. Gauge independence of the S matrix. The generalized Ward–Takahashi identity

In discussing the difficulties inherent in the theory of EM interactions of nuclei, we should particularly note two problems which have recently received a great deal of attention:

1. Ensuring the gauge invariance and gauge independence of the description of EM processes on nuclei.
2. Satisfying the requirements of special relativity.

The properties of gauge invariance for a system of charged particles (fields) interacting with an electromagnetic field can be formulated on the basis of the Weyl criterion:[113]

$$H\{A_\mu'\}=UH\{A_\mu\}U^++iU^+\frac{\partial U}{\partial t}, \tag{3.35}$$

where the functional $H\{A_\mu\}$ is the Hamiltonian of the system (nucleus) in an EM field with potential

$$A_\mu(\vec{x},t)=(A^0(\vec{x},t),\vec{A}(\vec{x},t)).$$

The condition (3.35) expresses the invariance of the Schrödinger equation

$$i\frac{\partial\Psi}{\partial t}=H\{A_\mu\}\Psi$$

under a gauge transformation

$$A_\mu'(\vec{x},t)=A_\mu(\vec{x},t)+\partial_\mu G(\vec{x},t) \tag{3.36}$$

with an arbitrary function $G(\vec{x},t)$, which, by definition, can be associated with a unitary transformation U: $\Psi'=U\Psi$.

The existence of U is demonstrated by direct construction (see Ref. 42, for example, where this is done for problems in nonrelativistic quantum mechanics and quantum field theory). Since for a system of interacting nonrelativistic nucleons, when $H\{A_\mu\}$ is obtained from the nuclear Hamiltonian by using the recipe of minimal substitution $\partial_\mu\rightarrow\partial_\mu+ieA_\mu$, the desired transformation can be defined as

$$U=e^{i\chi},\quad \chi=\int\rho(\vec{x})G(\vec{x},t)d\vec{x}, \tag{3.37}$$

where $\rho(\vec{x})$ is the charge-density operator. We split H into the unperturbed part H_0 and the interaction between the nucleus and the EM field H_I:

$$H=H_0+H_I,\quad H_I=H^{(1)}\{A_\mu\}+H^{(2)}\{A_\mu\}+\dots . \tag{3.38}$$

Here the superscript denotes the order in e. In canonical form we have

$$H^{(1)}\{A_\mu\}=\int A_\mu(\vec{x})J^\mu(\vec{x})d\vec{x},$$

where $J^\mu(\vec{x})=(\rho(\vec{x}),\mathbf{J}\ (\vec{x}))$ is the operator for the nuclear EM current density.

The expression for H_I without expanding in powers of the charge e in the case of NN forces with an arbitrary velocity dependence can be found in Ref. 99. The corresponding current[5)] is the sum of the one-body current $J^{[1]}$ and the two-body current $J^{[2]}$:

$$\mathbf{J}(\vec{x})=\mathbf{J}^{[1]}(\vec{x})+\mathbf{J}^{[2]}(\vec{x}), \tag{3.39}$$

$$\mathbf{J}^{[1]}(\vec{x})=(2m)^{-1}\sum_{\alpha=1}^{A}\{\vec{p}_\alpha\rho_\alpha(\vec{x})+\rho_\alpha(\vec{x})\vec{p}_\alpha\},$$

$$\mathbf{J}^{[2]}(\vec{x})=-\frac{i}{2}\sum_{\alpha<\beta}\int d\vec{y}\int_0^1 ds\left[\rho_\alpha\left(\vec{x}+\frac{1}{2}\vec{y}s\right)-\rho_\beta\left(\vec{x}-\frac{1}{2}\vec{y}s\right)\right]\vec{y}\exp\left[-\frac{i}{2}(\vec{p}_\alpha-\vec{p}_\beta)\vec{y}\right]V(\vec{r}_\alpha-\vec{r}_\beta+\vec{y},\vec{r}_\alpha-\vec{r}_\beta),$$

where $\vec{r}_\alpha$ ($\vec{p}_\alpha$) is the coordinate (momentum) operator of the nucleon numbered α, the operator $\rho_\alpha(\vec{x})=e(\alpha)f(\vec{x}-\vec{r}_\alpha)$ contains the function $f(\vec{y})$ characterizing the charge distribution in the nucleon, and $\rho(\vec{x})=\Sigma_{\alpha=1}^{A}\rho_\alpha(\vec{x})$. The operator function $V(\vec{r}_\alpha-\vec{r}_\beta+\vec{y},\vec{r}_\alpha-\vec{r}_\beta)$ determines the NN interaction:

$$V(\alpha,\beta)=\int\exp\left[-\frac{i}{2}(\vec{p}_\alpha-\vec{p}_\beta)\vec{y}\right]\times V(\vec{r}_\alpha-\vec{r}_\beta+\vec{y},\vec{r}_\alpha-\vec{r}_\beta)d\vec{y}.$$

A direct relation is thereby established between the properties of the current $J^{[2]}$ (in particular, its short-distance behavior) and the properties of NN forces. This relation is particularly clear in the case of Majorana-type forces:

$$V_M(\alpha,\beta)=P_M(\alpha,\beta)V(\vec{r}_{\alpha\beta}),$$

for which

$$V(\vec{r}+\vec{y},\vec{r})=V(\vec{r})\delta(2\vec{r}+\vec{y}).$$

This case is considered in more detail in Ref. 99 (see also Ref. 38).

The Weyl criterion is important from the practical point of view, as it imposes certain restrictions on the $H^{(n)}\{A_\mu\}$. For example, for time-independent gauge transformations it gives

$$H^{(1)}\{A'_\mu\}=i[\chi,H_0]+H^{(1)}\{A_\mu\}, \tag{3.40}$$

$$H^{(2)}\{A'_\mu\}=\frac{i^2}{2!}[\chi,[\chi,H_0]]+H^{(2)}\{A_\mu\}+i[\chi,H^{(1)}\{A_\mu\}]. \tag{3.41}$$

From the first relation we find the continuity equation for the current:

$$\operatorname{div}\mathbf{J}(\vec{x})=i[\rho(\vec{x}),H_0], \tag{3.42a}$$

or, equivalently,

$$[\vec{P},\mathbf{J}(0)]=[H_0,\rho(0)], \tag{3.42b}$$

which can be useful for studying the role of MECs in processes involving two (Compton scattering) or more photons.

We have thus shown that the Weyl criterion generates the gauge-invariance condition in various orders in e at the operator level. It is important to stress the fact that, following Ref. 42, even when the corresponding operator relations [of the type (3.40)–(3.41)] are satisfied, it is necessary to worry about the independence of the amplitude of some EM transition from the choice of gauge.

Actually, the gauge-independence condition for a one-photon process with energy transfer ω and momentum transfer $\vec{q}$ is

$$\omega\langle f|\rho(0)|i\rangle=\vec{q}\langle f|\mathbf{J}(0)|i\rangle. \tag{3.43}$$

This relation is obviously a consequence of Eq. (3.42c) for the matrix elements between the exact eigenstates of the system:

$$H_0|i\rangle=E_i|i\rangle,\quad H_0|f\rangle=E_f|f\rangle$$

on the energy shell, and $\omega=E_f-E_i$ for photoabsorption.

In other words, satisfaction of (2.7) is not sufficient for the gauge independence of the EM transition amplitudes. It must be augmented with the additional requirement that the initial and final wave functions be eigenfunctions of the Hamiltonian H_0. Clearly, it is very difficult to satisfy this condition in actual calculations (especially nuclear ones) involving multiparticle wave functions.

It is interesting to note that the conditions (3.42)–(3.43) can be combined into a single operator generalization of the Ward–Takahashi identity if, using the continuity equation for the current, we write

$$q^\mu J_\mu(\vec{q})=\omega\rho(\vec{q})-[H,\rho(\vec{q})]=G(z_f)\rho(\vec{q})-\rho(\vec{q})G^1(z_i), \tag{3.44}$$

where $G(z)$ is the propagator $G(z)=(z-H)^{-1}$ for a given Hamiltonian H,[6)] and the free parameters z_i and z_f obey the condition $z_f-z_i=\omega$.

Inserting the two sides of (3.44) between eigenstates of H and setting $z_i=E_i$ and $z_f=E_f$, we immediately obtain the gauge-independence condition:

$$q^\mu\langle f|J_\mu(\vec{q})|i\rangle=0. \tag{3.45}$$

3.4. Effective ways of ensuring gauge independence. Extension of the Siegert theorem

Using the continuity equation, we can express the contribution of the longitudinal part of the current in terms of the matrix element of the charge density $\rho(\vec{x})$, which is less sensitive to the effect of MECs than the other components of the current (see the discussion in Ref. 7). Because of this, this trick is one effective way of including MECs in the description of inclusive and exclusive reactions induced by electrons (see Ref. 115, for example).

In this context we have the following useful generalization of the Siegert theorem,[116] which was essentially made long ago in the studies by Sachs[100] and Foldy[117] and rediscovered relatively recently.[118] As was shown in Ref. 118, the amplitude of a radiative process with the emission (absorption) of a single photon can be written in terms of the electric and magnetic field strengths $\vec{E}$ and $\vec{H}$ as follows:

$$T_{if}=\vec{E}(\vec{k}_\gamma)\langle f|\vec{D}(\vec{k}_\gamma)|i\rangle+\vec{H}(\vec{k}_\gamma)\langle f|\vec{M}(\vec{k}_\gamma)|i\rangle, \qquad (3.46)$$

where $\vec{D}(\vec{k}_\gamma)$ $[\vec{M}(\vec{k}_\gamma)]$ is the generalized dipole electric (magnetic) moment of the nucleus:

$$\vec{D}(\vec{k})=\int_0^1 d\lambda\int e^{i\lambda\vec{k}\vec{x}}\vec{x}\rho(\vec{x})d\vec{x}, \qquad (3.47)$$

$$\vec{M}(\vec{k})=\int_0^1 \lambda d\lambda\int \vec{x}\times\mathbf{J}(\vec{x})e^{i\lambda\vec{k}\vec{x}}d\vec{x}. \qquad (3.48)$$

Obviously, Eq. (3.46) is explicitly gauge-independent. We also note that $\vec{D}(\vec{k}=0)$ $[\vec{M}(\vec{k}=0)]$ coincides with the dipole electric (magnetic) moment operator of the system. It is easy to see that in the long-wavelength limit $(\vec{k}_\gamma\to 0)$ Eq. (3.46) gives the Siegert result widely used in the theory of photonuclear reactions. In contrast to its generalization at the level of various forms of multipole expansion of the EM current (see Ref. 119 and references therein), Eq. (3.46) makes it possible to avoid expansions completely, which simplifies the analysis at intermediate energies, where many multipole orders begin to contribute all at once.

In our earlier study[120] an expression similar to (3.46) was obtained without the traditional splitting of the EM current into a convection current related to the motion of the nucleus as a whole and an internal current. The corresponding result on the momentum shell is

$$T_{if}^{\text{on-shell}}=\vec{E}(\vec{k}_\gamma)\vec{D}_{if}(\vec{k}_\gamma)+\vec{H}(\vec{k}_\gamma)\vec{M}_{if}(\vec{k}_\gamma), \qquad (3.49)$$

$$\vec{D}_{if}(\vec{k})=(E^f_{\vec{P}_f}-E^i_{\vec{P}_i})\int_0^1\nabla_{\vec{k}}\times\Big\{(E^f_{\vec{P}_i+\lambda\vec{k}}-E_{\vec{P}_i}$$

$$\times\langle\vec{P}_i+\lambda\vec{k},f|\mathbf{J}(0)|\vec{P}_i,i\rangle\}\frac{d\lambda}{\lambda}, \qquad (3.50)$$

$$\vec{M}_{if}(\vec{k})=i\int_0^1\nabla\vec{k}\times\langle\vec{P}_iJ+\lambda\vec{k},f|\mathbf{J}(0)|\vec{P}_i,i\rangle d\lambda, \qquad (3.51)$$

where $E^i_{\vec{P}}$ $(E^f_{\vec{P}})$ is the energy of the initial (final) state of the hadronic system with momentum $\vec{P}$.

Equation (3.44) is applicable for ensuring the gauge independence of the calculations, both in the nonrelativistic description and in relativistic approaches (for example, in the Bethe–Salpeter formalism).

3.5. Conditions for covariance of the description of EM interactions of a hadronic system. The local analog of the Siegert theorem

Above, we have already used the property of transformation of the operator $J_\mu(x)$ under translations of the reference frame. The transformation properties of this operator under the Lorentz group can be formulated using the equation

$$U^+(\Lambda)J_\mu(0)U(\Lambda)\Lambda^\mu_\nu=J_\nu(0), \qquad (3.52)$$

where $U(\Lambda)$ is the operator corresponding to the Lorentz transformation

$$x'=\Lambda x \quad (x'_\mu=\Lambda^\nu_\mu x_\nu).$$

From (3.52) we find the equations involving the Lorentz-group generators $\mathscr{M}^{\mu\nu}$ (cf. Ref. 121):

$$i[\mathscr{M}^{\mu\nu},J_\lambda(0)]=I^{\mu\nu\rho}_\lambda J_\rho(0), \qquad (3.53)$$

$$I^{\mu\nu\lambda}_\rho=g^{\nu\lambda}\delta^\mu_\rho-g^{\mu\lambda}\delta^\nu_\rho,$$

where the metric tensor $g_{\mu\nu}$, as everywhere in the present study [see, for example, Eq. (2.10)], has the components

$$g_{00}=-g_{11}=-g_{22}=-g_{33}=1.$$

From this, for the boost generator $\vec{\mathscr{K}}=(\mathscr{M}^{10},\mathscr{M}^{20},\mathscr{M}^{30})$ we find

$$i\mathbf{J}(0)=[\vec{\mathscr{K}},J^0(0)], \qquad (3.54)$$

or

$$\langle f|J^l(0)|i\rangle=\frac{\partial}{\partial\beta_l}\langle f'|J^0(0)|i'\rangle|_{\beta_l}=0 \qquad (3.55)$$

$$(l=1,2,3),$$

where the transformed states in the motion of the reference frame along the lth axis with velocity v depend on the parameter $\beta_l=v/c$.

Comparing (3.55) with the gauge-independence condition (3.43), we see that whereas this condition makes it possible to express the matrix element of the longitudinal component of the current in terms of the matrix element of its time component, the spatial part of the current with the correct transformation properties under the Lorentz group can be completely reconstructed from this component.

Equation (3.54) can be used to obtain the local analog of the Siegert theorem:[122]

$$\mathbf{J}(0)=i[\mathscr{H}_S(0),\vec{D}], \qquad (3.56)$$

where $\vec{D}=\int\vec{x}J(\vec{x})d\vec{x}$ is the dipole electric moment operator of the system. We recall that, as in Sec. 3.1, capital letters are used here for operators acting in the background space of states of the system of interacting fields.

The proof of (3.56) can be based on the canonical expression for the Noether angular momentum:

$$\vec{\mathscr{K}}=\int\vec{x}\mathscr{H}_S(\vec{x})d\vec{x}, \qquad (3.57)$$

where the Hamiltonian density $\mathscr{H}_S(x)$ is equal to the component $\tau^{00}(\mathbf{x})$ of the symmetrized energy–momentum tensor $\tau^{\mu\nu}(\mathbf{x})=\tau^{\nu\mu}(\mathbf{x})$ (the Belinfante tensor).

Substituting (3.57) into (3.54) and noting that

$$\left[\int\vec{x}\mathscr{H}_S(\vec{x})d\vec{x},J^0(0)\right]=\int\vec{x}\mathbf{e}^{-i\vec{\mathscr{P}}\vec{x}}[\mathscr{H}_S(0),J^0(\vec{x})]\mathbf{e}^{-i\vec{\mathscr{P}}\vec{x}}d\vec{x},$$

for the eigenvectors of the momentum $\vec{\mathscr{P}}$ we find

$$\langle f|\mathbf{J}(0)|i\rangle=i\langle f|[\mathscr{H}_S(0),\quad\vec{D}(\vec{q})\}|i\rangle,$$

$$\vec{D}(\vec{q})=\int\mathbf{e}^{i\vec{q}\vec{x}}\vec{x}J^0(\vec{x})d\vec{x},$$

$$\vec{q}=\vec{P}_f-\vec{P}_i.$$

Furthermore, it can be shown that for any $\vec{q}$ we have

$$i[\mathscr{H}_S(0),\vec{D}(\vec{q})]=i[\mathscr{H}_S(0),\vec{D}]=\mathbf{J}(0).$$

Some of the consequences of (3.56) for the covariant and gauge-invariant description of EM interactions with nuclei are considered in Ref. 122. In particular, in the nucleon sector R_0 we have

$$\mathbf{J}^{\text{eff}}(0)=[\mathscr{H}^{\text{eff}}(0),\vec{D}^{\text{eff}}]. \quad (3.58)$$

This expression is valid if the diagonalization condition holds for $\mathscr{H}_S(0)$, i.e.,

$$Q_0(\mathscr{H}_S(0)-[A_0,\mathscr{H}_S(0)]-A_0\mathscr{H}_S(0)A_0)P_0=0, \quad (3.59)$$

which is equivalent to (3.4) as long as the desired operator A_0 is translationally invariant (cf. the discussion in Ref. 66).

Just as important is the fact that when (3.59) holds the noncommuting operators are simultaneously put in quasidiagonal form, e.g.,

$$U_0^+\vec{\mathscr{K}}U_0=\begin{Bmatrix} \vec{K}_{P_0P_0} & 0 \\ 0 & \vec{K}_{Q_0Q_0} \end{Bmatrix},$$

$$U_0^+\mathscr{H}_S U_0=\begin{Bmatrix} H_{P_0P_0} & 0 \\ 0 & H_{Q_0Q_0} \end{Bmatrix}.$$

The generator $\vec{K}^{\text{eff}}\equiv\vec{K}_{P_0P_0}$ determines the transformations of vectors in $\in R_0$ under boosts.

Then, combining (3.59) and (3.42b), we obtain the expression

$$[H_S^{\text{eff}},\rho(0)]=i[\vec{P},[H_S^{\text{eff}}(0),\vec{D}^{\text{eff}}]], \quad (3.60)$$

or

$$\omega\langle f|\rho(0)|i\rangle=i\vec{q}\langle f|[H_S^{\text{eff}}(0),\vec{D}^{\text{eff}}|i\rangle, \quad (3.61)$$

which impose certain restrictions on the density operator $\rho(\vec{x})$ of the nucleon charge distribution in the nucleus, which enters into the expression

$$\vec{D}^{\text{eff}}=\int \vec{x}\rho(\vec{x})d\vec{x}. \quad (3.62)$$

We are presently working on applications of the results obtained in Secs. 3.4 and 3.5.

4. METHODS AND RESULTS OF THE CALCULATIONS

4.1. The reaction $d(e,e'p)n$. Proton polarization in the Saclay kinematics

Our calculations differ from those carried out by Arenhövel *et al.*[13,39] In particular, we have not made the standard expansion of the current in multipoles, the electric part of which was calculated by those authors using the Siegert recipe.[7)] Because of this, we have not been forced to calculate and monitor simultaneously the contributions of many partial transitions between the initial and final states. In addition, we have performed our analysis in momentum space. Without dwelling on the details, which can be found in Refs. 12 and 15, we note that the partial waves $\Psi_{p_0ll'}^{(-)JST}(p)$ in the expansion of the final state have been calculated using the so-called matrix-inversion method.[106,123] The characteristic feature of this method is the isolation of the "radial" dependence of the distorted wave:

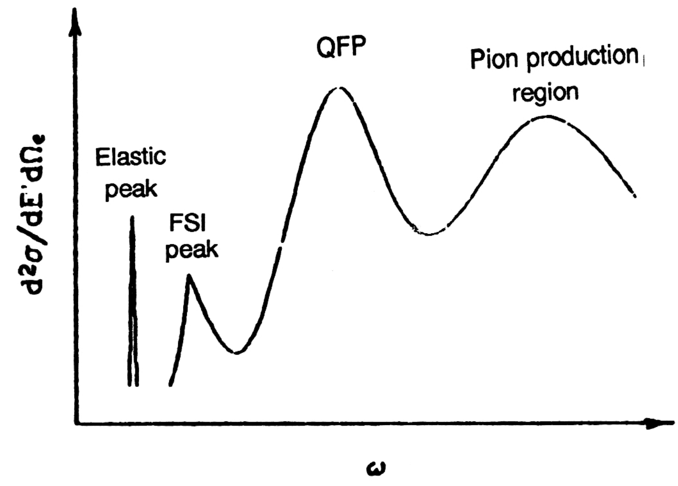

FIG. 6. Schematic depiction of the characteristic regions in the energy spectra of electrons for the inclusive $d(e,e')$ reaction.

$$\Psi_{ll'}^a(p)=\sum_{k=1}^{k=N+1} B_{ll'}^a(k)\delta(p-p_k)/p_k^2, \quad (4.1)$$

where the coefficients $B_{ll'}^a(k)$ are the solutions of an algebraic system of equations approximately equivalent to the original integral equation of the scattering problem (in this case, for the R matrix of np scattering), N is the dimensionality of this system, and $\{p_k\}$ is the set of points in p space related to the Gaussian quadrature points $[-1,1]$.

The structure of (4.1) considerably simplifies the analogous calculation of the amplitudes (2.3) (for example, sixfold overlap integrals involving meson-exchange currents can be reduced to single integrals[12,15]).

In Refs. 12 and 15 the angular distributions and proton polarizations in $d(e,e'\vec{p})n$ reactions were calculated, primarily, far from the quasifree peak in the cross sections for the inclusive (e,e') reaction on the deuteron (Fig. 6). It can be expected that FSI and MEC effects play an important role in this kinematics. These calculations were carried out with the Paris potential.[82] The FSI distortions were taken into account in the np partial-wave states with total angular momentum $J\leqslant J_{\max}=2$. The convergence of the results when FSI effects in higher partial waves are included is discussed in Ref. 15.

The direct mechanism of proton knockout [using the plane-wave impulse approximation (PWIA)] and the recoil mechanism arising from the EM interaction with the spectator neutron [using the Born approximation] have been studied.

In Figs. 7–8 we show the results of our calculations together with the Saclay data.[40,41] We see that the effect of the recoil mechanism becomes stronger as the momentum of the spectator n' grows. In the Saclay III kinematics the corresponding contribution becomes comparable to that from the direct mechanism. As can be seen in Fig. 7, the results of the Born approximation (BA) differ (sometimes significantly) from the Saclay data. The same trends were observed in the earlier nonrelativistic calculations.[39]

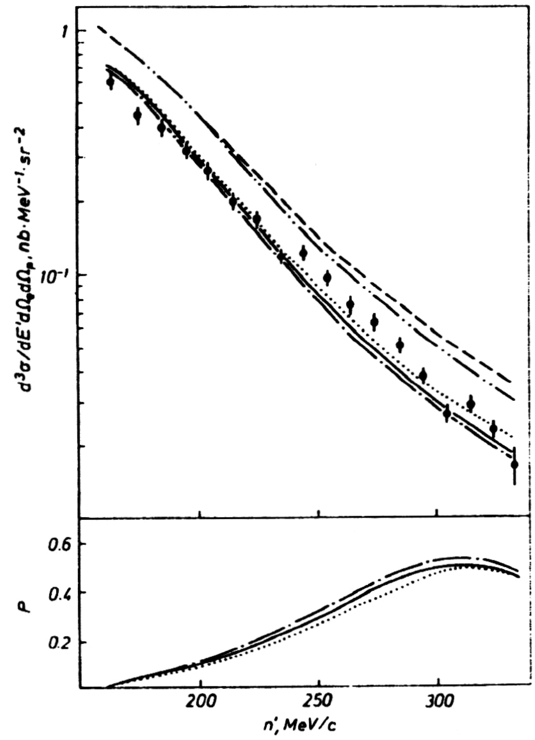

FIG. 7. Dependences of the differential cross sections (upper part) and proton polarization (lower part) for the $d(e,e'p)n$ reaction on the spectator-neutron momentum for the Saclay II kinematics. The calculations are for the PWIA (-···-), the Born approximation (- - -), the DWBA (-··), and with the FSI and MECs for two values of the cutoff parameter $\Lambda=4m_\pi$ and ∞ (— and ···).

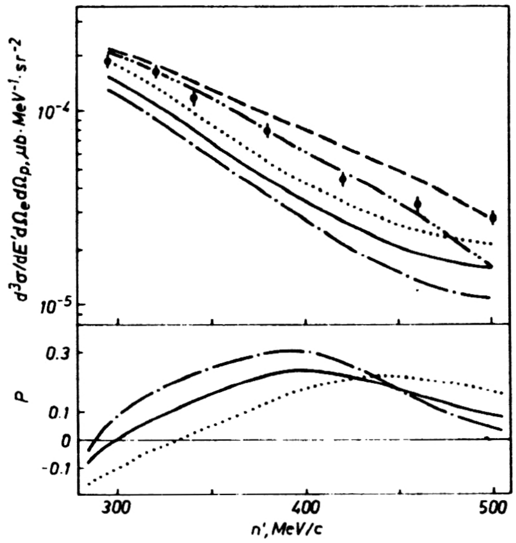

FIG. 8. The same as in Fig. 7, for the Saclay III kinematics.

Comparing these studies with those of Ref. 124, carried out in the relativistic impulse approximation (RIA), we note that the cross sections[8)] from Ref. 124 differ from ours and from those calculated in Ref. 39: the curves in Fig. 1 of Ref. 124 corresponding to the t-pole contribution to the amplitude of the reaction $d(e,e'p)n$ lie much lower than the PWIA curves in Fig. 7 for $n'>200$ MeV/s. In addition, the competition of the contributions of the direct and recoil mechanisms established in Ref. 124 is the opposite of that shown in Fig. 7, viz., according to Ref. 124 the inclusion of the u-pole contribution, i.e., the interaction between the virtual photon and the spectator neutron, decreases the calculated cross sections.

Perhaps the main reason for these discrepancies is the subtraction procedure

$$J_\mu \rightarrow J_\mu - q_\mu(qJ/q_\mu^2) \tag{4.2}$$

used by the authors of Ref. 124 in their attempt to obtain a gauge-independent description of the ed interaction. This procedure is obviously not free of defects:

(a) It is not unique, because the subtraction of $p_\mu(qJ/pq)$ with any vector p_μ for which $pq\neq 0$ leads to a conserved current.

(b) Its application to a one-body operator again gives a one-body operator, whereas the above-mentioned consistency of the nuclear current with the NN interaction presupposes the introduction of, at least, two-body contributions to the electromagnetic interaction operator.

The trick based on the substitution of (4.2) is too artificial to substitute for the genuine solution of this complicated problem in the theory.

The inclusion of FSI distortions [the distorted-wave Born approximation (DWBA)] decreases the cross sections obtained in the Born approximation, leading to a satisfactory description of the data for the kinematics II. We also see that the proton polarization under these conditions can be significant. It should be stressed that the FSI plays an important role in the kinematics III, even though the energy of the relative motion in the final states is relatively large ($E_{np}=179$ MeV in the c.m. frame).

In addition, the inclusion of MECs leads to an increase of the $d(e,e'p)n$ cross sections for these kinematics. The interference between the MEC and the FSI contributions to the cross section is destructive, and this confirms the conclusion reached in Ref. 39. Figure 8 shows that the predictions of MEC models with modified πNN vertices and pointlike nucleons differ noticeably (in particular, the proton polarization is qualitatively changed). This fact can prove useful in testing various models of the electromagnetic current of the deuteron.

The other discrepancies for the kinematics III can be diminished by taking into account MECs generated by ρ exchange and Δ-isobar excitation in intermediate states. The latter mechanism contributes to the transverse structure functions. Experience[96] shows that to estimate it accurately it is necessary to study the mutually canceling contributions from the currents j_Δ^π and j_Δ^ρ with the strong form factors. Of course, the relativistic effects mentioned of in the Introduction also must be considered.

We should note that it is probable that the description of the Saclay III data obtained by using just the Born approximation becomes poorer when more complicated reaction mechanisms are included. Measurements of the spin observables would be of great help in understanding the true role of these mechanisms in such situations.

4.2. Isolation of the structure functions. Parallel kinematics

Among the many problems associated with the analysis of polarization phenomena in electrodisintegration of nuclei, the isolation of the structure functions is of particular interest. Complete isolation can be done in experiments with noncoplanar geometry (see, for example, Ref. 33). However, it can be done partially in the coplanar case when some structure functions are defined in a relatively simple way.

Let us consider parallel kinematics, when the photon virtual momentum and the momentum of the knocked-out proton are collinear ($\vec{p}_0 \| \vec{q}$). Then the number of structure functions is decreased:

$$\sigma_0=\sigma_M\left\{\xi^2 W_C+\left(\frac{1}{2}\,\xi+\eta\right)W_T\right\}R, \tag{4.3}$$

$$\sigma_0 P=\sigma_M \xi\sqrt{\xi+\eta}\Sigma_I R. \tag{4.4}$$

Therefore, first of all, by measuring the cross section for $e'p$ coincidence in this kinematics, we can isolate the longitudinal structure function W_C and the transverse structure function W_T (the Rosenbluth plot). Second, by measuring $\vec{P}_Y \| \vec{k}' \times \vec{k}$, we can extract the interference structure function Σ_I This last procedure can be compared with the measurement of the azimuthal left–right asymmetry of the cross sections (see Fig. 4):

$$A_\phi \equiv [\sigma_0(\phi=0)-\sigma_0(\phi=\pi)][\sigma_0(\phi=0)+\sigma_0(\phi=\pi)]^{-1}=\xi\sqrt{\xi+\eta}W_I\left[\xi^2 W_C+\left(\frac{1}{2}\,\xi+\eta\right)W_T+(\xi+\eta)W_S\right]^{-1}, \tag{4.5}$$

which is proportional to the structure function W_I depending on the interference of the same components of the current J_0 and J_X as Σ_I In contrast to A_ϕ, the quantity P_Y carries information about spin-flip transitions in the np system.

Isolation of the structure functions $W_L=W_C$ and W_T in the $d(e,e'p)n$ cross sections was done recently at NIKHEF (Ref. 125). The measurements were carried out in parallel kinematics over the range $0.05 \leqslant q_\mu^2 \leqslant 0.27$ (GeV/s)^2 for values of the missing (recoil) momentum $p_m \lesssim 100$ MeV/s. Similar experiments were also performed at Saclay,[55,126] where the q dependence ($200 \leqslant q \leqslant 670$ MeV/s) of the same structure functions was studied for the two values $p_m=20$ and 100 MeV/s.

The next advance was the isolation of the three in-plane structure functions W_L, W_T, and $W_{LT}=W_I$ for the $d(e,e'p)n$ reaction in Refs. 54 and 127 for $q_\mu^2=0.21$ (GeV/s)^2 in the wider range $p_m \lesssim 200$ MeV/s and in Ref. 126 for $q=400$ MeV/s and $p_m=50$, 100, and 150 MeV/s. These studies were carried out for quasifree kinematics, when the Bjorken variable is $x=q_\mu^2/2m\omega=1$, i.e., near the maximum of the quasifree peak (Fig. 6). The azimuthal asymmetry A_ϕ has been measured at Bonn[128] and at SLAC.[129] Some of the results of these measurements will be discussed in Sec. 4.8.

Figures 9 and 10 show our calculations[15] at transferring electron energies $E=1$ GeV. The values of the other variables are given in Table I. We see from these figures that the cross sections for $e'p$ coincidences have a clearly expressed azimuthal asymmetry relative to the case of $\theta=0°$ (parallel kinematics). The polarization of the knocked-out protons also has a noticeable azimuthal asymmetry.

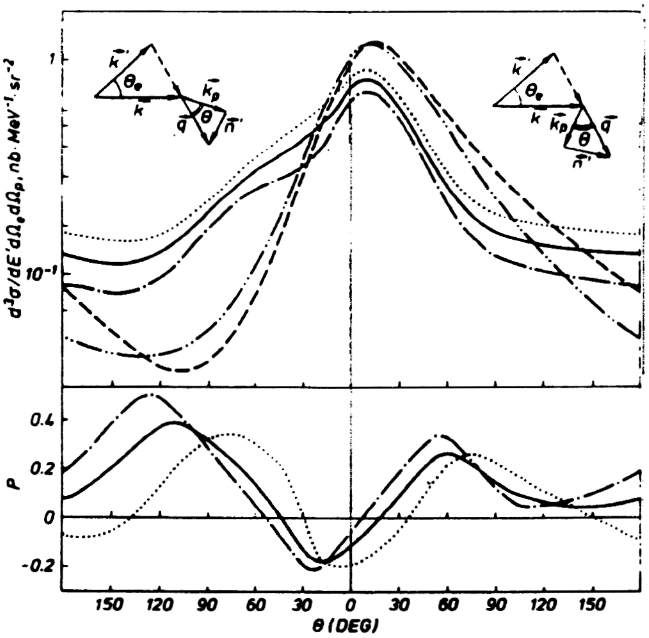

FIG. 9. The same as in Fig. 7, as a function of the angle θ between $\vec{k}_p$ and $\vec{q}$ for the right-hand part of the quasifree peak.

This is easily explained when we consider the properties of the transformation

$$R_Z(\pi)J_{X,Y}(q)R_Z^{-1}(\pi)-J_{X,Y}(\vec{q}), \tag{4.6}$$

with rotation $R_Z(\pi)$ of the reference frame about the vector $\vec{n}_Z$ by 180°. From (4.6) it follows that

$$W_{C,T,S}(\phi=0)=W_{C,T,S}(\phi=\pi),$$
$$W_I(\phi=0)=-W_I(\phi=\pi) \tag{4.7}$$

and

$$\Sigma_{C,T,S}(\phi=0)=-\Sigma_{C,T,S}(\phi=\pi),$$
$$\Sigma_I(\phi=0)=\Sigma_I(\phi=\pi). \tag{4.8}$$

The values of the polarization are more sensitive to the choice of current model. In going from one to another we observe qualitative changes in the angular dependence of the polarization.

On the left-hand part of the quasifree peak, proton emission is possible only into the forward hemisphere. The maximum proton emission angle is given by

$$\cos\theta_{\lim}=\{(\omega+m_d)^2-[(\omega+m_d)^2+m_p^2-m_n^2-\mathbf{q}^2]^2/4m_p^2\}^{1/2}/q, \tag{4.9}$$

where $m_p(m_n)$ is the proton (neutron) mass.

The corresponding cross section (Fig. 10) has a special feature: as θ tends to $\theta_{\lim}$ (in this case $\theta_{\lim} \simeq 16.6°$), the cross section increases sharply. This growth is due to the behavior

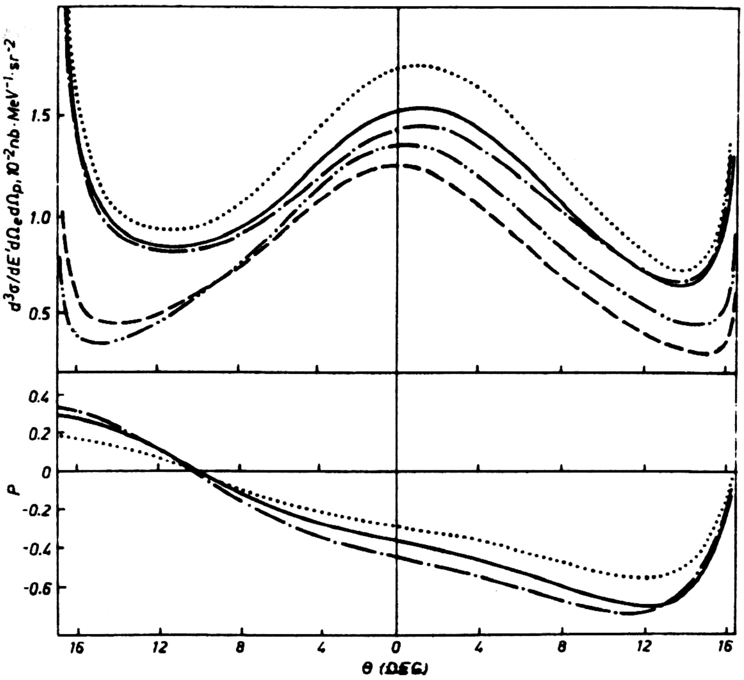

FIG. 10. The same as in Fig. 9 for the left-hand part of the quasi-free peak.

of the kinematical factor R: $R\to\infty$ if $\theta\to\theta_{\lim}$. However, this feature is rather weak, so that in an experiment (with finite angular resolution) the cross section takes a finite value.

The curves corresponding to different current models come closer together for $\theta\to\theta_{\lim}$. The differences between them are most noticeable for $\theta=0°$.

As can be seen from Fig. 10, the polarization of protons emitted in the direction of the vector $\vec{q}$ reaches a sizable value of $\simeq 40\%$. The θ dependence of the polarization changes significantly in going from the case with $\phi=0°$ to the case with $\phi=180°$.

Equations (4.7)–(4.8) make it possible to extract the θ dependence of the structure function Σ_I:

$$\Sigma_I=\frac{\sigma_0(\phi=0)P(\phi=0)+\sigma_0(\phi=\pi)P(\phi=\pi)}{2\sigma_M R\xi\sqrt{\xi+\eta}}. \quad (4.10)$$

The results of the calculations[130] using Eq. (4.10) are shown in Figs. 11 and 12. In our opinion, measurements of this azimuthal asymmetry could be a good test of our understanding of deuteron electrodisintegration mechanisms.

4.3. Polarization observables for the reaction $d(\vec{e},e'\vec{p})n$. Polarization transfer. The MIT–Bates experiment

Let us consider the breakup of unpolarized deuterons by longitudinally polarized electrons under conditions where the Bjorken variable is $x=1$. Theoretical research (Refs. 6, 18, and 131) in this area has to a significant degree been stimulated by the proposals[4,11] for the MIT program. It is suggested that the measurements[11] of the polarization transfer in $d(\vec{e},e'\vec{p})n$ reactions be measured for initial electron energy $E=880$ MeV. The other parameters are given in Table II.

Before commenting on our calculation in Fig. 13, we note that in the parallel kinematics, of the two structure functions for each component $P'_{X,Z}$ only one survives, because

$$\Sigma_I'^{Z}=\Sigma_T'^{X}=0. \quad (4.11)$$

The angular dependences of the structure functions in (2.13)–(2.14) can be studied by forming polarization-transfer asymmetries like (4.10) (Ref. 18).

As shown in Fig. 13, the components of the proton polarization vector can take large values which can be measured. In the parallel kinematics the FSI and MEC effects are

TABLE I. Values of the kinematical parameters for $E=1$ GeV.

	E', MeV	θ_e, deg	$\vec{q}$, MeV/s	E^*_{np}, MeV	T_p, MeV	θ, deg	n', MeV/s
Right side	830	10	233	154.5	128.4	0	274.8
					39.45	180	507.5
Left side	827	50	788	13.2	131.8	0	273.4
					71.1	16.58	444.2

Only the limiting values of θ, the neutron momentum n', and the proton kinetic energy T_p are given in this table.

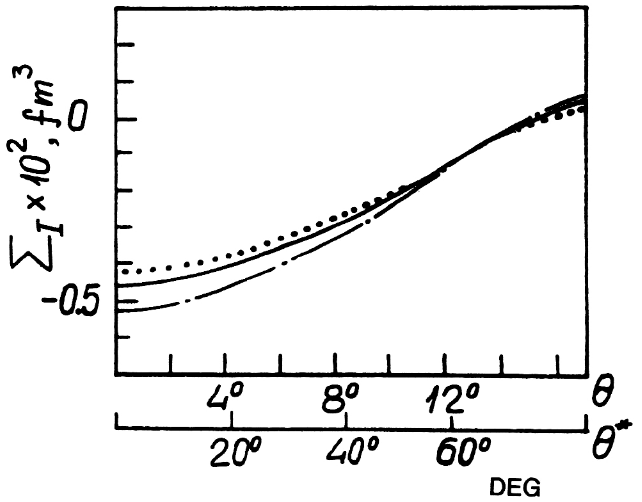

FIG. 11. Angular dependence of the interference (longitudinal–transverse) structure function for the proton polarization in the reaction $d(e,e'\vec{p})n$ on the left-hand part of the quasifree peak; θ^* is the angle between the momentum of the knocked-out proton and the momentum transfer in the c.m. frame.

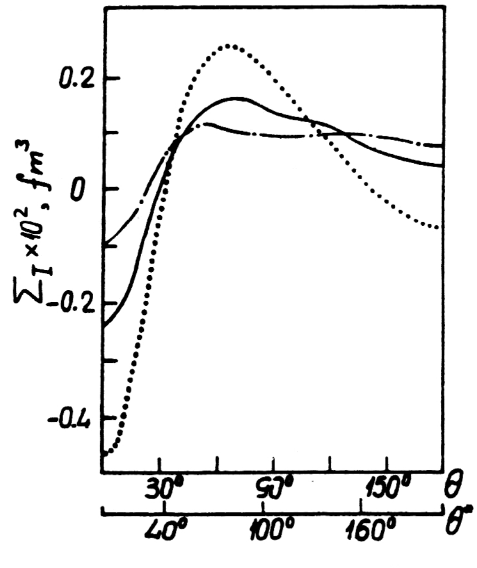

FIG. 12. The same as in Fig. 11 for the right-hand part of the quasifree peak.

insignificant. The same is true near $\theta_{\lim}=90°$ (parallel kinematics for neutrons with $\vec{k}_n=\vec{q}$. At intermediate angles FSI effects are important and the MEC contributions are small.

Detailed analysis shows that for proton emission angles $\theta\leqslant45°$ the dominant contribution to the cross section for $e'p$ coincidences comes from direct proton knockout (for example, for the MIT-1 kinematics, with $\theta=45°$ this contribution is $\simeq75\%$). As θ increases the electromagnetic interaction with the neutron plays an ever greater role, so that at $\theta\simeq\theta_{\lim}$ the cross sections are completely determined by the contribution of this recoil mechanism (cf. our results in Ref. 132 for the reactions $^4\mathrm{He}(\vec{\gamma},p)^3\mathrm{H}$ and $^4\mathrm{He}(\vec{\gamma},n)^3\mathrm{He}$ with linearly polarized photons). The same pertains to the observables $P'_{X,Z}$. When this mechanism is neglected, they depend weakly on θ.

The relations between quantities in the lab frame ($\vec{P}_d=0$) and in the c.m. frame of the final np pair, in which, according to the Madison convention, the Z^* axis points along the momentum $\vec{k}_p^*$ (Fig. 14; Appendices B and D), need to be explained.

In particular, as shown in Appendix D, up to terms of order q/m_d we have for $\phi^*=180°$

$$P_l=P'_Z\cos\theta^*-P'_X\sin\theta^*,$$

$$P'_t=P'_Z\sin\theta^*+P'_X\cos\theta^*, \qquad (4.12)$$

$$P_n=P_Y,$$

where P'_l, P'_t, and P_n are the longitudinal (along $\vec{k}_p^*$), transverse (along the X^*axis, i.e., perpendicular to $\vec{k}_p^*$ and lying in the reaction plane), and normal (along $\vec{k}_p^*\times\vec{q}$) components of the polarization vector $\vec{p}_X^*$ in the c.m. frame. These definitions are equivalent to those often used.[11] Arguments in favor of using results in the lab frame (especially at large momentum transfers) can be found in Ref. 18.

4.4. Extraction of the neutron electric form factor from polarization experiments. Exclusive and inclusive reactions

It is well known that the quality of the available information about the electromagnetic properties of the neutron leaves much to be desired. As was stressed in Refs. 7, 12, and 15, study of the induced polarization P as a function of G_E^n can improve this situation. In fact, as can be seen from Fig. 15, this observable changes significantly in going from a current model with $G_E^n=0$ to one with a scaling version[133] of G_E^n: $G_E^n=\tau\kappa_n G_E^p$, where $\tau=q_\mu^2/4m^2<0$ and κ_n is the neutron anomalous magnetic moment. The corresponding variations are especially large in the parallel kinematics, where they are almost 30%. Another calculation (Fig. 16) demonstrates the qualitative changes in the angular dependence $P_Y(\theta)$ for the reaction $d(\vec{e},e'\vec{p})n$ with $G_E^n=0$ replaced by G_E^n from Ref. 133.

As was shown in Ref. 18, the component P'_X of the polarization transferred to the proton is also sensitive to this substitution at angles close to $\theta_{\lim}=90°$. This is due to the

TABLE II. Kinematical conditions of the MIT–Bates experiment.

	ω, MeV	θ_e, deg	q, MeV/s	E^*_{np}, MeV	T_p, MeV	θ_p, deg
I	142	−56.8	531	69	140	37.0
II	210	−49.1	659	101	208	48.0
III	282	−41.6	779	136	281	60.1

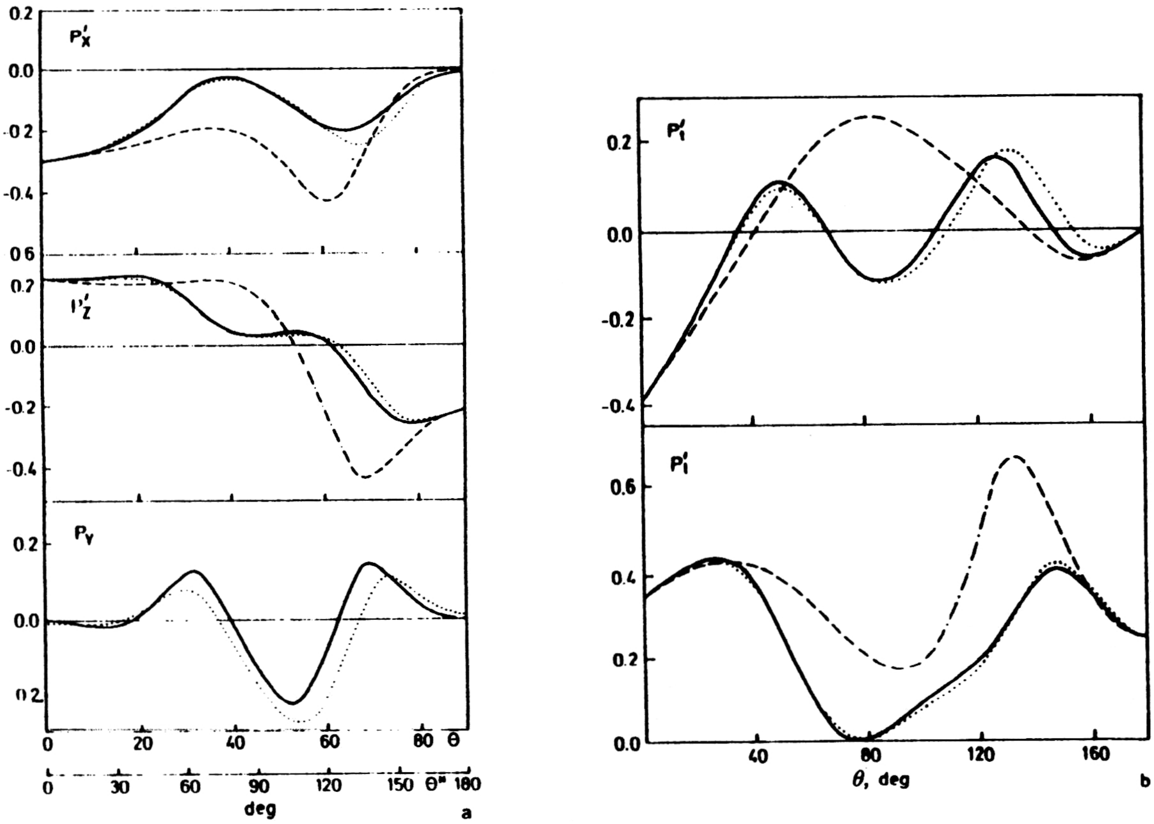

FIG. 13. Polarization observables in the reaction $d(\vec{e},e'\vec{p})n$ for the MIT-I kinematics. The curves were calculated (Ref. 18) using the Born approximation (- - -), including the FSI and MECs for $\Lambda=4m_\pi$ (—), and including the FSI but not MECs (···). Curves b were obtained from curves a using Eq. (4.12).

increased importance of the recoil mechanism, which was discussed in Sec. 4.3. In this regard it is preferable to measure the polarization transferred directly to the neutron in the reaction $d(\vec{e},e'\vec{n})p$.[9)]

Actually, in the PWIA, which, as we have seen, works well in the $\vec{k}_n \| \vec{q}$ kinematics, we find (as in the case of $\vec{e}n \rightarrow e'\vec{n}'$ scattering):

$$I_0 P'_X = -\xi\sqrt{\eta} G_E^n G_M^n \frac{q}{m},$$

$$I_0 P'_Z = \sqrt{\eta(\xi+\eta)}[G_M^n]^2 \frac{\vec{q}^2}{2m^2}, \tag{4.13}$$

$$I_0 = \xi^2 [G_E^n]^2 + \left(\frac{1}{2}\xi + \eta\right)[G_M^n]^2 \frac{\vec{q}^2}{2m^2}.$$

In other words, the observable P'_X in this approximation is determined by the product $G_E^n G_M^n$.[10)] We also note that these components of the polarization vector in this case are independent of nuclear-structure effects (the deuteron wave function).

The mixed asymmetry $A'_\nu(\theta_H=\pi/2,\phi_H=0)$ for the reaction $\vec{d}(\vec{e},e'n)p$, which in the parallel kinematics depends on a single structure function,

$$\sigma_0 A'_\nu\left(\frac{\pi}{2},0\right) = -\sigma_M \sqrt{\eta/2}\,\xi W'^{11}_{LT} R, \tag{4.14}$$

in the PWIA has a simple relation to P'_X:

$$A'_\nu\left(\frac{\pi}{2},0\right) = \sqrt{\frac{2}{3}} P'_X. \tag{4.15}$$

It therefore depends on the same combination of neutron form factors.

The components of the neutron polarization vector P'_l, P'_t, and P_n and the asymmetry $A'_\nu[(\pi/2,0)]$ from Ref. 21 calculated for the kinematical conditions of the MIT experiment[4] (Table III) are shown in Figs. 17 and 18. Here we see that the observables P_t and A'_ν depend strongly on the model of the neutron electric form factor at neutron emission angles close to $\theta^*=0$ (cf. the dot–dashed and solid lines 1). We also see that they are weakly sensitive to FSI effects for neutrons emitted along $\vec{q}$. As far as MEC contributions are concerned, their effect in this case with $x=1$ is insignificant in the entire angular range.

Strong dependence on G_E^n is seen (Figs. 19 and 20) in the calculated[20] polarization transfer to the neutron P_{1z} in the reaction $\vec{d}(e,e'\vec{n})p$ and in the double polarization transfer to the proton $P^n_{2x}(p)$ in the reaction $\vec{d}(\vec{\nu},e'\vec{p})n$. Again the corresponding structure functions depend on G_E^n through the product $G_E^n G_M^n$.

This product enters into one of the formulas of the impulse approximation for the spin-dependent response functions in (2.50):[72]

$$R_{TL'}(Q^2,\omega_{\max}) = -2\sqrt{2\xi^{-1}(\xi^{-1}-1)}\{P_n G_E^n G_M^n$$

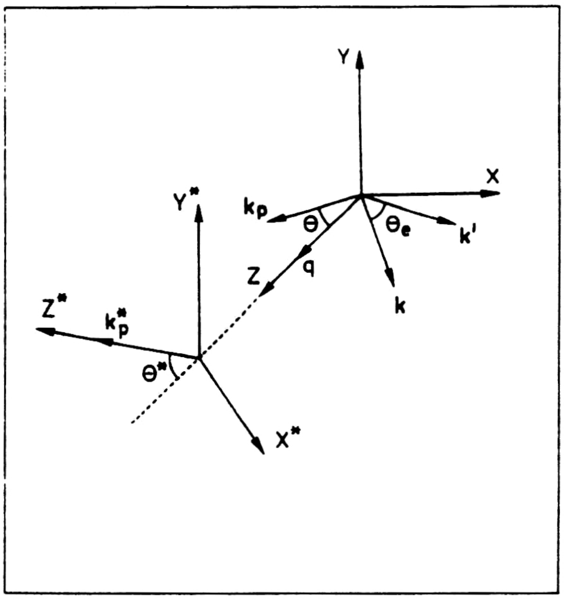

FIG. 14. Particle momenta in the reaction $d(\vec{e},e'\vec{p})n$ for coplanar geometry. All the starred notation refers to the c.m. frame, and the unstarred notation to the lab frame. For this arrangement of the vectors the angle ϕ (ϕ^*) is 180°.

$$+2P_pG_E^pG_M^p\}F(\omega_{\max}), \tag{4.16}$$

$$R_{T'}(Q^2,\omega_{\max})=2(\xi^{-1}-1)\{P_n[G_M^n]^2$$
$$+2P_p[G_M^p]^2\}F(\omega_{\max}), \tag{4.17}$$

where $F(\omega_{\max})$ is the scaling function for quasifree scattering on the ^{3}He nucleus at the maximum of the quasifree peak, $x=1$. The nucleon polarization P_p (P_n) is the difference of the probabilities for the nucleon to have spin up and spin down, averaged over the momenta.

If, following Ref. 73, we assume that in polarized ^{3}He the nucleon spins are arranged so that the neutron spin on the

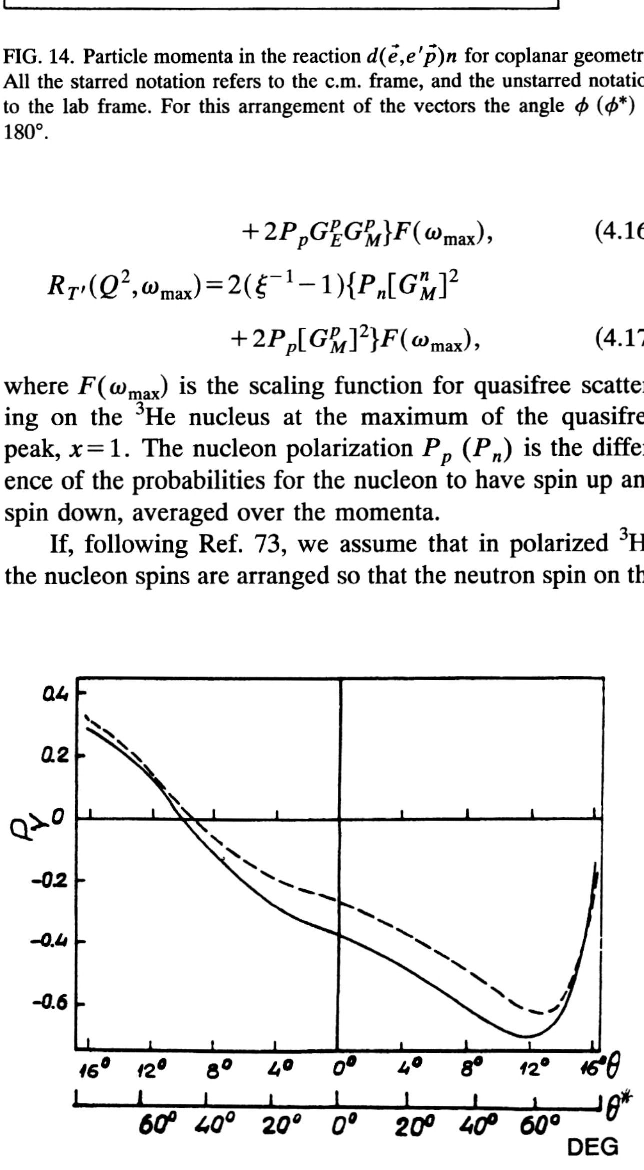

FIG. 15. Dependence of the proton polarization in the reaction $d(e,e'\vec{p})n$ on the choice of G_E^n on the right-hand part of the quasifree peak (Table I). The curves were calculated using the MEC model with $\Lambda=4m_\pi$. The solid line is for G_E^n from Ref. 133, and the dotted line is for $G_E^n=0$.

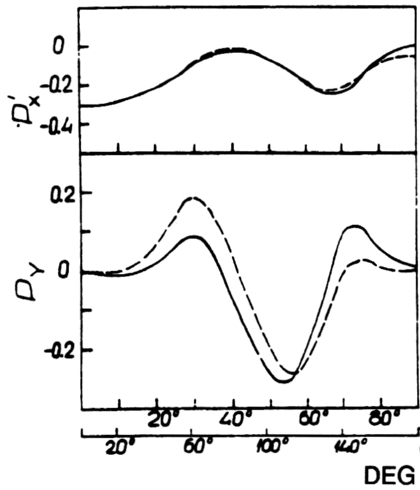

FIG. 16. The same as in Fig. 15 for the MIT-I kinematics.

average points along the ^{3}He spin, and the spins of the two protons nearly cancel each other ($|P_p| \ll |P_n|$), favorable conditions can be created for the separation of the neutron contributions (4.16) and (4.17). This argument was the main motivation for the "one-shoulder" experiments.[71,72]

As above, an attractive object for study is the function $R_{TL'}$, which depends linearly on G_E^n, i.e., not only on the modulus of this form factor, but also on its sign.

In contrast to this, the nucleon form factors enter quadratically into the longitudinal and transverse response functions for unpolarized particles:

$$R_T(Q^2,\omega_{\max})=2(\xi^{-1}-1)\{[G_M^n]^2+2[G_M^p]^2\}F(\omega_{\max}), \tag{4.18}$$

$$R_L(Q^2,\omega_{\max})=\xi^{-1}\{[G_E^n]^2+2[G_E^p]^2\}F(\omega_{\max}). \tag{4.19}$$

Two quantities have been measured[72] for separating the different contributions: the asymmetry $A_{T'} \sim R_{T'}$ (for $\theta_H=0,\pi$) and the asymmetry $A_{TL'} \sim R_{TL'}$ (for $\theta_H=\pi/2,3\pi/2$). The value $A_{TL'}=(+1.75\pm1.2\pm0.3)\%$ at $Q^2=-0.2$ (GeV/s)^2 is not very accurate. Using the predictions of Ref. 73 for the proton and neutron polarization in polarized ^{3}He and taking into account the existing uncertainties (for example, for G_M^n), the authors of Ref. 72 arrive at the result $G_E^n=0.044\pm0.074$, which, of course, cannot be considered satisfactory. This situation may improve with increasing $|Q^2|$, when a decrease of the relative contribution proportional to P_p in (4.16) can be expected.

Some of the uncertainties mentioned above originate in the assumptions made in deriving Eqs. (4.16)–(4.19); along with the impulse approximation, they are:

TABLE III. Values of the kinematical parameters for the $d(e,e'n)p$ reactions.

E, MeV	E', MeV	θ_e, deg	q, MeV/s	E^*_{np}, MeV
868	730	37	524	68

E^*_{np} is the relative energy of the np pair in the c.m. frame.

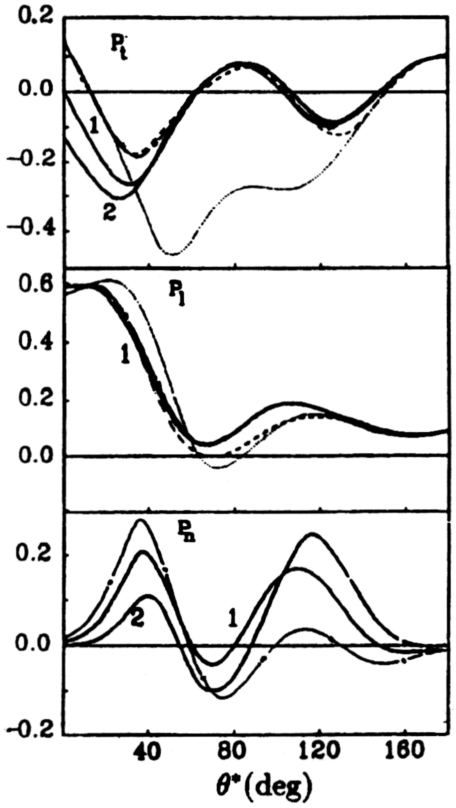

FIG. 17. Angular dependence of the components of the neutron polarization vector in the reaction $d(\vec{e},e'\vec{n})p$. Calculations of Ref. 21 in the PWBA (dotted lines), DWBA (dashed lines), DWBA+MEC+RA (dot-dashed lines) with $F_1^n=0$, i.e., from Ref. 133, DWBA+MEC+RA (solid lines *1*), and DWBA+MEC (solid lines *2*) with $F_1^n=-\tau\kappa_n G_E^p(1-\tau)^{-1}$, i.e., $G_E^n=0$.

1. Neglect of the FSI of the knocked-out nucleon in the reaction $^3\vec{He}(\vec{e},e'N)$ with the residual system.[11)]

2. Use of the completeness condition for the vectors of the final $2N$ states after introduction of the average (fitted) mass (the closure approximation).

3. Restriction to only the one-body virtual-photon absorption mechanism without including MECs.

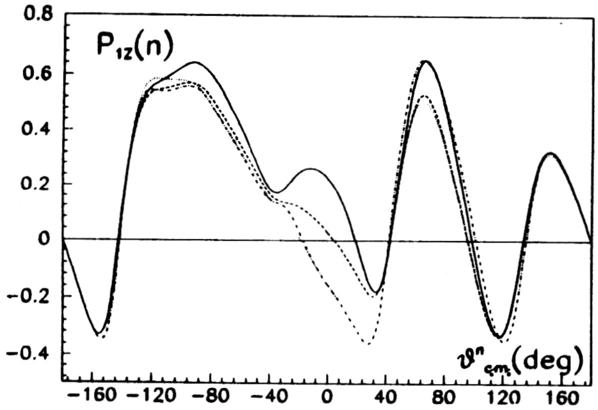

FIG. 19. Polarization transfer in the reaction $\vec{d}(e,e'\vec{n})p$. Results of Ref. 20 obtained in the DWBA (dot-dashed line), DWBA+MEC+contributions of isobar configurations (ICs) (dotted line), DWBA+MEC+IC+RA (solid line) using the model of Ref. 135, and DWBA+MEC+IC+RA (dashed line) with $G_E^n=0$.

These approximations give the scaling behavior of the inclusive cross sections with the so-called y_1 variable, which is different from the West variable (see Ref. 137). In further studies we hope to go beyond this simplified approach.[35,138]

The Mainz experiment has certainly led to great progress in the study of spin physics for the ^{3}He nucleus.[70] Here for $\bar{q}_\mu^2=0.31$ (GeV/s)^2 the two asymmetries $\bar{A}_\perp$ ($\vec{S}_{\rm He}\perp\vec{q}$) and $\bar{A}_\parallel$ ($\vec{S}_{\rm He}\|\vec{q}$) were measured with the values $\bar{A}_\perp/\bar{A}'_X=(0.89\pm0.30)\%$ and $\bar{A}_\parallel=\bar{A}'_Z=(-7.40\pm0.73)\%$. The ratio $\bar{A}_\perp/\bar{A}_\parallel$ is independent of the degree of polarization of the electron beam and the target and gives $G_E^n=0.035\pm0.012\pm0.005$. Of course, it should be borne in mind that the data in this case were analyzed in the impulse approximation, which is not completely satisfactory from the theoretical point of view. The studies of the Bochum group[84,85] may be of orientational value for obtaining more reliable information about nuclear-structure effects and the electromagnetic properties of the bound neutron.

There is yet another assumption[16] which is made in the inclusive scattering of polarized electrons on polarized deu-

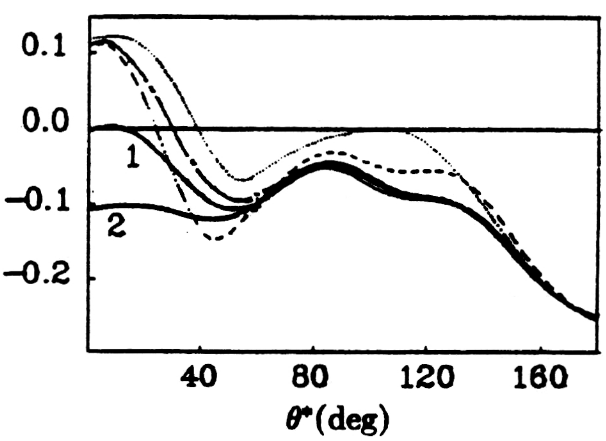

FIG. 18. Mixed asymmetry $A'_\nu(\pi/2,0)$ in the reaction $\vec{d}(\vec{e},e'n)p$ for the case $\phi=0$. The notation is the same as in Fig. 17.

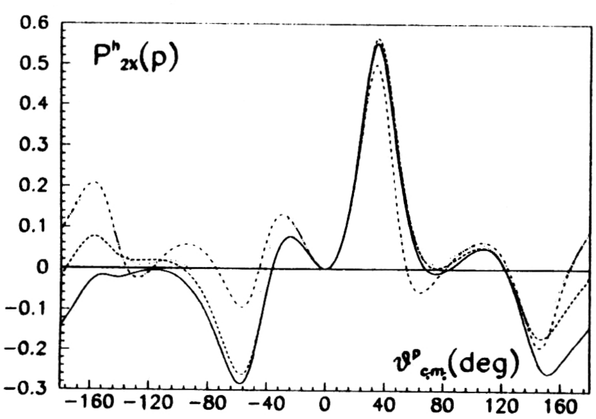

FIG. 20. Double polarization exchange in the reaction $\vec{d}(\vec{e},e'\vec{p})n$. The differences between the curves are given in the caption to Fig. 19.

terons. As shown in Fig. 21, at the maximum of the quasifree peak the structure function[12] $F_{LT}^{\prime 1-1}$ changes by 10% and 17% in going from the model with $G_E^n=0$ to the parametrizations of Refs. 135 and 136, respectively. Owing to the weak dependence on the contributions of non-nucleon degrees of freedom and on the np interaction model, this result makes the reaction $\vec{d}(\vec{e},e')np$ one of the most promising candidates for solving the problem in question.

We see from Fig. 22 that even at small values of q^* the choice of G_E^n significantly affects the asymmetry α_{ed}^V. As q^* increases this effect becomes even stronger.

In relation to this, we note that according to our calculations,[139] the cross sections for the reaction $d(e,e')np$ at threshold, i.e., far from the quasifree peak, for $q_\mu^2 \gtrsim 20$ F^{-2} change by several times in going from one model of the neutron electric form factor to another. Of course, this observation is not very important, owing to the dominant contributions of meson-exchange currents, which can be calculated by model-dependent methods.

4.5. MEC and FSI effects in electrodisintegration of polarized deuterons. The VEPP experiment in Novosibirsk

The results of our studies of the target asymmetries and azimuthal asymmetries for the reaction $\vec{d}(e,e'p)n$ as a function of the model of the EM current of the deuteron and FSI effects have been presented at the conference in Adelaide[140] and published in Ref. 19. There it was shown that the FSI in the np pair plays an important role in forming the angular and energy dependences of these asymmetries. Our calculations have been carried out both near the maximum of the quasifree peak and far from it. Some of the asymmetries depend significantly on G_E^n and on the spin–orbit EM interaction with the nucleons.

In Figs. 23 and 24 we show our results for the conditions of the experiment in Ref. 45 with a tensorially polarized (internal) deuterium target for energy of the electrons in the storage ring $E=2$ GeV. In this experiment the scattered electron was not detected, and np coincidences were recorded. Events corresponding to the situation where electrons are scattered at zero angle, i.e., $\theta_e \simeq 0°$, were selected. In other words, the cross sections for the reaction $\vec{d}(e,pn)e'$ at the photon point ($q_\mu^2=0, q=\omega$) were measured. The average degree of tensor polarization of the deuterium jet obtained in Ref. 45 was $P_{ZZ}=\pm(0.778\pm0.075)$. We note that $P_2=P_{ZZ}/\sqrt{2}$. Other details and explanations can be found in Refs. 19 and 45.

In this case it follows from Eqs. (2.27)–(2.29) that

$$\sigma^{(0)}=W_T,$$

$$\sigma^{(2)}=P_2\sum_{M\geqslant 0} W_T^{2M}\cos[M(\phi-\phi_H)]d_{M0}^2(\theta_H).$$

The quantities of interest to us are defined as ratios

$$T_{2M}=W_T^{2M}/W_T \tag{4.20}$$

of transverse structure functions.

In the PWIA we obtain

$$T_{20}=2u(k_n)d_{00}^2(\theta_H),\quad T_{22}=4u(k_n)d_{20}^2(\theta_H), \tag{4.21}$$

$$u(k_n)=\left[u_0(k_n)-\frac{1}{\sqrt{8}}u_2(k_n)\right]\frac{u_2(k_n)}{u_0^2(k_n)+u_2^2(k_n)}, \tag{4.22}$$

where u_0 (u_2) are the S (D) components of the deuteron wave function, and θ_n is the neutron emission angle in the lab frame relative to $\vec{q}$.

Equations (4.21)–(4.22) have to a considerable degree provided the motivation for measurements which have revealed a way of directly probing the properties of the deuteron. However, as can be seen from Fig. 23, the simple PWIA predictions are strongly distorted by FSI and MEC effects (especially with increasing momentum of the neutron in the deuteron). Meanwhile, these factors must be taken into account in describing the experimental data (Fig. 24). Of course, the data of Ref. 45 contain large uncertainties. Future measurements at electron accelerators with high duty-factor will ensure a qualitatively new level of research.

4.6. Mechanisms of the reaction ^{3}He($\vec{\gamma}$,p)d. Calculation using Faddeev wave functions

An important element determining the amplitude (2.53) is the wave function of the ^{3}He nucleus. This function can be expressed in terms of the Faddeev component $\Psi^{(1)}$:

$$|\Psi\rangle=[1-(1,2)-(1,3)]|\Psi^{(1)}\rangle, \tag{4.23}$$

where (α,β) is the operator permuting the nucleons numbered α and β.

In our calculations the vector $|\Psi\rangle$ is projected onto the basis of vectors $|\vec{p},\vec{q};SM_Sm;(Tt)\mathcal{T}\mathcal{T}_Z\rangle$ (see Refs. 9 and 10). Each such vector is the product of space, spin, and isospin parts. The relative momenta $\vec{p}$ and $\vec{q}$ are related to the nucleon momenta in ^{3}He as

$$\vec{p}=\frac{1}{2}(\vec{p}_2-\vec{p}_3),\quad \vec{q}=\frac{1}{3}(2\vec{p}_1-\vec{p}_2-\vec{p}_3).$$

The spin part of the basis vector is an eigenstate of the commuting operators

$$\vec{S}^2=(\vec{s}_2+\vec{s}_3)^2,\vec{s}_1^2,\vec{s}_2^2,\vec{s}_3^2,\quad S_Z\quad\text{and } s_{1Z},$$

and the isospin part is one of the operators

$$\vec{T}^2=(\vec{t}_2+\vec{t}_3)^2,\vec{t}_1^2,\vec{t}_2^2,\vec{t}_3^2,\quad \mathcal{T}^2=(\vec{T}+\vec{t})^2\quad\text{and } \mathcal{T}_Z,$$

where $\vec{s}_\alpha$ ($\vec{t}_\alpha$) is the nucleon spin (isospin) operator. The wave function of the ^{3}He nucleus in this basis is determined by a set of 16 complex numbers at each point of phase space:

$$\Psi_{SMmT}(\vec{p},\vec{q})=\langle\vec{p},\vec{q};SMsm;(Tt)\mathcal{T}\mathcal{T}_Z|\Psi_{J=J_Z=1/2}\rangle,$$

where J (J_Z) is the total angular momentum (its projection on the Z axis) of the ^{3}He nucleus.

The wave function $\Psi_{SMmT}(\vec{p},\vec{q})$ has been calculated from the expressions of Ref. 10, using the parametrization of Ref. 141 for the solutions of the Faddeev equations with the Reid soft-core potential. The good agreement between the values of the charge form factor $F_{ch}(Q)$ of the ^{3}He nucleus obtained with the exact and the parametrized functions for momentum transfers $Q\lesssim 8$ F^{-1}, i.e., up to the second mini-

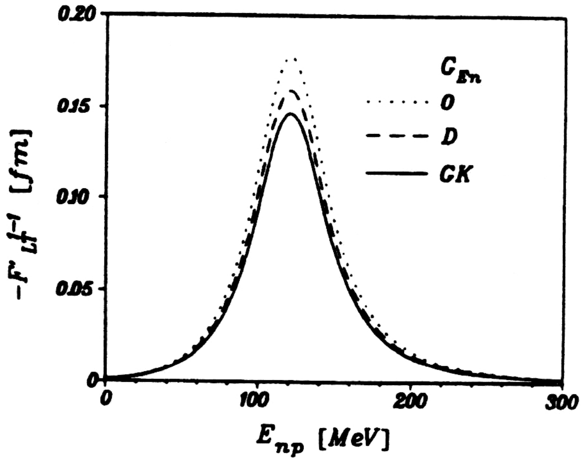

FIG. 21. Longitudinal–transverse response function for the reaction $d(\vec{e},e')np$ for $q^{*2}=12$ F^{-2}. The curves were calculated (Ref. 16) for: $G_E^n=0$ (dotted line), Ref. 135 (dashed line), and G_E^n from Ref. 136 (solid line). Further explanation can be found in Ref. 16.

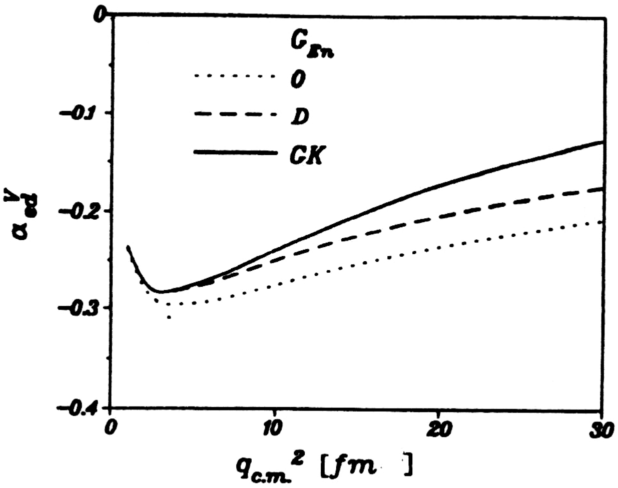

FIG. 22. Effect of G_E^n on the mixed asymmetry $\alpha_{ed}^V(\pi/2,0)$ in the reaction $\vec{d}(\vec{e},e')np$ for quasifree kinematics with $\theta_l=60°$. The differences between the curves are the same as in Fig. 21.

mum (see Fig. 1 in Ref. 141), indicates that the quality of this parametrization is quite high. Our calculations of $F_{\rm ch}(Q)$ confirm this.

The amplitude (2.53) without the FSI is

$$T_\lambda(m_pM_dJ_Z)=-e(6\pi/E_\gamma)^{1/2}\vec{\varepsilon}_\lambda \times\langle\varphi^{(1)}_{\vec{k}_pm_p}\varphi_{\vec{k}_dM_d}(2,3)|\mathbf{J}(\vec{k}_\gamma)|\Psi_{1/2J_Z}\rangle, \tag{4.24}$$

where the plane wave $\varphi_{\vec{k}m_p}(1)$ $[\varphi_{\vec{k}_dM_d}(2,3)]$ describes the state of the emitted proton (deuteron).

Using the properties of the current (2.10), it is easily seen that

$$T_\lambda=(-m_p,-M_d,-J_Z)=(-1)^{m_p+M_d+J_Z}T_\lambda^*(m_pM_dJ_Z). \tag{4.24$'$}$$

In other words, for each λ only six of the matrix elements (4.24) are independent.

Furthermore, taking into account the symmetry of the amplitudes under reflection in the reaction plane, we find[9]

$$T_\parallel(m_pM_dJ_Z)=T_\parallel^*(m_pM_dJ_Z), \tag{4.25}$$

$$T_\perp(m_pM_dJ_Z)=-T_\perp^*(m_pM_dJ_Z). \tag{4.26}$$

Therefore, when $\vec{\varepsilon}_\lambda$ lies in the reaction plane (perpendicular to it) the amplitude of the reaction (2.52) without the FSI is real (purely imaginary). In particular, these relations are good tests for the complicated numerical calculations involving the Faddeev wave functions.

It follows from (4.24′) that

$$\sigma_\lambda\equiv d\sigma_\lambda/d\Omega_p=R\sum_{m_pM_d}|T_\lambda(m_pM_d)|^2, \tag{4.27}$$

where

$$T_\lambda(m_pM_d)=T_\lambda\left(m_pM_dJ_Z=+\frac{1}{2}\right).$$

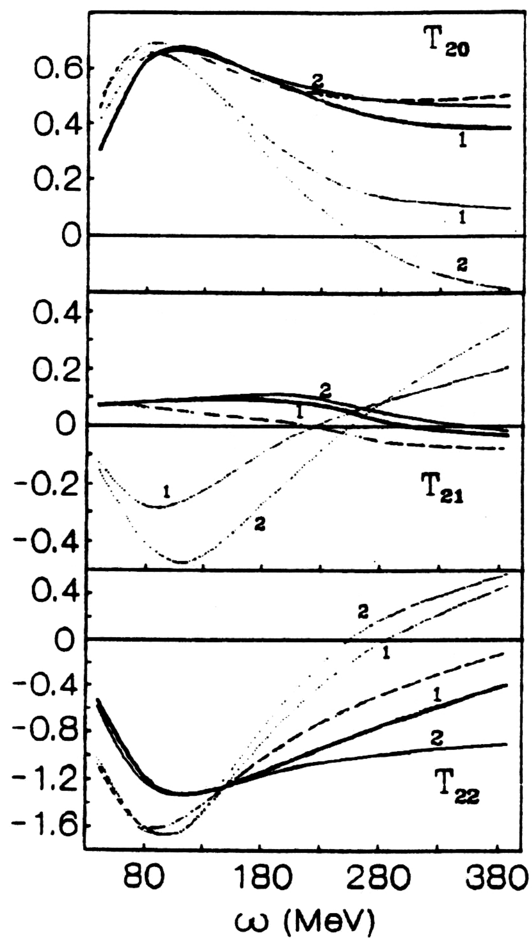

FIG. 23. Tensor asymmetries for $^2\vec{H}(e,pn)e'$ under the VĚPP-3 conditions. The curves show our results (Ref. 19) in the PWBA (dotted lines *1*), PWIA (dotted lines *2*), DWBA (dashed lines), and DWBA+MEC ($\Lambda=4m_\pi$; solid lines).

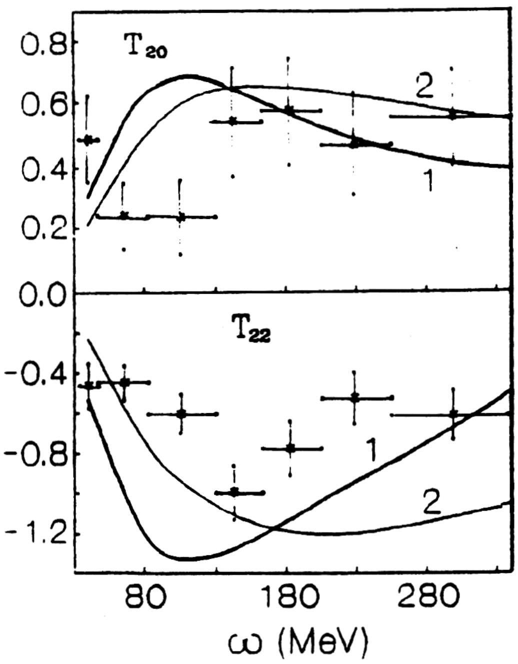

FIG. 24. Comparison of the calculated asymmetries T_{20} and T_{22} with the data of Ref. 45. The solid (dashed) lines were calculated with inclusion of FSI and MEC effects with $\Lambda=4m_\pi$ ($\Lambda=1.2$ GeV).

In addition, in the plane-wave approximation the cross section is the sum of two incoherent parts:

$$\sigma_\lambda=\sigma_\lambda(\mathrm{CC+MEC})+\sigma_\lambda(\mathrm{MC+SO}), \tag{4.28}$$

where the abbreviations CC, MEC, (MC), and SO stand for the convection current, meson-exchange current, magnetization current, and spin–orbit contributions. These properties simplify not only the calculations, but also the estimates of the various contributions to the cross sections.

Our results are compared with the experimental data and with calculations of other authors in Figs. 25–30. All the calculations have been carried out using Faddeev wave functions of the ^{3}He nucleus for the Reid soft-core potential (Refs. 31, 51, 75, 76, 79, 110, and 148) and the Paris potential (Ref. 89). The quantitative discrepancies between the results of our calculations and those of Ref. 79 are most likely due to the differences between the ^{3}He wave functions that are used: whereas in Ref. 79 this wave function contains 11 components with relative angular momenta $L,l\leqslant 3$, in our approach Ψ is constructed by using Eq. (4.23) for the five partial components of $\Psi^{(1)}$ (Ref. 141) with $L,l\leqslant 2$. We note that in Ref. 79 (Ref. 141) the solutions of the Faddeev equations obtained in Ref. 149 (Ref. 150) were used.

In Fig. 25 we see that the addition of three D waves to the two S waves in the partial-wave expansion of $\Psi^{(1)}$ (Ref. 141) significantly increases the cross section for $E_\gamma\gtrsim 100$ MeV, making the energy dependences and asymmetries smoother, and filling in the dip whose location is determined by the line of nodes in the ^{3}He wave function (cf. Ref. 10). The reason for the large discrepancies with the Laget calculations[89] remains unclear.

The MEC contributions nearly always increase the differential cross section. As shown in Fig. 26a, this enhancement is about 50% beginning at $E_\gamma=30$ MeV.[13)] Meson-exchange currents have nearly the same effect on the proton angular distribution in Fig. 27a up to angles $\theta_p\simeq 120°$. For $\theta_p\simeq 150°$ there is destructive interference of the CC and MEC contributions, which leads to a decrease of the cross section. Moreover, more detailed analysis (see Ref. 110, for example) reveals a strong mutual cancellation of the contributions from seagull and pionic currents. Their total contribution can be enhanced by increasing the value of Λ (for example, taking $\Lambda=1.2$ GeV). However, our calculations show that this leads to even greater discrepancies between theory and experiment for the asymmetry. We again find it necessary to have a consistent definition of the MECs and NN interaction, and we see that it is important to carry out combined studies involving unpolarized and polarized particles.

As far as the competition of the (CC) and MEC contributions is concerned, we should note the inequality $\sigma_\parallel(\mathrm{kT})\gg\sigma_\perp(\mathrm{kT})$, except for certain angular ranges of the forward and backward proton emission, where the asymmetry falls rapidly from 1 to zero because we approach the collinear kinematics. As can be seen in Fig. 27b, the corresponding range in the forward hemisphere is very narrow. Meson-exchange current contributions lead to a noticeable deviation of Σ from 1 beyond these ranges. For $\theta_p=90°$ the asymmetry Σ(MEC) is a function of E_γ with changing sign (Fig. 26b).

The addition of the magnetization current to the CC and MEC contributions increases the differential cross section, since its contribution calculated without the FSI is, as noted above, incoherent with respect to these currents. As expected, the magnetic interaction is manifested most strongly at angles θ_p close to 0° and 180°. For proton emission angles in the backward hemisphere the recoil mechanism dominates; it corresponds to photon absorption by spectator nucleons. A similar result was obtained in the study of the reactions $^4\mathrm{He}(\vec{\gamma},p)^3\mathrm{H}$ and $^4\mathrm{He}(\vec{\gamma},n)^3\mathrm{He}$ (Ref. 132).

We note that whereas the contribution of the recoil mechanism related to the CC is determined by the components of the wave function Ψ with $S=1$ and $T=0,1$,[14)] in the case of the MC the corresponding amplitude depends on the entire set of components of this wave function. Our analysis of the formation of the angular dependence of the cross section in Fig. 28a has shown that the contribution of the recoil mechanism for the MC depends on the components of the ^{3}He wave function with $T=1.0$. However, owing to the inequality $(\mu_p-\mu_n)^2\gg(\mu_p+\mu_n)^2$, where μ_p (μ_n) is the proton (neutron) magnetic moment, the relative importance of transitions via the intermediate state with $T=1$ is noticeably enhanced. Therefore, this result does not correspond to the ideas of the quasideuteron mechanism of photonuclear reactions at intermediate energies.[151]

The MC has a significant effect on the asymmetry coefficient. The photon interaction with the nucleon magnetic moments increases $\sigma_\perp$, so that $\sigma_\perp(\mathrm{MC})>\sigma_\parallel(\mathrm{MC})$ for $10\leqslant E_\gamma\leqslant 110$ MeV. The equation $\sigma_\perp(\mathrm{MC})=\sigma_\parallel(\mathrm{MC})$ holds if

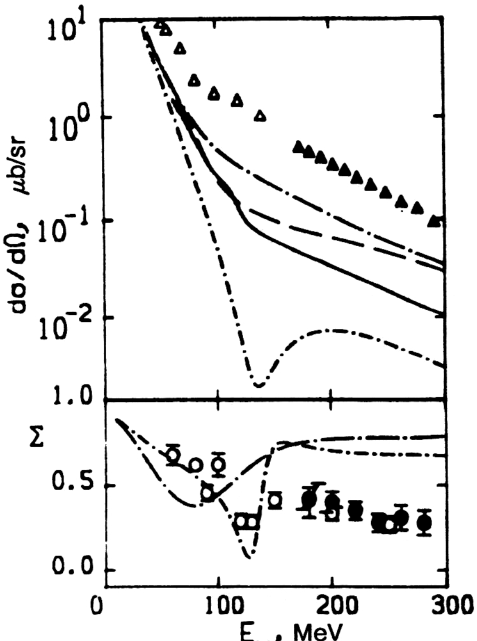

FIG. 25. Differential cross section and asymmetry coefficient for two-body photodisintegration of the ^{3}He nucleus versus the photon energy at proton emission angle in the lab frame $\theta_p^*=90°$. The results of the calculations with only the CC and MC contributions are shown. The solid (dashed) line is taken from Ref. 79 (Ref. 89). The dot–dashed lines with short (long) dashes were calculated in Refs. 75 and 110 using S ($S+D$) waves in $\Psi^{(1)}$ and $S+D$ waves in the deuteron wave function. The points △, ▲, ○, and ● are the data of Refs. 142, 143, 144, and 145, respectively.

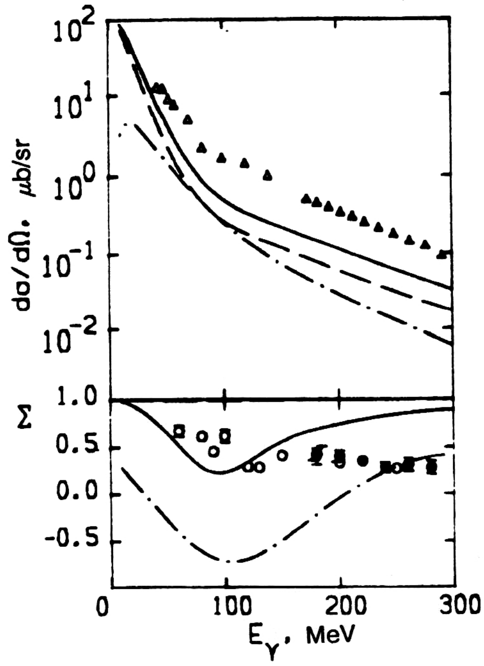

FIG. 26. The same as in Fig. 25. The dashed (dot–dashed) lines were calculated with CCs (MECs), and the solid lines were calculated with both CTs and MECs.

we restrict ourselves to only S waves in $\Psi^{(1)}$, and it is violated when D waves are included in $\Psi^{(1)}$ or the ^{3}He wave function.

In trying to improve the agreement between theory and experiment, we studied other mechanisms of photon absorption by the ^{3}He nucleus, viz., inclusion of the π-meson current with Δ-isobar excitation in the intermediate state, the ρ-MEC, and the nucleon spin–orbit electromagnetic interaction. The role of the latter is discussed in Sec. 4.7; here we note that the inclusion of the Δ-isobar current[96] does not have any noticeable effect on the energy dependences in Fig. 25. This is the case because its contribution is suppressed, for example, relative to the seagull current by a factor $\sim k/m$ where k is the virtual pion momentum. The ρ-MEC effects are shown in Fig. 30.

4.7. Relativistic corrections to deuteron electrodisintegration and two-body breakup of ^{3}He by linearly polarized photons

Let us begin our discussion of relativistic corrections (RCs) in these processes by defining the spin–orbit (SO) current mentioned in Secs. 3.2 and 4.6. Earlier it was shown[152,153] that the inclusion of the SO current improves the description of the cross sections and the polarization observables for deuteron photodisintegration below and above the pion-production threshold. This contribution is usually viewed as the result of the nonrelativistic reduction of the one-body current $J_\mu^{[1]}(\vec{q})$:

$$\rho_{SO}^{[1]}(\vec{q})=\vec{q}\vec{g}(\vec{q}), \tag{4.29}$$

$$\mathbf{J}_{SO}^{[1]}(\vec{q})=[K,\vec{g}(\vec{q})], \tag{4.30}$$

$$\vec{g}(\vec{q})=-\frac{i}{4m^2}\sum_\alpha (F_{1\alpha}+2F_{2\alpha})e^{i\vec{q}\vec{r}_\alpha}[\vec{\sigma}_\alpha\times\vec{p}_\alpha].$$

Following Ref. 153, we define the spatial components of the SO current as

$$\mathbf{J}_{SO}(\vec{q})=\mathbf{J}_{SO}^{[1]}(\vec{q})+\mathbf{J}_{SO}^{[2]}(\vec{q})=[H,\vec{g}(\vec{q})]. \tag{4.31}$$

The current $J_{SO}(\vec{q})=(\rho_{SO}^{[1]}(\vec{q}),\mathbf{J}_{SO}(\vec{q}))$ is conserved, since

$$\vec{q}\mathbf{J}_{SO}(\vec{q})=[H,\rho_{SO}^{[1]}(\vec{q})], \tag{4.32}$$

i.e., this inclusion of the SO electromagnetic interaction does not spoil the gauge invariance of the theory.

It is easy to see that the on-energy-shell matrix element of $\mathbf{J}_{SO}(\vec{q})$ coincides with the well known result[107] for the SO contribution.

We also note that, according to the classification used in Ref. 154, the current (4.31) is of order m^{-3} and is therefore a relativistic correction to the CC and the MC, which are $\sim m^{-1}$. As shown in Fig. 28a, the contribution of $\mathbf{J}_{SO}$ to the differential cross section for $\theta_p=90°$ is small compared with that of MECs for $E_\gamma \lesssim 300$ MeV. The relative importance of this current increases with the photon energy.

In the proton angular distribution the contribution of the SO current is concentrated in the forward hemisphere, and $\sigma_{SO}(\theta_p=0°)\gg\sigma_{SO}(\theta_p=180°)$. This property is explained by the fact that the contribution of the recoil mechanism due to $\mathbf{J}_{SO}$ is not really noticeable in the background of direct proton knockout in the entire range of angles θ_p.

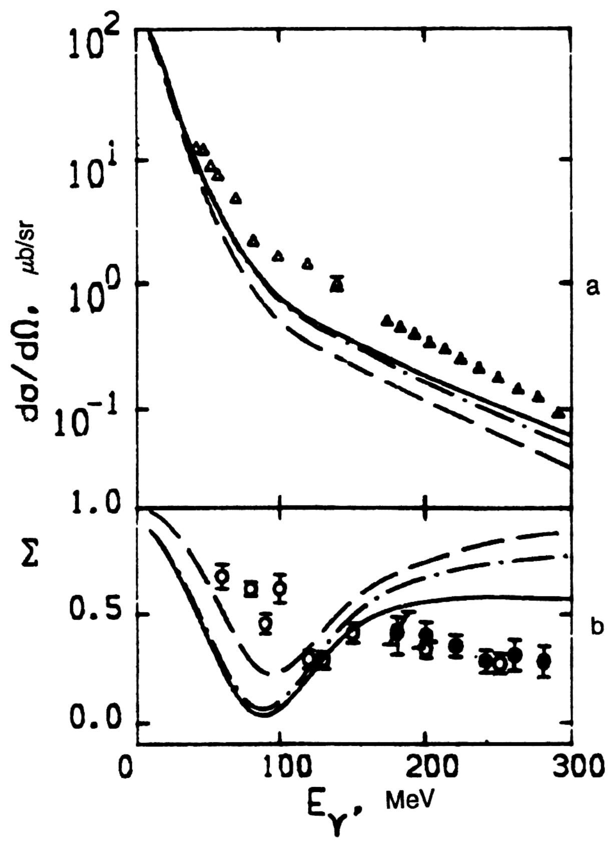

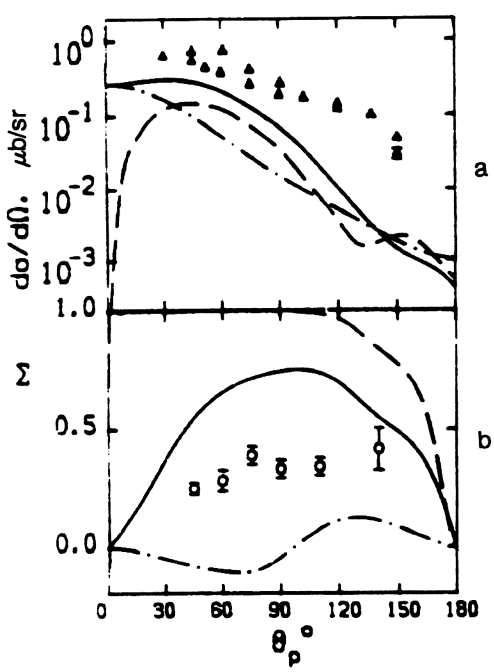

FIG. 28. The same as in Fig. 26. The dashed (dot–dashed) lines were calculated with the CC and MEC (CC, MEC, and MC) contributions, and the solid lines were calculated with the CC, MEC, MC, and SO-current contributions.

FIG. 27. Angular dependences of the differential cross section for $E_\gamma=240$ MeV and of the asymmetry coefficient for $E_\gamma=200$ MeV. The calculations were done using the same currents as in Fig. 26. The points △, ▲, and ○ are taken from Refs. 146, 147, and 144.

The spin–orbit interaction has a much greater effect on the Σ asymmetry. In particular, the values of Σ in Fig. 28b are significantly decreased for $E_\gamma>150$ MeV. For $E_\gamma=300$ MeV this relativistic effect reaches about 30%, making the calculated energy dependence of Σ approach the experimental data. As shown in Figs. 31–34, the RCs can affect various observables in deuteron electrodisintegration. In particular, our calculations of A_ϕ in which along with the *SO* interaction we included the Darwin–Foldy corrections to the charge-density operator, improve the agreement between theory and experiment (see the dotted and solid lines in Fig. 32). The dependence of A_ϕ that we calculated is, for small $p_m\leqslant150$ MeV/s, practically the same as the curve obtained in the relativistic description.[53] The main ingredients of the latter are:

(a) The use of the complete on-mass-shell current $J^{[1]}_\mu(q)$ with Dirac form factors F_1 and F_2 [cf. (3.25)].

(b) The solutions of the quasipotential equations for the initial and final states of the *np* pair with a relativistic *np* interaction generated by π, ρ, ε, ω, η, and δ exchange.

Meson-exchange currents were not considered in Ref. 53.

On the whole, the sizable discrepancy between the results of various groups, on the one hand, imposes stricter requirements on the theory, while, on the other, it requires of experimentalists more precise measurements at larger p_m

The behaviors of the calculated ratios shown in Fig. 33,

$$S_L/S_T=W_Lw_T/W_Tw_C,\quad S_{TL}/S_T=W_{LT}w_T/W_Tw_I,$$

where w_C, w_T, and w_I are defined according to the CC1 prescription in Ref. 69, display different trends after the inclusion of RCs. In particular, the inclusion of RCs in Fig. 32c leads to overestimation of the Saclay data.[157] The results of other authors are also overestimated (see Fig. 5 of Ref. 126).

The distinctive feature of the Bonn measurements[158] is that they probe the high-momentum components of the deuteron wave function ($314\leqslant p_m\leqslant653$ MeV/s). Under these conditions relativistic effects play an ever greater role. As our calculations (solid line in the upper part of Fig. 34a) show, they improve the agreement between theory and experiment, and they produce a qualitative change in the polarization of the knocked-out protons (particularly at large *W*). Of course, in order to understand the true role of the relativistic dynamics at these values of the invariant mass it is necessary to have a consistent covariant description of the reaction mechanisms and the deuteron structure.

Relativistic effects are manifested particularly clearly under conditions close to the parallel kinematics (cf. the solid lines *1* and *2* in Figs. 17 and 18), when small momenta of the nucleons inside the deuteron are probed. Our analysis shows that here the dominant contribution comes from Darwin–Foldy relativistic corrections.

4.8. Angular distributions and polarization of cumulative protons in the reaction $d(e,e'\vec{p})n$

Study of the polarization phenomena in deuteron electrodisintegration at large nucleon emission angles (≳90°) rela-

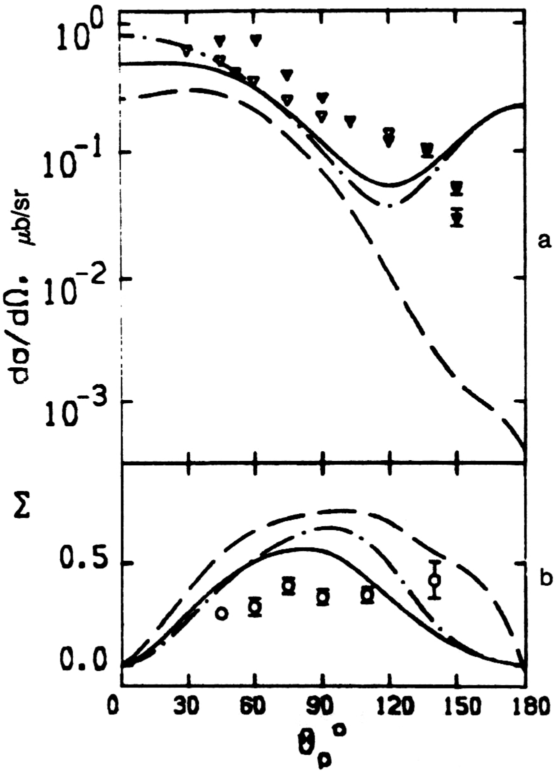

FIG. 29. The same as in Fig. 27. The differences between the curves are given in the caption to Fig. 28.

tive to the direction of the incident electron beam, i.e., in the so-called cumulative kinematics forbidden for eN scattering on a free nucleon at rest, can provide an additional test for the mechanisms of particle production at backward angles (see, for example, the reviews of Refs. 159 and 160 and references therein).

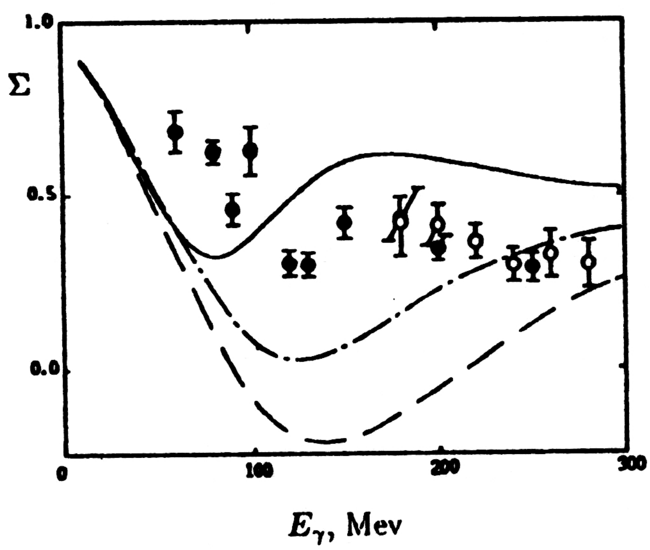

FIG. 30. The same as in Fig. 25. The solid line was calculated with the CC, MEC, and SO-current contributions, and the dashed (dot–dashed) line was calculated with the π-MEC (π- and ρ-MECs) for Λ_π=1.2 GeV, Λ_ρ=1.5 GeV and the tensor coupling parameter χ_ρ=6.6 (Ref. 96).

Here we present (Fig. 35) the results of our first calculations[67] of the angular dependences of the cross sections and polarization of cumulative protons in the case of deuteron electrodisintegration. We also show the left–right asymmetries $A_\sigma \equiv A_\phi$ and A_p:

$$A_i=[F_i(\pi)-F_i(0)][\sigma_0(\pi)+\sigma_0(0)]^{-1}, \tag{4.33}$$

where $F_\sigma(\phi)=\sigma_0(\phi)$ and $F_p=\sigma_0(\phi)P(\phi)$. These studies are also of independent interest, because cumulative processes on the simplest bound system of nucleons are important ingredients in searches for manifestations of short-range correlations in few-particle clusters embedded in a nuclear medium.[161,162] We prefer to use the meson–nucleon picture, because we think its possibilities are far from exhausted.

The calculations of Fig. 35 were carried out at fixed values of the energy $E=1.8$ GeV and $E'=1.64$ GeV of the incident and scattered electrons and at scattering angle $\theta_e=15°$. This situation corresponds to the so-called dip region with $x<1$, where manifestations of non-nucleon degrees of freedom can be expected.

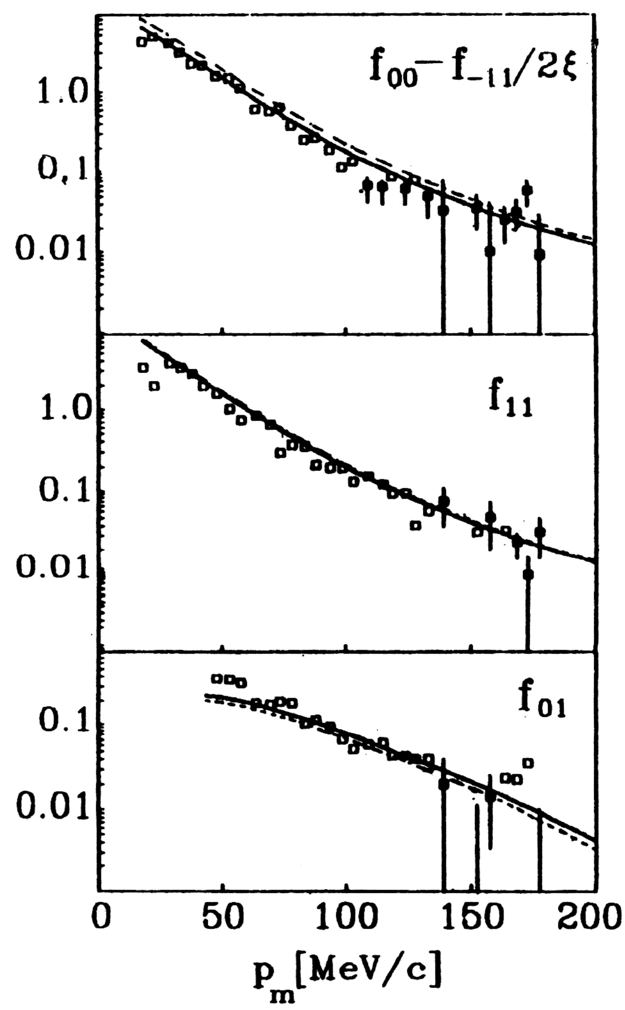

FIG. 31. Dependence of the structure functions isolated in the experiment of Ref. 54 on the missing momentum. The solid (dashed) lines were calculated with the FSI and MEC contributions (Λ=1.2 GeV) and with (without) relativistic corrections.

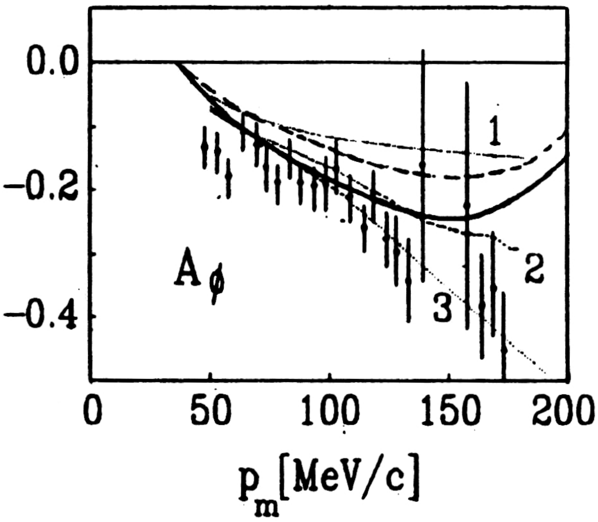

FIG. 32. Azimuthal (left–right) asymmetry versus p_m The dashed lines *1*, *2*, and *3* are the results of the calculations in the approaches of Refs. 39, 53, and 156, respectively. The differences between the dashed and solid lines are the same as in Fig. 31. The points are taken from Ref. 54.

We see that FSI effects play an important role in forming the cumulative proton angular distributions. The FSI distortions can probably be imitated by adding non-nucleon components to the deuteron wave function. However, when cumulative proton polarization is studied simultaneously this procedure is subjected to serious tests. The inclusion of MECs generated by π exchange slightly changes the DWBA predictions.

Work on off-shell and relativistic effects in this region is in progress.

5. CONCLUSION

Among the problems and successes in current studies of polarization phenomena in photo- and electrodisintegration of few-nucleon systems are the following:

(1) Measurements using polarized deuterium and helium targets and polarized high-intensity photon and electron beams are among the main activities at many scientific centers. This research, which has already produced rich information about the properties of bound nucleons, is constantly becoming broader (especially with the introduction of electron accelerators with a small off-duty factor).

(2) The presently existing theoretical results in the spin physics of very light nuclei using unpolarized and polarized photons and electrons (especially reactions with the detection of scattered electrons in coincidence with nuclear fragments) form a solid basis for future polarization experiments which will be even more informative. This joining of forces of theoreticians and experimentalists can lead to a deeper understanding of the effect of the nuclear environment on the electromagnetic interactions of a bound nucleon (for example, off-shell effects at the γNN vertex, which have been little studied so far), the role of meson exchange in forming the spin-dependent response functions of few-nucleon systems, and the behavior of nuclear wave functions at small distances in approaching momentum transfers $\sim$1 GeV/s.

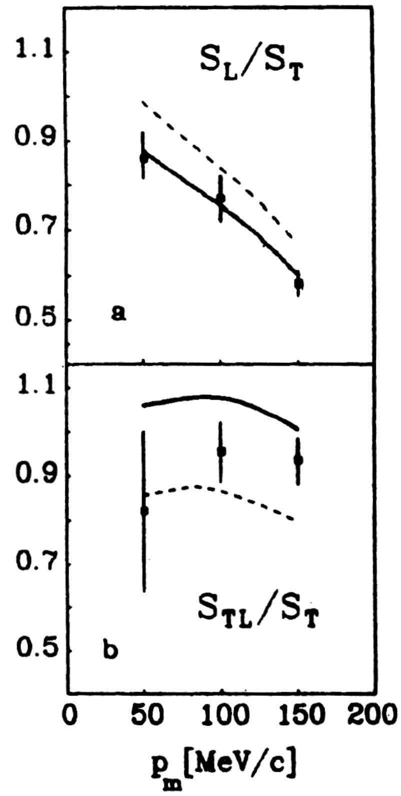

FIG. 33. Ratios S_L/S_T (a) and S_{TL}/S_T (b) versus p_m for $q=400$ MeV/*s*. The differences between the curves are given in Fig. 31. The points are taken from Ref. 157.

(3) Satisfaction of the requirements of gauge independence of the theory is important for achieving these goals. In particular, as shown by our calculations, the proton polarization for the reaction $d(e,e'\vec{p})n$, the tensor asymmetries of the target for the reaction $\vec{d}(e,e'p)n$, and the beam asymmetry in the reaction ^{3}He$(\vec{\gamma},p)d$ with linearly polarized photons are very sensitive to inconsistency of the electromagnetic current of the nucleus and the NN-interaction model (especially when high-momentum components of the deuteron and the ^{3}He nucleus are probed).

(4) The strong interaction of the products of (real or virtual) photon-induced nuclear breakup is an important ingredient in the description of various spin observables. In particular, in the theory without P and T violation the proton polarization in the reactions $d(e,e'\vec{p})n$ and ^{3}He$(\gamma,\vec{p})d$ is identically equal to zero if the FSI is included. Therefore, comparison of the corresponding theoretical predictions and the results of measurements can be a source of additional information about the dependences of the functions describing the continuous spectrum of $2N$ and $3N$ systems on nuclear-force models. In many cases the distortions introduced by the FSI must be included for reliable testing of the nucleon electromagnetic interaction mechanisms and nuclear-structure effects. They can be very noticeable not only far from the quasifree kinematics (cf. our analysis of the asymmetries of the cross sections for disintegration of tensor deuterons by electrons near the photon point with $q_\mu^2=0$), but also in the vicinity of the quasifree peak, when the

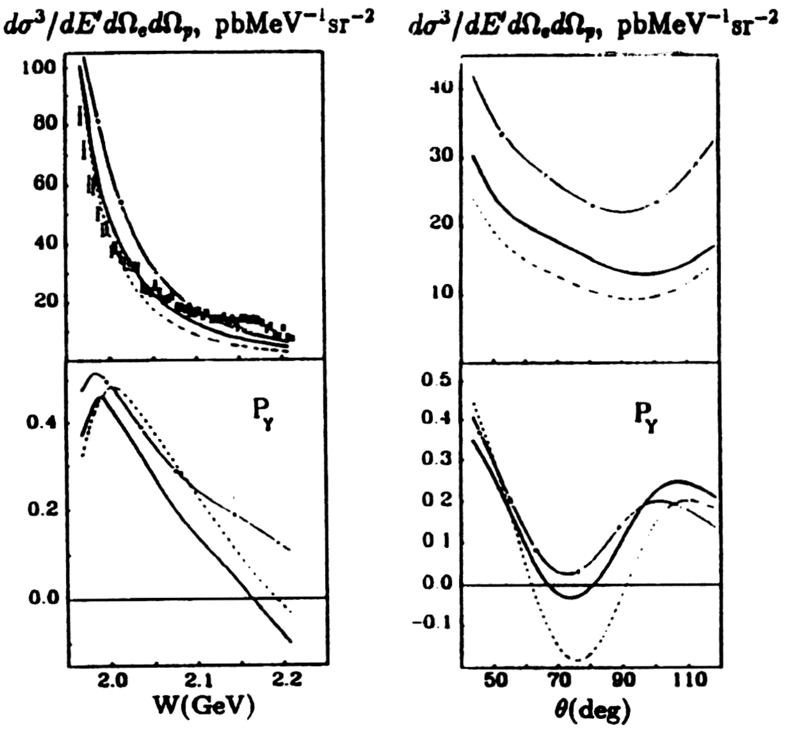

FIG. 34. Differential cross sections (upper part) and proton polarization (lower part) for the reaction $H(e,e'\vec{p})n$ as functions of the invariant mass W of the final np pair (left) and the angle θ between $\vec{k}_p$ and $\vec{q}$ for $W=2.03$ GeV (right). The dashed, solid, and dot–dashed lines were calculated by us (Ref. 155) with the DWBA, DWBA+MEC+RA, and DWBA +MEC, respectively. The experimental data were obtained in Bonn.[158]

Bjorken variable is $x \cong 1$. As we have seen, FSI effects are clearly manifested in the formation of the angular distributions and polarization of cumulative protons in the reaction $d(e,e'\vec{p})n$. For photo- and electrodisintegration of $3N$ nuclei at medium energies, the inclusion of the FSI in calculations involving realistic NN potentials remains a challenge for theorists.

(5) The spin observables in the electrodisintegration of the deuteron and the ^{3}He nucleus are of great interest for extracting the electric form factor of the neutron. Among the ideas in this area which are either being pursued now or which pertain to machines of the new generation (AmPS, SHR, ELSA, CEBAF), noteworthy ones are measurements of the polarization transferred to the nucleon in the reactions $d(\vec{e},e'\vec{n})p$, $\vec{d}(e,e'\vec{n})p$, and $\vec{d}(\vec{e},e'\vec{p})n$, of the mixed asymmetry in the reaction $\vec{d}(\vec{e},e'n)p$ with a vector polarized target, and of the beam asymmetry for the reactions $^3\vec{He}(\vec{e},e'n)pp$ (the Mainz experiments) and ^{3}He$(\vec{e},e')$ (the experiments at the MIT–Bates Laboratory). Extensive theoretical studies have shown that the most favorable kinematical conditions for exclusive reactions of this type are realized in the parallel kinematics, where FSI and MEC effects are small, so that one is dealing with quasifree $eN-e'N'$ scattering. The proton polarization induced by the FSI in the reaction $d(e,e'\vec{p})n$ undergoes a qualitative change in going from one model of G_E^n to another, which makes this reaction (without a polarized electron beam) yet another candidate for the extraction of this fundamental quantity.

(6) We find two regions corresponding to the left- and right-hand sides of the quasifree peak where the proton polarization in the reaction $d(e,e'\vec{p})n$ takes values which can be measured in a continuously working accelerator like that at CEBAF. From the physical point of view it would be interesting to perform such measurements in the parallel kinematics, where this polarization is described most simply, i.e., by a single structure function depending on the LT interference of the components of the deuteron current.

(7) The significant discrepancies between the results of theoretical studies of photon-induced two-particle breakup of the ^{3}He nucleus at photon energies $E_\gamma > 100$ MeV make it necessary to perform additional (perhaps more careful) calculations of the high-momentum components of the wave function of this $3N$ system. It should be stressed that all these results, which have been obtained without the FSI in the pd system, do not give a satisfactory description of the data on the cross sections for the reaction ^{3}He$(\gamma,p)d$ and the asymmetry coefficient. The inclusion of meson-exchange currents improves the description of the cross sections, but at the same time it increases the discrepancies between the calculated and measured asymmetries.

(8) Calculations show that some observables in the processes that we have considered depend strongly on the RCs to the nuclear electromagnetic current and the nuclear wave functions. For example, under the conditions of quasifree kinematics the corresponding effects in the angular dependences of the asymmetry A_ϕ, the polarization transfers $P_t'(n)$, $P_{1Z}(n)$, and $P_{2X}^h(p)$, and the mixed asymmetry $A_V'(\pi/2,0)$ for the exclusive breakup of the deuteron are manifested at relatively small q_μ^2. Since in such situations these observables are determined by the longitudinal–transverse structure functions, the isolation of the structure functions can give new information about the role of relativistic effects in nuclei.

Of course, when the high-momentum components of the nuclear wave functions are probed it is necessary to relativize the theory further, including, for example, the retardation effects in meson-exchange currents and the solutions of the relativistic equations for the states of the hadron system ei-

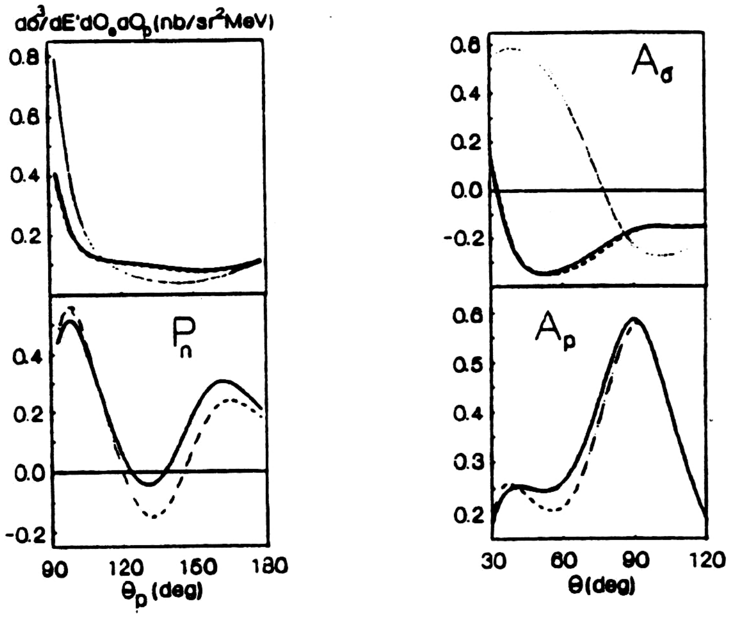

FIG. 35. The angular dependences of the differential cross section σ_0 in the reaction $d(e,e'p)n$ and the polarization P in the reaction $d(e,e'\vec{p})n$ versus the angle θ_p between $\vec{k}_p$ and $\vec{k}$ for the case $\phi=\pi$ are shown on the left, and A_σ and A_p versus the angle θ between $\vec{k}_p$ and $\vec{q}$ are shown on the right. The calculations were done using the PWBA (dotted lines), DWBA (dashed lines), and DWBA+MEC with $\Lambda=4m_\pi$ (solid lines).

ther in the Okubo approach, which is based on on-mass-shell particles, or in the Bethe–Salpeter formalism with off-mass-shell particles in intermediate states.

APPENDIX A

We would like to show that the Okubo method described in Sec. 3.1 is an example of the solution of the general algebraic problem of diagonalization of a Hermitian matrix by means of a unitary transformation.

For this we turn to the model of interacting fields, a neutral scalar field (scalar meson field) and a spinless fermion field in which the recoil of the "heavy" fermion is neglected:

$$\mathscr{H}=\mathscr{H}_0+\mathscr{H}_I, \tag{A1}$$

$$\mathscr{H}_0=m_0\int \psi^+(\vec{p})\psi(\vec{p})d\vec{p}+\int \omega(\vec{k})a^+(\vec{k})a(\vec{k})d\vec{k}, \tag{A2}$$

$$\mathscr{H}_I=\frac{g}{(2\pi)^{3/2}}\int d\vec{p}\int d\vec{k}\,\frac{f(\vec{k}^2)}{\sqrt{2\omega(\vec{k})}}\,\psi^+(\vec{p}+\vec{k})\psi(\vec{p})\times[a(\vec{k})+a^+(-\vec{k})], \tag{A3}$$

where $\omega(\vec{k})=\sqrt{\vec{k}^2+\mu^2}$, μ is the meson mass, $f(\vec{k}^2)$ is a cutoff factor, and m_0 is the bare fermion mass.

The nontrivial commutation relations for the fermionic creation (annihilation) operators $\psi^+(\vec{p})$ $[\psi(\vec{p})]$ and $a^+(\vec{k})$ $[a(\vec{k})]$ are

$$\{\psi(\vec{p}),\psi^+(\vec{p}\,')\}=\delta(\vec{p}-\vec{p}\,'),$$
$$[a(\vec{k}),a^+(\vec{k}')]=\delta(\vec{k}-\vec{k}'). \tag{A4}$$

Let us consider the unitary transformation

$$V=\exp(iS), \tag{A5}$$

$$iS=\frac{g}{(2\pi)^{3/2}}\int\frac{f(\vec{k}^2)}{\sqrt{2\omega^3(\vec{k})}}\{B(\vec{k})a(\vec{k})-B^+(\vec{k})a^+(\vec{k})\}\equiv g(X-X^+), \tag{A6}$$

where we have introduced the notation $B(\vec{k})$ for the Fourier transform of the baryon density:

$$B(\vec{k})=\int e^{i\vec{k}\vec{x}}\psi^+(\vec{x})\psi(\vec{x})d\vec{x}=\int\psi^+(\vec{p}+\vec{k})\psi(\vec{p})d\vec{p}. \tag{A7}$$

Using the commutation relations, in particular, the identity

$$[AB,CD]=A[B,C]D+C[A,D]B,$$

which is valid when $[A,C]=[B,D]=0$, we find

$$[X,X^+]=\int\frac{f^2(\vec{k}^2)}{2\omega^3(\vec{k})}\frac{B(\vec{k})B^+(\vec{k})}{(2\pi)^3}d\vec{k} \tag{A8}$$

and

$$[X,[X,X^+]]=0. \tag{A9}$$

However, when (A9) is satisfied it can be shown that

$$V=e^{g(X-X^+)}=e^{-gX^+}e^{gX}e^{(g^2/2)[X,Xx^+]}.$$

From this we obtain

$$V^+a(\vec{k})V=a(\vec{k})-g\frac{f(\vec{k}^2)}{\sqrt{2(2\pi)^3\omega^3(\vec{k})}}B^+(\vec{k}) \tag{A10}$$

and

$$\mathscr{H}_V\equiv V^+\mathscr{H}V=mB(0)-\delta mB(0)-\int\omega(\vec{k})a^+(\vec{k})a(\vec{k})d\vec{k}$$

$$-\frac{g^2}{(2\pi)^3}\int \frac{f^2(\vec{k}^2)}{2\omega^2(\vec{k})} B^+(\vec{k})B(\vec{k})d\vec{k}. \quad \text{(A11)}$$

In (A11) we have isolated the mass counterterm with $\delta m = m - m_0$. It arises naturally as soon as we are interested in the potential part without self-interaction:

$$\int \frac{f^2(\vec{k}^2)}{2\omega^2(\vec{k})} B^+(\vec{k})B(\vec{k})d\vec{k} = \int \frac{f^2(\vec{k}^2)}{2\omega^2(\vec{k})} d\vec{k}B(0) - \int d\vec{k}\frac{f^2(\vec{k}^2)}{2\omega^2(\vec{k})}\int d\vec{p}\int d\vec{p}\,'\psi^+(\vec{p}+\vec{k})\psi^+(\vec{p}\,')\psi(\vec{p})\psi(\vec{p}\,'+\vec{k}), \quad \text{(A12)}$$

from which

$$\delta m = -\frac{g^2}{(2\pi)^3}\int \frac{f^2(\vec{k}^2)}{2\omega^2(\vec{k})} d\vec{k}. \quad \text{(A13)}$$

The second term in (A12) can be written in the canonical form for the potential energy (a two-body operator):

$$V = \int d\vec{x}\int d\vec{x}\,'\psi^+(\vec{x})\psi^+(\vec{x}\,')V(\vec{x}-\vec{x}\,')\psi(\vec{x})\psi(\vec{x}), \quad \text{(A14)}$$

$$V(\vec{x}-\vec{x}\,') = -\frac{g^2}{(2\pi)^3}\int \frac{f^2(\vec{k}^2)}{2\omega^2(\vec{k})} e^{i\vec{k}(\vec{x}-\vec{x}\,')}d\vec{k}. \quad \text{(A15)}$$

Therefore,

$$\mathcal{H}_V = mB(0) + H_M + V, \qquad H_M = \int \omega(\vec{k})a^+(\vec{k})a(\vec{k})d\vec{k}. \quad \text{(A16)}$$

We see that the significant difference between $\mathcal{H}_V$ and $\mathcal{H}$ is the splitting into the part H_M acting in the meson sector and the remaining part R_0 acting in the fermion sector:

$$H^{\text{eff}} \equiv P_0\mathcal{H}_V P_0 = mP_0B(0)P_0 + P_0VP_0, \quad \text{(A17)}$$

where, using the notation of Sec. 3.1, we have introduced the operator for projection onto the subspace P_0 without mesons:

$$P_0 = |0\rangle\langle 0| + |N;0\rangle\langle N;0| + |NN;0\rangle\langle NN;0| + \dots .$$

By definition, we have

$$a(\vec{k})|0\rangle = 0, \quad \psi(p)|0\rangle = 0 \quad \text{(A18)}$$

for the bare vacuum and

$$|N;0\rangle = \psi^+(p)|0\rangle \quad \text{(A19)}$$

for one-fermion states. From this it follows that

$$\mathcal{H}_0|0\rangle = 0.$$

In addition, in this model $\mathcal{H}|0\rangle = 0$,[15] but

$$\mathcal{H}|N;0\rangle \neq \lambda|N;0\rangle.$$

Regarding this, we note that the solution of the eigenvalue problem

$$H^{\text{eff}}|\chi\rangle = E|\chi\rangle \quad \text{(A20)}$$

is associated with the unitary partner

$$\mathcal{H}|\Psi\rangle = E|\Psi\rangle, \quad |\Psi\rangle = U|\chi\rangle. \quad \text{(A21)}$$

We see that

$$H^{\text{eff}}|0\rangle = 0, \quad \text{(A22)}$$

i.e., the bare vacuum is an eigenstate of H^{eff} with zero energy. Furthermore, according to (A20)–(A21) we have

$$\mathcal{H}|\Psi_0\rangle = 0, \quad |\Psi_0\rangle = V|0\rangle.$$

However, in this model

$$V|0\rangle = |0\rangle,$$

i.e.,

$$|\Psi_0\rangle = |0\rangle. \quad \text{(A23)}$$

From

$$H^{\text{eff}}|N;0\rangle = m|N;0\rangle \quad \text{(A24)}$$

we find that

$$\mathcal{H}|\psi_N\rangle = m|\psi_N\rangle, \quad \text{(A25)}$$

$$|\psi_N\rangle = V|N;0\rangle = \psi_d^+(\vec{p})|\Psi_0\rangle = \psi_d^+(\vec{p})|0\rangle, \quad \text{(A26)}$$

where $\psi_d^+(\vec{p}) = V\psi^+(\vec{p})V^+$ is the dressed fermion operator. We also note that

$$H^{\text{eff}}|N;0\rangle = H_0(m)|N;0\rangle, \qquad H_0(m) = mB(0),$$

while

$$\mathcal{H}_0|N;0\rangle = m_0|N;0\rangle. \quad \text{(A27)}$$

In other words, we can take

$$|\psi_N\rangle = |N;m\rangle = |N;out\rangle = V|N;0\rangle. \quad \text{(A28)}$$

This relation underscores the differences between descriptions of fermion states in the *in* (*out*) formalism (a vector in the Fock space R) and the Okubo approach (a vector in the sector $R_0 \subset R$). In exactly the same way we can construct the effective generator of boosts $\vec{K}^{\text{eff}}$ illustrating the statement that two noncommuting Hermitian operators $\mathcal{H}$ and **K** can be brought by the same unitary transformation [in this case, (A5)] to quasidiagonal form (see the discussion in Ref. 122).

APPENDIX B

The coefficients of the expansion

$$\bar{u}(p')\Gamma_\mu(p',p)u(p) = \varphi^+(A_\mu + \vec{B}_\mu\vec{\sigma})\varphi \quad \text{(B1)}$$

are determined by the expressions

$$A_\mu = \frac{1}{2}\,\text{Tr}\left\{(\not{p}'+m)\Gamma_\mu(p',p)(\not{p}+m)\frac{1+\gamma_0}{2}\right\}, \quad \text{(B2)}$$

$$\vec{B}_\mu = \frac{1}{2}\,\text{Tr}\left\{(\not{p}'+m)\Gamma_\mu(p',p)(\not{p}+m)\frac{1+\gamma_0}{2}\vec{\gamma}\gamma_5\right\}. \quad \text{(B3)}$$

After simple calculations we find

$$A_\mu=N_{\vec p'}N_{\vec p}\Big\{G_M[m^2+p'p]\delta_{\mu 0}-i(p'_\mu(E_{\vec p}+m)+p_\mu(E_{\vec p'}+m))\Big]+\frac{i}{2m}F_2(p'+p_\mu)[m^2-pp'+m(E_{\vec p'}+E_{\vec p})], \quad \text{(B4)}$$

$$\vec B_\mu=N_{\vec p'}N_{\vec p}\left\{-\frac{F_2}{2m}(p'+p)_\mu[\vec p'\times\vec p]+G_M[i[\vec p'\times\vec p]\delta_{\mu 0}-(1-\delta_{\mu 0})([\hat{\vec n}^{(\mu)}\times\vec p'](E_{\vec p}+m)-[\hat{\vec n}^{(\mu)}\times\vec p](E_{\vec p}+m))]\right\}, \quad \text{(B5)}$$

$$N_{\vec p}=[2E_{\vec p}(E\vec p+m)]^{-1/2}, \quad G_M=F_1+F_2,$$

where $\hat{\vec n}^{(k)}$, for $k=1,2,3$, are unit vectors with components $\hat n_i^{(k)}=\delta_{ik}$. The arguments $(p'-p)^2$ in the form factors F_1, F_2, and G_M have been dropped.

It follows from (3.27) that

$$(p'-p)^\mu A_\mu=0, \quad \text{(B6)}$$

$$(p'-p)^\mu \vec B_\mu=0. \quad \text{(B7)}$$

APPENDIX C

Let us consider in more detail the situation regarding

$$x=\frac{\vec q^2-\omega^2}{2m\omega}=1. \quad \text{(C1)}$$

In this case, setting $m_p=m_n=m$, for the invariant $s=(\omega+m_d)^2-\vec q^2$ we have

$$s=(\omega+m_\alpha)^2-\vec q^2,$$

$$s=4m^2\left(1+\frac{\omega}{2m}\right)\left[1-\frac{\varepsilon_d}{m}+O\left(\frac{\varepsilon_d^2}{m^2}\right)\right], \quad \text{(C2)}$$

where $\varepsilon_d>0$ is the deuteron binding energy. The limiting angle $\theta_{\lim}$ is given by

$$\sin^2\theta_{\lim}=\left(\frac{\gamma_p^*v_p^*}{\gamma v}\right)^2=\frac{sk_p^{*2}}{m^2q^2}\leqslant 1, \quad \text{(C3)}$$

where v is the speed of the c.m. frame relative to the lab frame, v_p^* is the speed of the knocked-out proton in the c.m. frame, and γ and γ_p^* are the corresponding Lorentz factors.

Using (C2), we find

$$\sin^2\theta_{\lim}=\left(1-\frac{\varepsilon_d}{m}\right)\left[1-\frac{2\varepsilon_d}{\omega}\left(1+\frac{\omega}{2m}\right)\right]. \quad \text{(C4)}$$

Therefore, with the condition (C1) we have $\theta_{\lim}=\pi/2$ up to terms $\sim\varepsilon_d/m$ and $\sim\varepsilon_d/\omega\ll 1$. Moreover, using the Lorentz transformation

$$\vec k_p^*=\vec k_p+\left[\frac{\vec k_p\vec q}{\omega+m_d+\sqrt{s}}-E_{\vec p}\right]\frac{\vec q}{\sqrt{s}} \quad \text{(C5)}$$

and neglecting terms $\sim\varepsilon_d/m_d$, ε_d/ω, and $\omega^2/m^2\ll 1$, it can be shown that

$$\cos\theta^*=\cos 2\theta-\frac{\omega}{4m}\sin^2 2\theta, \quad \text{(C6)}$$

i.e., to a good approximation $\theta^*=2\theta$ for the Bjorken variable $x=1$ and $\omega/4m\ll 1$.

APPENDIX D

Here we shall be interested in the transformation properties of the vector

$$\vec p=\frac{\mathrm{Tr}\{\vec\sigma(1)T_{\rho_e}T^+\}}{\mathrm{Tr}\{T_{\rho_e}T^+\}}, \quad \text{(D1)}$$

where ρ_e is the polarization density matrix for electrons relative to the Lorentz group.

By definition, the T matrix has the following properties:

$$\langle\vec k_p\sigma_p\vec k_n\sigma_n\vec k'\sigma'|T|\vec k\sigma\vec k_d\sigma_d\rangle=\langle\vec k_p\sigma_p\vec k_n\sigma_n\vec k'\sigma'|V^+(\Lambda)TV(\Lambda)|\vec k\sigma\vec k_d\sigma_d\rangle. \quad \text{(D2)}$$

The correspondence $\Lambda\to V(\Lambda)$ realizes some unitary representation of the Lorentz group. Keeping in mind the well known independence of the trace of a matrix from the choice of basis, it is convenient to choose the canonical basis $|p\sigma\rangle\equiv|[ms]\vec p\sigma\rangle$. Each vector in the latter describes the state of a particle of mass m, spin s, momentum $\vec p$, and spin projection σ on the quantization axis.

By definition,

$$V(\Lambda)|\vec p\sigma\rangle=D^{(s)}_{\sigma'\sigma}(R(\Lambda\vec p,\vec p))|\Lambda\vec p\sigma'\rangle, \quad \text{(D3)}$$

where the Wigner rotation $R(\Lambda\vec p,\vec p)$ can be written as

$$R(\Lambda\vec p,\vec p)=L^{-1}(\Lambda\vec p)\Lambda L(\vec p). \quad \text{(D4)}$$

The boost $L(p)$ transforms $m(1,0,0,0)$ into $p=(\sqrt{\vec p^2+m^2},\,\vec p)$. It can now be shown that

$$\vec P=R(\Lambda\vec k_p,\vec k_p)\vec P(\Lambda), \quad \text{(D5)}$$

$$\vec P(\Lambda)=\frac{\mathrm{Tr}\{\vec\sigma(1)T(\Lambda)\rho_e(\Lambda)T^+(\Lambda)\}}{\mathrm{Tr}\{T(\Lambda)\rho_e(\Lambda)T^+(\Lambda)\}}, \quad \text{(D6)}$$

where $\rho_e(\Lambda)=V(\Lambda)\rho_eV^+(\Lambda)$ and $T(\Lambda)$ denotes the T matrix in which the 4-momenta of all the particles are replaced by the transformed momenta: $k_p\to\Lambda k_p$, $k'\to\Lambda k'$, and so on.

Therefore, in transforming from one reference frame to another the polarization vector (D1) undergoes a Wigner rotation (D5).

If Λ is a boost $\vec L$ with velocity v, the corresponding transformation $R(L\vec k_p,\vec k_p)$ is a rotation about the $\vec v\times\vec k_p$ direction by the angle ψ given by the relation

$$\left(1+\gamma+\frac{E^*_{\vec p}}{m}+\frac{E_{\vec p}}{m}\right)\tan\frac{\psi}{2}=\frac{\gamma|\vec v\times\vec k_p|}{m}. \quad \text{(D7)}$$

In the case under consideration, where

$$\gamma\vec v=\vec q/\sqrt{s}, \quad \text{(D8)}$$

we obtain

$$\tan\frac{\psi}{2}<\frac{1}{4}\frac{q}{\sqrt{s}}\frac{k_p}{m}\sin\theta. \quad \text{(D9)}$$

In other words, the components of the proton polarization change significantly under the rotation (D5) in the ultrarelativistic case if the 3-momentum k_p is comparable to the proton mass. This effect becomes more important with increasing θ. Moreover, in the coplanar geometry the component P_Y remains fixed.

A careful treatment of the transformation $\rho_e \to \rho_e(\Lambda)$ can be found in our earlier study.[18]

APPENDIX E

The structure functions W_i^{JM} and $\bar{W}_i^{JM}$ in the lab frame are related to the structure functions f_i^{JM} from Ref. 13 as follows:

$$W_i^{JM}=d_i f_i^{JM} \quad (i=L,T), \tag{E1}$$

$$W_k^{JM}=d_k f_k^{JM(+)}, \quad \bar{W}_k^{JM}=d_k(1-2\delta_{Y_2})f_k^{JM(-)}, \tag{E2}$$

$$f_k^{JM(\pm)}=\frac{1}{2}(2-\delta_{M0})[f_k^{JM}\pm(-1)^{J-M}f_k^{J,-M}]$$

$$(k=LT,TT).$$

Here we have introduced the notation

$$d_i=\frac{c\bar{\rho}_i}{\sigma_M R}\frac{d\Omega_{np}^*}{d\Omega_p}, \tag{E3}$$

$$\bar{\rho}_L/\beta^2=\bar{\rho}_T=-\bar{\rho}_{TT}=\sqrt{2}\bar{\rho}_{LT}/\beta=q_\mu^2/2\eta, \tag{E4}$$

where the kinematical factor C is given in Ref. 13 and $\beta=|\vec{q}|/|\vec{q}^*|$.

The Jacobian of the transformation from the c.m. frame to the lab frame is

$$\frac{d\Omega_{np}^*}{d\Omega_p}=k_p\left[k_p^*\gamma\left(1-\frac{E_p}{k_p}\nu\cos\theta\right)\right]^{-1}. \tag{E5}$$

The inclusive response function $R_{LT}'^{11}$ in (2.42) is proportional to the response function $F_{LT}'^{1-1}$ from Ref. 16:

$$R_{LT}'^{11}=-\frac{6c}{\sigma_M}\bar{\rho}_{LT}F_{LT}'^{1-1}. \tag{E6}$$

Regarding the asymmetries (2.39)–(2.41), it is easily seen that

$$A_{\nu,t}=A_d^{V,T}, \tag{E7}$$

$$A'_{\nu,t}=A_{ed}^{V,T}, \tag{E8}$$

where the quantities on the right-hand sides are defined in Ref. 17.

1)The more general situation with noncoplanar arrangement of the vectors $\vec{k}$, $\vec{k}'$, and $\vec{k}_p$ is considered in Sec. 2.3.

2)As far as we know, the corresponding measurements have been performed at the MIT–Bates Laboratory.

3)This series is generated by iterations of the corresponding integral equation in the t matrix for a given $V(\alpha,\beta)$.

4)In Appendix A the problem of diagonalizing the "strong" Hamiltonian is studied for an exactly solvable field-theoretical model.[105]

5)For simplicity we omit nonminimal contributions.

6)In contrast to Ref. 114, where the result (3.44) was obtained while focusing on the nonrelativistic problem ($H=K+V$), we see that it is valid in the more general case (for example, for the Noether current and the corresponding $\mathscr{H}$).

7)In our opinion, this trick is not necessary, since in deriving the working expressions (2.4) and (2.8) the longitudinal component of the current has been eliminated twice.

8)The nucleon polarization vanishes in the RIA [see the discussion following (2.10)].

9)As far as we know, the data of the corresponding MIT–Bates experiment are being analyzed right now (R. Madey, private communication).

10)Preliminary results of the first measurements of the neutron (proton) polarization in the reaction $d(\vec{e},e'\vec{n})p$ $[d(\vec{e},e'\vec{p})n]$ at the microtron in Mainz were presented in Amsterdam.[134]

11)In Ref. 73 the hadron tensor is obtained by integrating the spectral function for this exclusive reaction over the solid angle of the knocked-out nucleon.

12)The relation between $F_{LT}'^{1-1}$ and $R_{LT}'^{11}$, in terms of which the asymmetry $a'_\nu(\theta_H=\pi/2,\phi_H=0)$ is expressed, and other relations between various quantities can be found in Appendix E.

13)Our results in Figs. 25–29 are for the MEC model of Sec. 3.2 with the parameter $\Lambda=4m_\pi$.

14)Here $S(T)$ denotes the spin (isospin) of the np pair from which the deuteron is formed in the final state.

15)This would not be so if antifermions were included in it.

[1] W. Meyer, Nucl. Phys. **A446**, 381 (1985).

[2] H. G. Andresen, in *Proc. of the Sixth Seminar on Electromagnetic Interactions of Nuclei at Low and Medium Energies*, Moscow, 1986, p. 318.

[3] T. W. Donnelly and A. S. Raskin, Ann. Phys. (N.Y.) **169**, 247 (1986).

[4] R. Madey and S. Kowalski (spokespersons), Proposal 85-05 to MIT–Bates Research Program, 1985.

[5] M. P. Rekalo, G. I. Gakh, and A. P. Rekalo, Ukr. Fiz. Zh. **31**, 1293 (1986) [in Russian].

[6] H. Arenhövel, Phys. Lett. **199B**, 13 (1987).

[7] A. V. Shebeko, in *Proc. of the Intern. Conf. on the Theory of Few-Body and Quark–Hadronic Systems*, Dubna, 1987, p. 183.

[8] M. V. Mostovoy, D. M. Nikolenko, K. T. Ospanov *et al.*, Phys. Lett. **188B**, 181 (1987).

[9] V. V. Kotlyar and A. V. Shebeko, Yad. Fiz. **45**, 984 (1987) [Sov. J. Nucl. Phys. **45**, 610 (1987)].

[10] V. V. Kotlyar and A. V. Shebeko, Z. Phys. A **327**, 301 (1987).

[11] J. M. Finn, R. W. Lourie, C. F. Perdrisat, and P. E. Ulmer (spokespersons), Proposal 88-21 to MIT–Bates Research Program, 1988.

[12] A. Yu. Korchin, Yu. P. Mel'nik, and A. V. Shebeko, Yad. Fiz. **48**, 387 (1988) [Sov. J. Nucl. Phys. **48**, 243 (1988)].

[13] H. Arenhövel, W. Leidemann, and E. L. Tomusiak, Z. Phys. A **331**, 123 (1988); **334**, 363(E) (1989).

[14] V. V. Burov, V. N. Dostovalov, and S. É. Sus'kov, Fiz. Elem. Chastits At. Yadra **23**, 721 (1992) [Sov. J. Part. Nucl. **23**, 317 (1992)].

[15] A. Yu. Korchin, Yu. P. Mel'nik, and A. V. Shebeko, Few-Body Syst. **9**, 211 (1990).

[16] W. Leidemann, E. L. Tomusiak, and H. Arenhövel, Phys. Rev. C **43**, 1022 (1991).

[17] H. Arenhövel, W. Leidemann, and E. L. Tomusiak, Phys. Rev. C **46**, 455 (1992).

[18] Yu. P. Mel'nik and A. V. Shebeko, Few-Body Syst. **13**, 59 (1992).

[19] Yu. P. Mel'nik and A. V. Shebeko, Phys. Rev. C **48**, 1259 (1993).

[20] B. Mosconi, J. Pauschenwein, and P. Ricci, Phys. Rev. C **48**, 332 (1993).

[21] Yu. P. Mel'nik, in *Proc. of the Nat. Conf. on the Physics of Few-Body and Quark–Hadronic Systems*, Kharkov, 1992, edited by V. Boldyshev, V. Kotlyar, and A. Shebeko (1994), p. 293.

[22] Th. Walcher, in *Proc. of the Thirteenth European Conf. on Few-Body Problems in Physics*, Isola d'Elba, 1991, edited by C. Ciofi degli Atti, E. Pace, G. Salme, and S. Simula, Few-Body Syst. Suppl. 6 (Springer-Verlag, 1992), p. 393.

[23] P. K. A. de Witt Huberts, *ibid.*, p. 408.

[24] J. Mougey, *ibid.*, p. 421.

[25] A. Bernstein, *ibid.*, p. 485.

[26] W. F. Hersman, *ibid.*, p. 499.

[27] R. Gilman, in *Proc. of the Nat. Conf. on the Physics of Few-Body and Quark–Hadronic Systems*, Kharkov, 1992, edited by V. Boldyshev, V. Kotlyar, and A. Shebeko (1994), p. 273.

[28] A. Saha, *ibid.*, p. 416.

[29] P. V. Sorokin, in *Proc. of the Sixth Seminar on Electromagnetic Interactions of Nuclei at Low and Medium Energies*, Moscow, 1986, p. 318.

[30] H. Arenhövel and M. Sanzone, Few-Body Syst. Suppl. 3 (Springer-Verlag, 1991).

[31] V. V. Kotlyar and A. V. Shebeko, in *Proc. of the Tenth Intern. Seminar on High Energy Physics Problems*, Dubna, 1990, edited by A. M. Baldin, V. V. Burov, and L. P. Kaptari (World Scientific, Singapore, 1991), p. 392.
[32] S. Boffi, in *Proc. of the CEBAF Summer Workshop*, edited by F. Gross and R. Minehart, Newport News, SURA, 1986, p. 133.
[33] F. Gross, in *Research Program at CEBAF (III)*, Newport News, SURA, 1988, p. 183.
[34] R. D. McKeown, in *Proc. of the Fourteenth European Conf. on Few-Body Problems in Physics*, Amsterdam, 1993, edited by B. L. G. Bakker and R. van Dantzig (Springer-Verlag, 1994), p. 104.
[35] C. Ciofi degli Atti, S. Scopetta, E. Pace, and G. Salme, *ibid.*, p. 458.
[36] A. V. Shebeko, in *Proc. of the Twenty-Seventh Winter School of the PINP*, St. Petersburg, 1993, p. 89 [in Russian].
[37] A. V. Shebeko, in *Proc. of the Sixth Seminar on Electromagnetic Interactions of Nuclei at Low and Medium Energies*, Moscow, 1986, p. 200.
[38] A. V. Shebeko, Lecture given at the V. M. Galitskiĭ All-Union School on Theoretical Nuclear Physics, Moscow Engineering Physics Institute, 1991.
[39] H. Arenhövel, Nucl. Phys. **A384**, 287 (1982).
[40] M. Bernheim, A. Bussiere, J. Mougey *et al.*, Nucl. Phys. **A365**, 349 (1981).
[41] S. Turk-Chieze, P. Barreau, M. Bernheim *et al.*, Phys. Lett. **142B**, 145 (1984).
[42] E. Kazes, T. E. Feuchtwang, P. H. Cutler *et al.*, Ann. Phys. **142**, 80 (1982).
[43] A. V. Shebeko, in Lecture given at the V. M. Galitskiĭ All-Union School on Theoretical Nuclear Physics, Moscow Engineering Physics Institute, 1991.
[44] A. V. Shebeko, Vopr. At. Nauki Tekh. Ser. Yad. Fiz. Issled. No. 2(20), 3 (1991) [in Russian].
[45] S. I. Mishnev, D. M. Nikolenko, S. G. Popov *et al.*, Phys. Lett. **302B**, 23 (1993).
[46] D. Day (spokesperson), CEBAF Proposal 89-018, 1989.
[47] B. Mosconi, J. Pauschenwein, and P. Ricci, Few-Body Syst. Suppl. 6 (Springer-Verlag, 1992), p. 223.
[48] K. Tamura, T. Niwa, S. Sato, and H. Ohtsubo, Nucl. Phys. **A536**, 597 (1992).
[49] G. Beck and H. Arenhövel, Few-Body Syst. Suppl. 13 (Springer-Verlag, 1992), p. 165.
[50] H. Arenhövel, H. Goller, and G. Beck, in *Proc. of the Nat. Conf. on the Physics of Few-Body and Quark–Hadronic Systems*, Kharkov, 1992, edited by V. Boldyshev, V. Kotlyar, and A. Shebeko (1994), p. 132.
[51] V. V. Kotlyar, *ibid.*, p. 145.
[52] T. Wilbois, G. Beck, and H. Arenhövel, Preprint T-93-10, Mainz (1993).
[53] E. Hummel and J. A. Tjon, Phys. Rev. C **49**, 21 (1994).
[54] M. van der Schaar, H. Arenhövel, H. P. Block *et al.*, Phys. Rev. Lett. **68**, 776 (1992).
[55] J. E. Ducret, PhD Thesis, Univ. de Paris-Sud, Orsay, 1992.
[56] W. Jaus and W. S. Woolcock, Helv. Phys. Acta **57**, 644 (1984).
[57] F. Gross and D. O. Riska, Phys. Rev. C **36**, 1928 (1987).
[58] A. Yu. Korchin and A. V. Shebeko, Preprint 88-56, Khar'kov Physico–Technical Institute, Kharkov (1988).
[59] A. Yu. Korchin and A. V. Shebeko, Yad. Fiz. **54**, 357 (1991) [Sov. J. Nucl. Phys. **54**, 214 (1991)].
[60] A. Yu. Korchin, in *Proc. of the Nat. Conf. on the Physics of Few-Body and Quark–Hadronic Systems*, Kharkov, 1992, edited by V. Boldyshev, V. Kotlyar, and A. Shebeko (1994), p. 105.
[61] F. M. Renard, Tran Thanh Van, and M. Bellac, Nuovo Cimento **38**, 565, 1688 (1965).
[62] J. Adam, Jr., E. Truhlik, and D. Adamova, Nucl. Phys. **A492**, 556 (1989).
[63] S. Okubo, Prog. Theor. Phys. **12**, 603 (1954).
[64] N. Fukuda, K. Sawada, and M. Taketani, *ibid.*, p. 156.
[65] M. Gari and H. Hyuga, Nucl. Phys. **A274**, 333 (1976).
[66] W. Glöckle and L. Muller, Phys. Rev. C **23**, 1183 (1981).
[67] Yu. P. Mel'nik and A. V. Shebeko, PANIC XIII, Perugia, Italy, 1993, Abstracts, Vol. 1, p. 322.
[68] K.-M. Schmitt and H. Arenhövel, Few-Body Syst. Suppl. 4 (Springer-Verlag, 1991).
[69] T. de Forest, Nucl. Phys. **A392**, 232 (1983).
[70] M. E. Meyerhoff, D. Eyl, A. Frey *et al.*, Phys. Lett. **327B**, 201 (1994).
[71] C. E. Jones-Woodward, E. J. Beise, J. E. Belz *et al.*, Phys. Rev. C **44**, R571 (1991); C. E. Jones, E. J. Beise, J. E. Belz *et al.*, Phys. Rev. C **47**, 110 (1993).
[72] A. K. Thompson, A. M. Bernstein, T. E. Chupp *et al.*, Phys. Rev. Lett. **68**, 2901 (1992).
[73] B. Blankleider and R. M. Woloshyn, Phys. Rev. C **29**, 538 (1984).
[74] V. V. Kotlyar and A. V. Shebeko, *Contrib. P4 to the Europhysics Conf. on Nuclear Physics with Electromagnetic Probes*, Paris, 1985, Conf. Abstracts, p. 290.
[75] V. V. Kotlyar and A. V. Shebeko, Yad. Fiz. **51**, 1008 (1990) [Sov. J. Nucl. Phys. **51**, 645 (1990)].
[76] V. V. Kotlyar and A. V. Shebeko, Yad. Fiz. **52**, 1320 (1990) [Sov. J. Nucl. Phys. **52**, 836 (1990)].
[77] A. A. Belyaev, V. A. Get'man, V. G. Gorbenko *et al.*, Pis'ma Zh. Eksp. Teor. Fiz. **40**, 448 (1984) [JETP Lett. **40**, 1275 (1984)].
[78] A. A. Belyaev, V. A. Get'man, V. G. Gorbenko *et al.*, Yad. Fiz. **44**, 289 (1986) [Sov. J. Nucl. Phys. **44**, 181 (1986)].
[79] B. A. Craver and Y. E. Kim, and A. Tubis, Nucl. Phys. **A276**, 237 (1977).
[80] S. Aufleger and D. Drechsel, Nucl. Phys. **A364**, 81 (1981).
[81] R. V. Reid, Ann. Phys. (N.Y.) **50**, 411 (1968).
[82] M. Lacombe, B. Loiseau, J. M. Richard *et al.*, Phys. Rev. C **291**, 861 (1980).
[83] T. Sasakawa, Few-Body Syst. Suppl. 1 (Springer-Verlag, 1986), p. 558.
[84] W. Glöckle, H. Kamada, and H. Witala, in *Proc. of the Nat. Conf. on the Physics of Few-Body and Quark–Hadronic Systems*, Kharkov, 1992, edited by V. Boldyshev, V. Kotlyar, and A. Shebeko (1994), p. 132.
[85] S. Ishikawa, H. Kamada, W. Glöckle *et al.*, Preprint, Institut für Theor. Physik II, Ruhr-Universität Bochum (1992).
[86] J. M. Laget, Phys. Lett. **151B**, 325 (1985); **199B**, 493 (1987).
[87] E. van Meijgaard and J. A. Tjon, Phys. Rev. Lett. **57**, 3011 (1986); Phys. Rev. C **42**, 74, 96 (1990).
[88] S. I. Nagornyĭ, Yu. A. Kasatkin, V. A. Zolenko, and I. K. Kirichenko, Yad. Fiz. **55**, 2385 (1992) [Sov. J. Nucl. Phys. **55**, 1325 (1992)].
[89] J. M. Laget, Phys. Rev. C **38**, 2993 (1988).
[90] S. A. Coon, Few-Body Syst. Suppl. 1 (Springer-Verlag, 1986), p. 41.
[91] A. Stadler, W. Glöckle, and P. U. Sauer, Phys. Rev. C **44**, 2319 (1991).
[92] A. V. Shebeko, Vopr. At. Nauki Tekh. Ser. Obshch. Yad. Fiz., No. 2(27), 6 (1984) [in Russian].
[93] *Mesons in Nuclei*, edited by M. Rho and D. H. Wilkinson (North-Holland, Amsterdam, 1979).
[94] *Proc. of the Eleventh Europhysics Conf. on Nuclear Physics with Electromagnetic Probes*, edited by A. Gerard and C. Samour (North-Holland, Amsterdam, 1985).
[95] J.-F. Mathiot, Phys. Rep. **173**, 63 (1989).
[96] D. O. Riska, Phys. Rep. **181**, 207 (1989).
[97] V. R. Brown and J. Franklin, Phys. Rev. C **8**, 1706 (1973).
[98] K. Ohta, Nucl. Phys. **A495**, 564 (1989).
[99] A. Yu. Korchin and A. V. Shebeko, Yad. Fiz. **40**, 1114 (1984) [Sov. J. Nucl. Phys. **40**, 708 (1984)].
[100] R. G. Sachs, Phys. Rev. **74**, 433 (1948).
[101] L. G. Levchuk and A. V. Shebeko, Yad. Fiz. **50**, 974 (1989) [Sov. J. Nucl. Phys. **50**, 607 (1989)].
[102] L. G. Levchuk and A. V. Shebeko, Vopr. At. Nauki Tekh. Ser. Yad. Fiz. Issled. No. 2(20), 66 (1991) [in Russian]; Report presented at the Int. Symp. *Meson-94*, Dubna, 1984 [in Russian]; Yad. Fiz., in press (1994) [Phys. At. Nucl. (1994)].
[103] S. Deister, M. F. Gari, W. Krumpelmann, and M. Mahlke, Few-Body Syst. **10**, 1 (1991).
[104] A. Yu. Korchin and A. V. Shebeko, Yad. Fiz. **56**, No. 12, 77 (1993) [Phys. At. Nucl. **56**, 1663 (1993)].
[105] O. W. Greenberg and S. S. Schweber, Nuovo Cimento **8**, 378 (1958).
[106] A. Yu. Korchin and A. V. Shebeko, Preprint 77-35, Khar'kov Physico–Technical Institute, Khar'kov (1977) [in Russian].
[107] K. W. McVoy and L. van Hove, Phys. Rev. **125**, 1034 (1962).
[108] C. Giusti and F. D. Pacati, Nucl. Phys. **A336**, 247 (1980).
[109] J. D. Bjorken and S. D. Drell, *Relativistic Quantum Fields* (McGraw-Hill, New York, 1965) [Russ. transl., Nauka, Moscow, 1978].
[110] V. V. Kotlyar and A. V. Shebeko, Vopr. At. Nauki Tekh. Ser. Yad. Fiz. Issled. No. 2(20), 83 (1991) [in Russian].
[111] V. V. Burov, S. M. Dorkin, A. Yu. Korchin *et al.*, Preprint E2-93-467, JINR, Dubna (1993).
[112] M. A. Maize and Y. E. Kim, Nucl. Phys. **A420**, 365 (1984).
[113] H. Weyl, *Gruppentheorie und Quantenmechanik* (Leipzig, 1928).
[114] J. L. Friar and S. Fallieros, Phys. Rev. C **46**, 2393 (1992).
[115] H. Arenhövel, Nuovo Cimento **76A**, 256 (1983).
[116] A. J. F. Siegert, Phys. Rev. **52**, 787 (1937).
[117] L. L. Foldy, Phys. Rev. **92**, 178 (1953).
[118] J. L. Friar and S. Fallieros, Phys. Rev. C **29**, 1645 (1984); **34**, 2029 (1986).

[119] A. V. Shebeko, Yad. Fiz. **49**, 46 (1989) [Sov. J. Nucl. Phys. **49**, 30 (1989)].
[120] L. G. Levchuk and A. V. Shebeko, Yad. Fiz. **56**, No. 2, 145 (1993) [Phys. At. Nucl. **56**, 227 (1993)].
[121] F. E. Close and H. Osborn, Phys. Lett. **34B**, 400 (1971).
[122] A. V. Shebeko, Yad. Fiz. **52**, 1535 (1990) [Sov. J. Nucl. Phys. **52**, 970 (1990)].
[123] G. E. Brown and A. D. Jackson, *The Nucleon–Nucleon Interaction* (North-Holland, Amsterdam, 1976) [Russian transl., Atomizdat, Moscow, 1979].
[124] M. P. Rekalo, G. I. Gakh, and A. P. Rekalo, Ukr. Fiz. Zh. **30**, 1125 (1985) [in Russian].
[125] M. van der Schaar, H. Arenhövel, Th. S. Bauer *et al.*, Phys. Rev. Lett. **66**, 2855 (1991).
[126] J. E. Ducret, M. Bernheim, J. F. Danel *et al.*, Phys. Rev. C **49**, 1783 (1994).
[127] P. K. A. de Witt Huberts, in *Proc. of the Eighth Seminar on Elecromagnetic Interactions of Nuclei at Low and Medium Energies*, Moscow, 1991, p. 96.
[128] B. H. Schoch, in *Proc. of the Fourteenth European Conf. on Few-Body Problems in Physics*, Amsterdam, 1993, edited by B. L. G. Bakker and R. van Dantzig (Springer-Verlag, 1994), p. 144.
[129] J. F. J. van den Brand, *ibid.*, p. 151.
[130] A. Yu. Korchin, Yu. P. Mel'nik, and A. V. Shebeko, *Contrib. T-43 to PANIC XII*, MIT, Cambridge (1990).
[131] A. Yu. Korchin, Yu. P. Mel'nik, and A. V. Shebeko, Coll. Physique **51**, 6-499 (1990).
[132] Yu. P. Mel'nik and A. V. Shebeko, Preprint 84-27, Khar'kov Physico–Technical Institute, Moscow, TsNII Atominform, 1984 [in Russian].
[133] A. O. Barut, D. Corrigan, and H. Kleinert, Phys. Rev. Lett. **20**, 167 (1968).
[134] Th. Walcher, *Invited Talk at the Fourteenth European Conf. on Few-Body Problems in Physics, Few-Body XIV Conference Handbook*, edited by L. P. Kok (Amsterdam, 1993), p. 46.
[135] S. Galster, H. Klein, and J. Moritz, Nucl. Phys. **B32**, 221 (1971).
[136] M. Gari and W. Krumpelmann, Z. Phys. A **322**, 689 (1985).
[137] A. Yu. Korchin and A. V. Shebeko, Z. Phys. A **321**, 687 (1985).
[138] R.-W. Schülze and P. U. Sauer, Phys. Rev., 1993, V. C48, p. 38.
[139] A. Yu. Korchin and A. V. Shebeko, Yad. Fiz. **39**, 12 (1984) [Sov. J. Nucl. Phys. **39**, 7 (1984)].
[140] Yu. P. Mel'nik and A. V. Shebeko, *Contrib. to the Thirteenth Intern. Conf. on Few-Body Problems*, Flinders Univ., Adelaide, 1992, pp. 212, 214, 218.
[141] Ch. Hajduk, A. M. Green, and M. E. Sainio, Nucl. Phys. **A337**, 13 (1980).
[142] N. M. O'Fallon, L. J. Koester, and J. H. Smith, Phys. Rev. C **5**, 1926 (1972).
[143] P. E. Argan, G. Audit, N. de Botton *et al.*, Nucl. Phys. **A237**, 447 (1975).
[144] V. B. Ganenko, V. A. Get'man, V. A. Gushchin *et al.*, Vopr. At. Nauki Tekh. Ser. Obshch. Yad. Fiz., No. 1(41), 17 (1988) [in Russian].
[145] F. L. Fabbri, P. Picozza, and C. Schaerf, Lett. Nuovo Cimento **3**, 63 (1972).
[146] H. J. Gassen, A. Hegerath, W. Loers *et al.*, Z. Phys. A **303**, 35 (1981).
[147] J. M. Cameron, P. Kitching, W. J. McDonald *et al.*, Nucl. Phys. **A424**, 549 (1984).
[148] V. V. Kotlyar and A. V. Shebeko, in *Proc. of the Fourth Workshop on High Energy Spin Physics*, Protvino, 1991, p. 346.
[149] R. A. Brandenburg, Y. E. Kim, and A. Tubis, Phys. Rev. C **12**, 1368 (1975).
[150] Ch. Hajduk and P. U. Sauer, Nucl. Phys. **A322**, 329 (1979).
[151] J. Ricco, in *Proc. of the Sixth Seminar on Electromagnetic Interactions of Nuclei at Low and Medium Energies*, Moscow, 1986, p. 78.
[152] A. Cambi, B. Mosconi, and P. Ricci, Phys. Rev. Lett. **48**, 462 (1982).
[153] P. Wilhelm, W. Leidemann, and H. Arenhövel, Few-Body Syst. **8**, 111 (1988).
[154] J. Friar, Phys. Rev. C **27**, 2078 (1983).
[155] Yu. P. Mel'nik, Preprint 93-40, Khar'kov Physico-Technical Institute, Khar'kov (1993).
[156] S. I. Nagorny, Yu. A. Kasatkin, and V. A. Zolenko, Preprint 92-46, Khar'kov Physico-Technical Institute, Khar'kov (1992).
[157] J. E. Ducret, M. Bernheim, M. K. Brussel *et al.*, *INPC 92, Book of Abstracts*, Wiesbaden, 1992, p. 2.2.15.
[158] H. Breuker, V. Burkert, E. Ehses *et al.*, Nucl. Phys. **A455**, 641 (1986).
[159] V. K. Lukyanov and A. I. Titov, Fiz. Elem. Chastits At. Yadra **10**, 815 (1979) [Sov. J. Part. Nucl. **10**, 321 (1979)].
[160] L. L. Frankfurt and M. I. Strikman, Phys. Rep. **160**, 235 (1988).
[161] G. A. Leksin *et al.*, CEBAF Proposal 89-036, 1989.
[162] K. Egiyan *et al.*, CEBAF Proposal 89-032, 1989.

Translated by Patricia A. Millard